NASA Contractor Report 4672

Analytical Investigations in Aircraft and Spacecraft Trajectory Optimization and Optimal Guidance

Nikos Markopoulos and Anthony J. Calise
Georgia Institute of Technology • Atlanta, Georgia

May 1995

Printed copies available from the following:

Analytical Investigations in Aircraft and Spacecraft Trajectory Optimization and Optimal Guidance[*]

Nikos Markopoulos[**] and Anthony J. Calise[†]

School of Aerospace Engineering
Georgia Institute of Technology, Atlanta, Georgia 30332

Summary

A collection of analytical studies is presented related to unconstrained and constrained aircraft energy-state modeling and to spacecraft motion under continuous thrust. With regard to aircraft unconstrained energy-state modeling, the physical origin of the singular perturbation parameter that accounts for the observed two-time-scale behavior of aircraft during energy climbs is identified and explained. With regard to the constrained energy-state modeling, optimal control problems are studied involving active state-variable inequality constraints. Departing from the practical deficiencies of the control programs for such problems that result from the traditional formulations, a complete reformulation is proposed for these problems which, in contrast to the old formulation, will presumably lead to practically useful controllers that can track an inequality constraint boundary asymptotically, and even in the presence of two-sided perturbations about it. Finally, with regard to spacecraft motion under continuous thrust, a thrust program is proposed for which the equations of two-dimensional motion of a space vehicle in orbit, viewed as a point mass, afford an exact analytic solution. The thrust program arises under the assumption of tangential thrust from the costate system corresponding to minimum-fuel, power-limited, coplanar transfers between two arbitrary conics. The trajectory equation describing the above exact analytic solution is identical in form with the trajectory equation corresponding to Keplerian motion (motion with zero thrust). This solution can be used to satisfy boundary conditions corresponding to arbitrary coplanar transfer and escape problems. The thrust program can be used not only with power-limited propulsion systems, but also with any propulsion system capable of generating continuous thrust of controllable magnitude, and, for propulsion types and classes of transfers for which it is sufficiently optimal the results of this report suggest a method of maneuvering during planetocentric or heliocentric orbital operations, requiring a minimum amount of

---

[*]   Chapters two and three have been *co-authored*. Chapter four and the Appendices have been *sole-authored* by Nikos Markopoulos.

[**] Former Graduate Research Assistant.

[†] Professor.

computation, and thus uniquely suitable for real-time feedback guidance implementations. The results pertaining to the thrust program and to the exact analytic solution of the equations of motion are summarized in Appendix H, and then generalized to a much wider class of thrust programs, given the name the "Keplerian class", in Appendix I, supplied at the very end of this report. It should be emphasized that the Appendices (with the exception of A and C) are an integral part of the research reported in the fourth chapter of this report. Specifically, any reader who knows anything about Keplerian motion (spacecraft motion in the absence of thrust) can get a preliminary idea about the primary contribution of Chapter four by examining just two Tables, namely, Table H.1 (page 135) of Appendix H, and Table I.1 (page 139) of Appendix I.

Contents

List of Tables

List of Illustrations

Nomenclature

For Chapter IV, and the Appendices:

t   = time

M   = angular momentum per unit mass

X   = radial velocity component

R   = radial distance from center of gravitational attraction

θ = argument of latitude

E_R = radial thrust acceleration component

E_θ = transverse thrust acceleration component

τ = nondimensional time

h   = nondimensional angular momentum per unit mass

x   = nondimensional radial velocity component

r   = nondimensional radial distance

V   = nondimensional speed of the vehicle

γ = flight path angle

ε_r = nondimensional radial thrust acceleration

ε_θ = nondimensional transverse thrust acceleration

a   = semimajor axis of a conic

e   = eccentricity of a conic

ω = orientation of a conic (on a given plane)

E   = generalized eccentric anomaly

H   = generalized hyperbolic anomaly, Hamiltonian

A   = throttling parameter

B   = generalized eccentricity of a transfer trajectory

C   = generalized orientation of a transfer trajectory

$(\ )_s$ = value of a quantity at reference radius R_s

$(\ )_0$ = value of a quantity at the initial time $\tau=0$

$(\ )_f$ = value of a quantity at the final time $\tau=\tau_f$

CHAPTER I

Introduction

In spite of all the recent technological breakthroughs regarding the speed of numerical computing, and the latest advances in new computational techniques, analytical methods still continue to play an essential role in problems related to aircraft and spacecraft trajectory optimization and optimal guidance, and to flight mechanics in general. One reason for this is that there is always much physical insight to be gained from any analytical procedure that extracts as much information as possible from the differential equations governing a problem, even without attempting to solve them. For example, in systems exhibiting multiple-time-scale behavior, the fundamental physical process that gives rise to such behavior can sometimes be uncovered and understood by an analysis of the governing differential equations. A second reason is certainly that all real physical problems are first reduced to mathematical formulations or models before any attempt is made toward their solution. Formulating a real physical problem in precise mathematical language is equivalent to asking precise questions, and one cannot expect to obtain the right answers unless one asks the right questions. Analytical techniques can sometimes be useful and result in further progress just by helping one ask the right questions. Finally, a third reason for the importance of such methods is that the real-time solution of the common two-point boundary value problems encountered in the field of aircraft and spacecraft trajectory optimization still remains a dream. Accordingly, the numerical computation of optimal trajectories and optimal feedback guidance laws has still to be aided and supplemented considerably by analytical methods.

The major objective of this report is the application of such methods to the areas of aircraft and spacecraft trajectory optimization related to energy-state modeling and Non-Keplerian orbital motion.

A systematic approach is presented in the second chapter for identifying the perturbation parameter in singular perturbation analyses of aircraft optimal trajectories and guidance. The approach is based on a nondimensionalization of the equations of motion. It can be used to evaluate the appropriateness of forced singular perturbation formulations that were used in the past for transport and fighter aircraft. It can also be used to assess the

applicability of energy-state approximations and singular perturbation analyses for airbreathing, transatmospheric vehicles with hypersonic cruise and orbital capabilities. In particular, the family of problems related to aircraft energy climbs is considered. For energy climbs constrained to a vertical plane it is shown that the singular perturbation parameter can logically be taken as the maximum allowable longitudinal load factor of the vehicle. Two-time-scale behavior is suggested when this load factor is sufficiently less than one.

In the third chapter the focus is on optimal control problems involving active state-variable inequality constraints. Such problems arise naturally in the context of aircraft trajectory optimization whenever functions of the state variables (such as dynamic pressure, aerodynamic heating rate, etc.) are constrained along a trajectory. Traditional analytical techniques that work fairly well in the absence of such constraints break down when such constraints are present, and therefore new methods are needed for an understanding of these problems. Departing from this premise, a transformation technique is introduced in the third chapter that splits the class of all piecewise continuous (in time) controllers that track a given hypersurface in the state space of a dynamical system into two disjoint classes. The first class contains all controllers that track the hypersurface in finite time. The second class contains all controllers that track the hypersurface asymptotically. Four theorems are presented that describe the two classes. The results are applied to the study of optimal control problems involving active state-variable inequality constraints. The controllers obtained from the traditional formulation of such problems are typically finite-time and one-sided, that is, they break down when a disturbance throws the system toward the prohibited side of a state-constraint boundary. These features tend to make such controllers quite unattractive from a practical point of view. This report proposes a reformulation of such problems in which the optimization is carried out only with respect to asymptotic controllers. The *reformulated* problem leads to controllers that are approximately optimal, asymptotic, but still one-sided. However, if the state constraint is regarded as a soft constraint, then one can show that there may exist controllers that are *asymptotic, two-sided*, and result in the same optimal value of the performance index corresponding to the *original* problem, that is, they are practically *optimal*, but at the expense of violating the state constraint.

The topic in the fourth chapter is orbital motion under continuous thrust. A continuous thrust program is presented for which the equations of two-dimensional motion of a space vehicle in orbit, viewed as a point mass, afford an exact analytic solution. The

thrust program is proportional to an arbitrary throttling parameter, and arises from the optimization problem corresponding to minimum-fuel, power-limited, coplanar transfers between two arbitrary conics. It is shown that, for this problem, the assumption that the thrust is tangent to the flight path results in the complete analytic solution of the system of state-costate equations governing the optimal trajectories. This approximation of tangential thrust is made only in the costate equations, affecting only optimality, resulting in the elimination of the costates, and giving rise to the thrust program, for which the state equations can be solved analytically with no further approximations. The most striking aspect of the motion suggested by this solution is the fact that it is described by a trajectory equation identical in form to the one corresponding to Keplerian motion (motion with zero thrust)! The difference is that, in the latter the angular momentum is a constant, while in the former it is a linear function of time, with slope equal to the throttling parameter. This similarity allows one to speak of the two motions by using more or less the same mathematical vocabulary. The transverse (horizontal) component of the thrust program is inversely proportional to the radial distance from the inverse-square attractive center, while the radial (vertical) component is such that the thrust is in the flight-path direction. The constant of proportionality (throttling parameter) appearing in the thrust program can be appropriately selected to satisfy the boundary conditions corresponding to arbitrary coplanar transfer and escape problems. To document these facts, and demonstrate the existence of such particular solutions, several examples are given of such maneuvers. Questions concerning the optimality of such trajectories are also dealt with, and hints are provided, suggesting that there should be at least some classes of transfers for which the resulting trajectories are sufficiently optimal, both for power-limited and constant ejection velocity types of propulsion. The results pertaining to the thrust program and to the exact analytic solution of the equations of motion are generalized to a much wider class of thrust programs, given the name the "Keplerian class", in Appendix I.

CHAPTER II

Aircraft Energy-State Modeling and Singular Perturbations

2.1 Introduction

The methods of matched asymptotic analysis in singular perturbation theory are based on the presence of small parameters in the differential equations of motion, that give rise to multiple time-scale behavior. It has been noted by several authors[1,2] that, in spite of a wide number of papers attesting to the applicability of singular perturbation methods to optimization problems in aircraft flight mechanics, few have been successful in first casting the equations of motion in a singular perturbation form. Exceptions are Refs. 1-4. Two methods of analysis for time-scale separability are proposed in Ref. 1. Both of these methods are based on an estimation of the state variables' relative speeds. In Ref. 2 a rescaling to nondimensional variables is recommended. However, it is noted that the proper scaling transformation is not obvious, even if the time-scale separation of the variables is well-known from analysis or experience. Both of these papers (and in particular Ref. 1) provide extensive references to earlier studies which employ so-called forced singular perturbation formulations, in which the perturbation parameter ε, nominally equal to one, is artificially introduced as a bookkeeping parameter, in a formal expansion of the solution about $\varepsilon = 0$. In particular, there exists a large number of publications on the optimization of aircraft energy climbs (see for example Refs. 5-8), none of which identify an appropriate perturbation parameter in terms of the relevant problem parameters. This disparity is particularly disturbing, especially considering the number of years that have passed since such analytical techniques were first introduced in the flight mechanics literature. Note in contrast, that there *have* been applications of singular perturbation theory to other areas of flight mechanics, in which the perturbation parameter *was* clearly identified in terms of the relevant problem parameters. For instance, with regard to aero-assisted orbit transfer, the perturbation parameter happens to be just the ratio of the atmospheric scale height to the minimum trajectory radius (see for example Refs. 9, 10). In any singular perturbation analysis, it is advantageous to identify the perturbation parameter ε in terms of the relevant problem parameters (which in general include the boundary conditions), so that the

physical process that gives rise to the two-time-scale behavior is clearly understood. Then, the range of parameter values for which the perturbation analysis is possible can be easily identified. In fact, knowledge of time-scale separability present in the system dynamics, and success in exploiting this characteristic to obtain approximate solutions, cannot in itself be a rigorous justification for artificially introducing ε.

In this chapter an attempt is made to partially rectify the situation described above by presenting a systematic (albeit still ad hoc) approach for identifying the singular perturbation parameter ε through nondimensionalization of the problem variables. Attention is focused on nonlinear optimization problems in flight mechanics, though most of the considerations that are presented apply in other fields as well. The main motivation for collecting and stating these considerations is to define the thought process by which it is possible to arrive at a suitable scaling of the aircraft energy climb problem. Of particular interest, from the point of view of future potential applications, is an assessment of energy-state approximations and singular perturbation analyses for airbreathing, transatmospheric vehicles with hypersonic cruise and orbital capabilities.

2.2 Subsonic-Supersonic Regimes, Flat Earth Approximation

Consider atmospheric flight of a conventional aircraft, viewed as a point mass, in a vertical plane over a flat Earth. The equations governing such flight can be reduced to a three-state model in mass specific energy E, flight path angle γ, and altitude h. The vehicle mass, m, is assumed to be constant. The equations are:

$$\frac{dE}{dt} = \frac{V(T-D)}{m} \tag{2.1}$$

$$\frac{d\gamma}{dt} = \left(\frac{L}{mV}\right) - \left(\frac{g\cos\gamma}{V}\right) \tag{2.2}$$

$$\frac{dh}{dt} = V\sin\gamma \tag{2.3}$$

where L, D and g denote the lift, the drag and the (constant) gravitational acceleration. It is assumed that the atmosphere is stationary, and that the thrust, T, is directed along the flight path. The specific energy (mechanical energy per unit mass of the vehicle) E and the speed V are related by:

5

$$E = \frac{V^2}{2} + gh \tag{2.4}$$

and E rather than V has been employed as a state variable.

For a singular perturbation analysis, Eqs. (2.2) and (2.3) are commonly written as:

$$\varepsilon \frac{d\gamma}{dt} = \left(\frac{L}{mV}\right) - \left(\frac{g\cos\gamma}{V}\right) \tag{2.5}$$

$$\varepsilon \frac{dh}{dt} = V\sin\gamma \tag{2.6}$$

where ε is artificially introduced, and its nominal value is said to be equal to 1.0. The main purpose of the present chapter is to avoid an artificial introduction of ε at the outset, thus, Eqs. (2.2) and (2.3) will be retained, while Eqs. (2.5) and (2.6) will be used only as a guide for the natural introduction of ε.

2.2.1 Nondimensional Form

The first step in seeking a natural introduction of the perturbation parameter ε is to put Eqs. (2.1) through (2.3) in nondimensional form. To this end one may start by defining the set S:

$$S = \{t_0, E_0, h_0, V_0, T_0, D_0, L_0\} \tag{2.7}$$

The elements of the set S are at this point *arbitrary positive quantities*, and the only restriction that one imposes upon them is that:

t_0 has dimensions of time

E_0 has dimensions of energy per unit mass

h_0 has dimensions of length

V_0 has dimensions of speed

T_0, D_0, and L_0 have dimensions of force

Using the elements of S to define the nondimensional quantities:

$$\bar{t} = \frac{t}{t_0} \quad ; \quad \bar{E} = \frac{E}{E_0} \quad ; \quad \bar{h} = \frac{h}{h_0} \quad ; \quad \bar{V} = \frac{V}{V_0} \tag{2.8}$$

6

$$T = \frac{T}{T_0} \quad ; \qquad D = \frac{D}{D_0} \quad ; \qquad L = \frac{L}{L_0} \tag{2.9}$$

Eqs. (2.1) through (2.3) can be put into the following nondimensional form:

$$\frac{dE}{dt} = V(TT_0 - DD_0)\left(\frac{t_0 V_0}{E_0 m}\right) \tag{2.10}$$

$$\frac{d\gamma}{dt} = \left(\frac{L}{V}\right)\left(\frac{L_0 t_0}{mV_0}\right) - \left(\frac{\cos\gamma}{V}\right)\left(\frac{g t_0}{V_0}\right) \tag{2.11}$$

$$\frac{dh}{dt} = \left(\frac{V_0 t_0}{h_0}\right) V \sin\gamma \tag{2.12}$$

The goal is now to put Eqs. (2.10) through (2.12) in the traditional singular perturbation form. Multiplying both sides of Eqs. (2.11) and (2.12) by ($h_0 / V_0 t_0$) results in:

$$\left(\frac{h_0}{V_0 t_0}\right)\frac{d\gamma}{dt} = \left(\frac{L}{V}\right)\left(\frac{L_0 h_0}{mV_0^2}\right) - \left(\frac{\cos\gamma}{V}\right)\left(\frac{g h_0}{V_0^2}\right) \tag{2.13}$$

$$\left(\frac{h_0}{V_0 t_0}\right)\frac{dh}{dt} = V \sin\gamma \tag{2.14}$$

Comparing the set of Eqs. (2.10), (2.13), and (2.14), with the set of Eqs. (2.1), (2.5) and (2.6), it is evident that one can make the two sets similar by imposing the following *four* conditions on the elements of the set S:

$$T_0 = D_0 \tag{2.15}$$

$$\frac{T_0 t_0 V_0}{E_0 m} = 1 \tag{2.16}$$

$$\frac{L_0 h_0}{m V_0^2} = 1 \tag{2.17}$$

$$\frac{g h_0}{V_0^2} = 1 \tag{2.18}$$

7

If one defines ε as:

$$\varepsilon = \frac{h_0}{V_0 t_0} \tag{2.19}$$

then, Eqs. (2.10), (2.13) and (2.14) assume the form:

$$\frac{dE}{dt} = V(T - D) \tag{2.20}$$

$$\varepsilon \frac{d\gamma}{dt} = \left(\frac{L - \cos\gamma}{V} \right) \tag{2.21}$$

$$\varepsilon \frac{dh}{dt} = V \sin\gamma \tag{2.22}$$

To summarize, it was shown in the present section that it is possible to introduce a parameter ε naturally into the equations of motion (Eqs. (2.1) - (2.3)) by first introducing a set of arbitrary positive quantities S (see Eq. (2.7)) to scale the variables of interest, and then by imposing four conditions (Eqs. (2.15) - (2.18)) on these quantities so that the resulting nondimensional equations assume the traditional singular perturbation form (Eqs. (2.20) - (2.22)). Note that only one of the arbitrary quantities in S is uniquely determined at this point. Combining Eqs. (2.17) and (2.18) it follows that L_0 is given by:

$$L_0 = mg \tag{2.23}$$

2.2.2 Specifying a Particular Nondimensional Form

As shown in the previous subsection, only four conditions are imposed on the seven elements of set S in transforming the equations of motion to the traditional singular perturbation format. This means that one can specify three of the elements of S to fit one's convenience and then determine the remaining four using Eqs. (2.15)-(2.18). The first conclusion therefore is that in general the value of ε is quite arbitrary. For example, by choosing h_0, V_0, and t_0 in two different ways ε can be made arbitrarily small or large. The separability of the time scales on the other hand is a property of the system and not of the particular nondimensional form of the equations of motion that is chosen. One therefore should expect that if the system does indeed possess the property of time scale separability,

8

it will exhibit it no matter what the actual value of ε is. This is precisely the reason for the success of so many singular perturbation treatments of the past in which ε was introduced artificially and its nominal value was said to be "fixed" at one.

Although there is no unique way of specifying a particular nondimensional form of the equations of motion, one can argue that there is at least one choice for the elements of set S that results in additional physical insight. First, in order to maintain the relationship in Eq. (2.4) in the transformed variables, a fifth condition is introduced:

$$E_0 = g h_0 \qquad (2.24)$$

which together with Eq. (2.18) implies:

$$E = \frac{V^2}{2} + h \qquad (2.25)$$

Using Eqs. (2.16) and (2.24) in Eq. (2.19), it follows that ε can be written as:

$$\varepsilon = \frac{T_0}{mg} \qquad (2.26)$$

Now, only two among the seven elements of set S need to be specified. Then, the five conditions, Eqs. (2.15) - (2.18) and (2.24), uniquely determine the remaining elements.

Eq. (2.26) implies that ε depends only on T_0 and is independent of the value of the remaining elements of S. The question therefore arises as to whether there is a particular choice of T_0 for which the resulting value of ε can be used as a strict criterion for the applicability of a singular perturbation analysis to Eqs. (2.20)-(2.22). The answer to this question is negative in general, because, in a given time interval, it is both the relative magnitudes of the three quantities:

$$\frac{dE}{dt}, \quad \frac{d\gamma}{dt}, \quad \frac{dh}{dt}$$

and the boundary conditions of interest that determine the validity of a singular perturbation analysis. Specifically, for an aircraft to exhibit the well-known two-time-scale behavior in a given time interval, it is necessary that *for some choice of control* the relations:

$$\frac{dE}{dt} \ll \frac{d\gamma}{dt} \qquad (2.27)$$

9

$$\frac{dE}{dt} \ll \frac{dh}{dt} \qquad (2.28)$$

be valid in that interval, and that the required change in E be sufficiently large to permit the boundary layer responses in h and γ to reach their equilibrium values. Hence, it will be assumed that the boundary conditions are such that the resulting change in E is sufficiently large. Then, the conditions in Eqs. (2.27) and (2.28) further require that the net change in E during the boundary layer response is sufficiently small to permit approximating E as a constant (to zero order in ε) in the boundary layer analysis. In addition, the aim here will be only to identify whether this two-time-scale property is a consequence of the inherent dynamics of the aircraft, and not whether it is a consequence of using a high gain control solution for L. Therefore, it will be assumed that the control L resulting from the boundary-layer analysis is of order one in Eq. (2.21).

Under the above assumptions, there is a choice for T_0 for which the value of ε can be used as a criterion for the existence of time intervals in which two-time-scale behavior is exhibited. If the choice of T_0 is such that dE/dt in Eq. (2.20) is at most of the same order of magnitude as $\varepsilon d\gamma/dt$ and $\varepsilon dh/dt$ in Eqs. (2.21) and (2.22), then, a value of ε sufficiently less than one indicates the possible existence of such intervals. By suitably choosing V_0 one can restrict V to be of order one. Then, by selecting the flight condition where the difference between thrust and drag, T-D, reaches a maximum, and by choosing T_0 to be equal to this difference:

$$T_0 = (T - D)_{max} \qquad (2.29)$$

one can guarantee that dE/dt is of order one, and both $d\gamma/dt$ and dh/dt are of order $1/\varepsilon$. For this choice of T_0, ε is given by:

$$\varepsilon_1 = \frac{(T - D)_{max}}{mg} \qquad (2.30)$$

and is equal to the *maximum longitudinal load factor* of the vehicle.

Eq. (2.30) actually represents an *upper bound* for ε (i.e. $\varepsilon < \varepsilon_1$) since it is obtained by selecting the flight condition where the difference between thrust and drag, T-D, reaches a maximum. The logical choice for V_0 is the speed at this flight condition. One can also adopt

10

the less conservative viewpoint of evaluating ε along the energy climb path that represents the reduced solution (the solution obtained for $\varepsilon = 0$). The value of ε as a function of E can then be used as a measure to distinguish energy levels at which a singular perturbation analysis may be appropriate from other energy levels at which it may not be valid.

It is important to emphasize here that having a high-gain control solution for lift, L, does not change the above conclusion, since high lift results in further time-scale separation between the flight path angle dynamics and the energy dynamics. It is precisely for this reason that the aim was only to identify whether the two-time-scale property is a consequence of the inherent dynamics, and not whether it is a consequence of using a high gain control solution for lift. It was done with the hope that this would lead to a conclusion independent of the performance index. One might also wish to exclude the situation wherein the open loop dynamics are not two-time-scale, but the closed-loop dynamics *are* two-time-scale. This would be the nonlinear counterpart to the so-called "cheap control problem" in linear quadratic optimization[11].

Much can be anticipated from Eq. (2.30) for conventional aircraft without exact numerical evaluation. The quantity $(T-D)_{max}$ divided by mg is approximately equal to $\sin\gamma_{max}$ where γ_{max} is the maximum climb angle that can be maintained at a given energy level without loss of airspeed. It follows therefore that $\varepsilon_1 < 1$ for all such aircraft types. For transport aircraft $\sin\gamma_{max}$ is approximately 0.1, while for many fighter aircraft $\sin\gamma_{max}$ is approximately 0.8 or less. This suggests that the forced singular perturbation analysis used in past studies of optimal aircraft trajectories is valid for most conventional subsonic and supersonic aircraft.

A second upper bound for ε can also be evaluated in terms of the quantities $(T/mg)_{max}$ and $(L/D)_{max}$ for a given aircraft. Since L is approximately equal to mg along the reduced solution corresponding to an energy climb path, it follows that:

$$\varepsilon < \varepsilon_2 \tag{2.31}$$

where ε_2 is defined as:

$$\varepsilon_2 = \left[(T/mg)_{max} - \frac{1}{(L/D)_{max}} \right] \tag{2.32}$$

Estimates of ε_2 are given in Table 2.1.

Table 2.1 Estimation of ε_2 based on Eq. (2.32)

Parameter	Transports	Fighters
$(T / mg)_{max}$	0.25	0.90
$(L / D)_{max}$	13 - 15	4 - 7
ε_2	0.17 - 0.18	0.65 - 0.76

2.3 Hypersonic Regime

Consider the flight of a hypersonic and possibly transatmospheric vehicle, viewed as a point mass, in a vertical plane over a spherical, non-rotating Earth, of gravitational strength μ. The equations governing such flight can be reduced to a four-state model in E, m, γ and radial distance from the center of the Earth, r. The equations are:

$$\frac{dE}{dt} = \frac{V(\eta T - D)}{m} \tag{2.33}$$

$$\frac{dm}{dt} = -f(r, V, \eta) \tag{2.34}$$

$$\frac{d\gamma}{dt} = \left(\frac{L}{mV}\right) - \left(\frac{\mu \cos\gamma}{Vr^2}\right) + \left(\frac{V \cos\gamma}{r}\right) \tag{2.35}$$

$$\frac{dr}{dt} = V \sin\gamma \tag{2.36}$$

where T is now the maximum available thrust at a given speed and altitude. The control variables are L and η, where $0 < \eta < 1$ is introduced as a nondimensional throttling variable. E and V are now related by:

$$E = \frac{V^2}{2} - \frac{\mu}{r} \tag{2.37}$$

Eqs. (2.35) and (2.36) now assume the form:

$$\varepsilon \frac{d\gamma}{dt} = \left(\frac{L}{mV}\right) - \left(\frac{\mu \cos\gamma}{Vr^2}\right) + \left(\frac{V \cos\gamma}{r}\right) \tag{2.38}$$

12

$$\varepsilon \frac{dr}{dt} = V \sin\gamma \qquad (2.39)$$

and again in order to avoid the artificial introduction of ε, Eqs. (2.38) and (2.39) will serve only as a guide for the natural introduction of ε.

2.3.1 Nondimensional Form

In order to put Eqs. (2.33) through (2.36) in nondimensional form one can now define the set of arbitrary positive quantities:

$$S = \{t_0, E_0, m_0, r_0, V_0, f_0, T_0, D_0, L_0\} \qquad (2.40)$$

and impose the restrictions that:

t_0 has dimensions of time

E_0 has dimensions of energy per unit mass

m_0 has dimensions of mass

r_0 has dimensions of length

V_0 has dimensions of speed

f_0 has dimensions of mass per unit time

T_0, D_0, and L_0 have dimensions of force

Using the elements of S to define the nondimensional quantities:

$$t = \frac{t}{t_0} \ ; \qquad E = \frac{E}{E_0} \ ; \qquad m = \frac{m}{m_0} \ ; \qquad r = \frac{r}{r_0} \ ; \qquad V = \frac{V}{V_0} \qquad (2.41)$$

$$f = \frac{f}{f_0} \ ; \qquad T = \frac{T}{T_0} \ ; \qquad D = \frac{D}{D_0} \ ; \qquad L = \frac{L}{L_0} \qquad (2.42)$$

Eqs. (2.33) through (2.36) can be put into the following nondimensional form:

$$\frac{dE}{dt} = \frac{V(\eta T T_0 - D D_0)}{m}\left(\frac{t_0 V_0}{E_0 m_0}\right) \qquad (2.43)$$

$$\frac{dm}{dt} = -\left(\frac{f_0 t_0}{m_0}\right) f(r, V, \eta) \qquad (2.44)$$

13

$$\frac{d\gamma}{dt} = \left(\frac{L}{mV}\right)\left(\frac{L_0 t_0}{m_0 V_0}\right) - \left(\frac{\cos\gamma}{V r^2}\right)\left(\frac{\mu t_0}{V_0 r_0^2}\right) + \left(\frac{V\cos\gamma}{r}\right)\left(\frac{V_0 t_0}{r_0}\right) \quad (2.45)$$

$$\frac{dr}{dt} = \left(\frac{V_0 t_0}{r_0}\right) V \sin\gamma \quad (2.46)$$

The goal is again to put Eqs. (2.43) through (2.46) in the traditional singular perturbation form, thus, multiplying both sides of Eqs. (2.45) and (2.46) by $(r_0 / V_0 t_0)$ results in:

$$\left(\frac{r_0}{V_0 t_0}\right)\frac{d\gamma}{dt} = \left(\frac{L}{mV}\right)\left(\frac{L_0 r_0}{m_0 V_0^2}\right) - \left(\frac{\cos\gamma}{V r^2}\right)\left(\frac{\mu}{V_0^2 r_0}\right) + \left(\frac{V\cos\gamma}{r}\right) \quad (2.47)$$

$$\left(\frac{r_0}{V_0 t_0}\right)\frac{dr}{dt} = V\sin\gamma \quad (2.48)$$

Comparing the set of Eqs. (2.43), (2.44), (2.47) and (2.48) with the set (2.33), (2.34), (2.38) and (2.39) results in the following *five* conditions on the elements of set S:

$$T_0 = D_0 \quad (2.49)$$

$$\frac{T_0 t_0 V_0}{E_0 m_0} = 1 \quad (2.50)$$

$$\frac{f_0 t_0}{m_0} = 1 \quad (2.51)$$

$$\frac{L_0 r_0}{m_0 V_0^2} = 1 \quad (2.52)$$

$$\frac{\mu}{V_0^2 r_0} = 1 \quad (2.53)$$

By defining ε as:

$$\varepsilon = \frac{r_0}{V_0 t_0} \quad (2.54)$$

14

Eqs. (2.43), (2.44), (2.47) and (2.48) assume the traditional singular perturbation form:

$$\frac{dE}{dt} = \frac{V(\eta T - D)}{m} \tag{2.55}$$

$$\frac{dm}{dt} = -f(r, V, \eta) \tag{2.56}$$

$$\varepsilon \frac{d\gamma}{dt} = \left(\frac{L}{mV}\right) - \left(\frac{\cos\gamma}{Vr^2}\right) + \left(\frac{V\cos\gamma}{r}\right) \tag{2.57}$$

$$\varepsilon \frac{dr}{dt} = V \sin\gamma \tag{2.58}$$

2.3.2 Specifying a Particular Nondimensional Form

For the hypersonic case, only five conditions on the nine elements of set S are needed in order to put the equations of motion in the traditional singular perturbation form. Thus, one can specify four of the elements of S to fit one's convenience and then determine the remaining five using Eqs. (2.49)-(2.53).

Again, in order to maintain the relationship in Eq. (2.37) in the transformed variables, a sixth condition is introduced:

$$E_0 = \frac{\mu}{r_0} \tag{2.59}$$

which together with Eq. (2.53) gives:

$$E = \frac{V^2}{2} - \frac{1}{r} \tag{2.60}$$

If one thinks of r_0 as a radial distance, then Eq. (2.53) restricts V_0 to be the circular orbital speed at r_0. Similarly, Eq. (2.52) restricts L_0 to be the centripetal force that a point mass m_0 would experience in a circular orbit at r_0. Using Eqs. (2.50), (2.53), and (2.59) one obtains:

$$\varepsilon = \frac{T_0 r_0^2}{\mu m_0} \tag{2.61}$$

15

Hence, by picking three among the nine elements of set S arbitrarily, the six conditions Eqs. (2.49)-(2.53), and (2.59) uniquely determine the remaining elements.

The question arises again as to whether there is a particular choice for these three elements for which the resulting value of ε can be used as a criterion for the applicability of a singular perturbation analysis to Eqs. (2.55)-(2.58). The right-hand-sides of Eqs. (2.55) and (2.58) can be made of the same order of magnitude by choosing the ratio T_0/m_0 as:

$$\frac{T_0}{m_0} = \left(\frac{\eta T - D}{m}\right)_{max} \tag{2.62}$$

Choosing r_0 as the sea level radius r_{SL}, r and V are of order one. Also, for these choices of T_0/m_0 and r_0, dE/dt is of order one, and both $d\gamma/dt$ and dr/dt are of order $1/\varepsilon$. By choosing f_0 as the value of f at the flight condition where the ratio $(\eta T - D)/m$ is a maximum, dm/dt can also be made of order one. With the above choices of T_0/m_0, r_0, and f_0, ε becomes:

$$\varepsilon = \left(\frac{r_{SL}^2}{\mu}\right)\left(\frac{\eta T - D}{m}\right)_{max} \tag{2.63}$$

The right-hand-side of Eq. (2.63) is the *maximum longitudinal load factor* of the vehicle in units of sea-level g's, and actually represents an upper bound for ε since it is obtained by selecting the flight condition where $(\eta T - D)/m$ reaches a maximum. One can again adopt the less conservative viewpoint of evaluating ε along the energy climb path that results from the reduced solution (the solution obtained with $\varepsilon = 0$). The value of ε as a function of E can then be used as a measure to distinguish energy levels where a singular perturbation analysis may be appropriate, from other levels where it may not be valid.

A hypersonic flight vehicle employing an airbreathing propulsion system and sized for acceleration to orbital velocity necessarily employs a multimode propulsion system. An example might include turbojet, ramjet, scramjet, and rocket modes. Each mode of propulsion when considered in its operating Mach regime can be characterized by a corresponding ε. Available models of this vehicle type exhibit large values of excess thrust at low hypersonic Mach numbers. In fact, Eq. (2.63) will produce an ε that is greater than one over such flight phases. Experience with hypersonic vehicle dynamics reported in Ref. 12 indeed suggests that the assumed time scale separation is not valid in these phases. However, as will be seen in the next section, over most of the trajectory corresponding to the reduced solution Eq. (2.63) results in an ε that is less than one, just as in the flat Earth, subsonic-supersonic case.

16

2.4 Numerical Validation

It was shown in the preceding sections that for aircraft energy climbs that take place in a vertical plane, the singular perturbation parameter ε can logically be identified as the maximum longitudinal load factor of the vehicle, measured in units of sea-level g's. In order to further explore the implications of this result, numerical evaluations of ε will be presented in this section for several types of vehicles. As stated earlier, it will be assumed that the required change in specific energy is sufficiently large to permit the boundary layer responses in altitude and flight path angle to reach their equilibrium values.

For a given aircraft, it may be sufficient to evaluate a single upper bound for ε, valid for the entire envelope, in order to provide a hint regarding possible two-time-scale behavior. If the resulting value of this upper bound is sufficiently less than one, and if the boundary conditions are appropriate, then two-time-scale behavior is implied for any energy climb that the aircraft is allowed to perform. If however the resulting value of the upper bound turns out to be greater than one, then no conclusion can be drawn. The way to proceed in the latter case would be to evaluate a less conservative (smaller) upper bound for ε and apply the same reasoning. Unfortunately, the less conservative the upper bound, the more computation one has to perform in order to evaluate it. In particular, ε in Eq. (2.30) or Eq. (2.63) can be evaluated as a function of energy E, using all the assumptions made in the evaluation of reduced solutions in aircraft energy climbs ($\gamma=0$, L=mg etc.). By evaluating in this sense, and at each energy level the absolute maximum value of the longitudinal load factor one obtains a curve C on the ε-E plane. The interesting properties of this curve are that for a given aircraft it need only be constructed *once* and that it lies above any other curve that may be evaluated similarly, but along the actual reduced solution corresponding to the specific problem of interest. In other words, points on curve C represent upper bounds for ε at the *corresponding* energy levels. The portions therefore of curve C where ε is sufficiently less than one immediately show the energy levels where two-time-scale behavior (boundary-layer transitions along constant E) can be expected. If there are any portions of curve C where ε is greater than one, then no conclusions can be drawn as to the possible two-time-scale behavior at the corresponding energy levels. In the latter case one has again to evaluate a still less conservative upper bound for ε at these energy levels. Such less and less conservative upper bounds would of course eventually lead to the maximum value of the longitudinal load factor evaluated as a function of E along the reduced solution corresponding to a specific problem.

If one is interested in the possible two-time-scale behavior of a vehicle along a particular trajectory (corresponding to a specific problem) then, the *least* conservative upper bound for ε would be the maximum longitudinal load factor encountered along that (exact) trajectory. Such a test for time-scale separability would require computation of the (exact) trajectory first and would not be very helpful. Hence, it makes much more sense to start with a more conservative (greater) upper bound and to proceed with less and less conservative upper bounds.

Numerical evaluations of ε are presented in Figs. 2.1 through 2.8 for four types of vehicles. For each type there is a plot showing the variation of the maximum longitudinal load factor of the vehicle with energy E, and one or more plots showing the variation of the longitudinal load factor with E along the reduced solution corresponding to a specific optimization problem. The odd-numbered figures are the energy-climb figures for the four vehicles. They distort the fact that the altitude profiles contain jumps, because they only needed to be constructed roughly, since they only served for the evaluation of ε as a function of the energy E, given in the even-numbered figures.

Figs. 2.1 and 2.2 show the results for an F-8 fighter[13]. The two optimization problems considered for this case were minimum time to a specified energy and minimum time to a specified downrange position. The reduced solutions corresponding to these problems are obtained by maximizing (with respect to V) at each energy level the quantities (T-D)V for the former and $[(T-D)V]/(V_0-V)$ for the latter. In this case V_0 is the maximum possible cruising speed of the aircraft and D is calculated at L=mg. Fig. 2.1 shows the actual paths in the envelope corresponding to these reduced solutions and to the maximum longitudinal load factor of F-8. Fig. 2.2 shows the results for ε evaluated along these climb paths. Since the maximum longitudinal load factor of F-8 remains below 1.0 in Fig. 2.2, it is reasonable to assume that for any optimization problem, if the required energy gain is sufficient, the transitions to the reduced solution will take place at nearly constant E, exhibiting the well known boundary layer structure.

Figs. 2.3 and 2.4 show similar results for an F-15 fighter[14]. Again, the problems of minimum time to a specified energy and minimum time to a specified downrange position were considered. A maximum dynamic pressure constraint of 1500 lbf per square feet is imposed on the climb paths in each case. Due to the large thrust to weight ratio of F-15, the ε levels in Fig. 2.4 are much higher than those of F-8 (i.e. in comparison with Fig. 2.2). In particular, there is a small region at low energy where ε exceeds one, implying that time-scale separation at these energy levels may not be appropriate for these problems.

Figs. 2.5 and 2.6 show the results for a conventional transport[15]. In this case, however, the two optimization problems considered were minimum fuel to a specified energy and minimum fuel to a specified downrange position. The reduced solutions corresponding to these problems are obtained by maximizing (with respect to V and η) at each energy level the quantities $[(T-D)V]/f$ for the former and $[(T-D)V]/(fV_0-f_0V)$ for the latter. Here V_0 represents the most fuel efficient cruising speed of the aircraft and f_0 is the fuel consumption rate at this cruising flight condition[7]. The magnitude of ε in Fig. 2.6 remains small in comparison to that in Figs. 2.2 and 2.4. Two-time-scale behavior for the entire transport aircraft envelope is therefore suggested.

Finally, Figs. 2.7 and 2.8 show the results for a hypersonic vehicle model, used by NASA and termed the "Langley Accelerator"[16]. The only optimization problem considered in this case was minimum fuel to a specified energy, the reduced solution corresponding to which is obtained by maximizing the quantity $[(\eta T-D)V]/(mf)$ at each energy level (mass is not constant in this case). A maximum dynamic pressure constraint of 2000 lbf per square feet is imposed on the climb paths for this case. This particular vehicle model employs a multimode propulsion system, sized for acceleration to orbital velocity, and consisting of turbojet, ramjet, scramjet, and rocket modes. Optimal switching between propulsion modes was not included in the generation of Figs. 2.7 and 2.8. Instead, within allowable Mach regimes the cycle that maximizes $[(\eta T-D)V]/(mf)$ and $(\eta T-D)/m$ was selected. The points of cycle transitions are shown in the figures. In Fig. 2.8, ε is plotted against the speeds at which the constant energy contours intersect the zero altitude axis. The reason for this is that E is negative in this case so that its size is no longer intuitively obvious. Thus, sea-level speed was used as the abscissa, because at hypersonic speeds practically all the energy of the vehicle corresponds to kinetic energy. The calculated value of ε will likely be reduced if a practical method for cycle transition is employed. Note that as the energy increases the boundary of the envelope is approached and ε goes to zero. This is a basic characteristic of all aircraft (see also Figs. 2.2, 2.4, and 2.6), suggesting that transitions to the reduced solution can be treated as boundary layers with relatively greater success at higher energy levels. The physical explanation for this rests on understanding the behavior of the difference between thrust and drag. At low energy levels both the speed and altitude are low, resulting in high thrust and low drag, so that the difference between thrust and drag is high. This large amount of excess power can be used to effect a change in energy even during a transition. However, at higher energy levels, either speed or altitude or both are high, and the corresponding difference between thrust and drag is low. Thus,

19

transitions to the reduced solution at higher energy levels occur for the most part by interchanging kinetic for potential energy (or vice versa), with the total energy remaining more nearly constant. The expression found for ε (see Eqs. (2.30) and (2.63)) captures and quantifies this effect in a straightforward manner.

2.5 Conclusions

A systematic procedure has been introduced to identify a singular perturbation parameter in the differential equations of motion for both the conventional (subsonic-supersonic, flat Earth) and the transatmospheric (hypersonic, spherical Earth) flight regimes. The procedure uses a set of arbitrary scaling constants to nondimensionalize all the variables of interest. Nondimensionalization alone is not sufficient to clearly identify if a system will exhibit two-time-scale behavior. However, there is a useful choice of the scaling constants that leads to the conclusion that two-time-scale behavior can be expected when the maximum longitudinal load factor is sufficiently less than one. The important point here is that this statement is valid independent of the performance index that is being optimized.

This explains the past successes in singular perturbation treatments of aircraft energy climbs, despite an inability to explicitly identify a perturbation parameter. These observations also apply to the family of future hypersonic vehicles. If such a vehicle is employed as a passenger transport, its acceleration will necessarily be constrained in the interest of human comfort. To constrain the maximum longitudinal load factor of such a vehicle to be sufficiently less than one would imply two-time-scale behavior for any type of energy climb that such a vehicle would be allowed to perform.

20

CHAPTER III

State-Constrained Energy-State Modeling

3.1 Introduction

State-variable inequality constraints are commonly encountered in the study of dynamic systems. The study of rigid body aircraft dynamics and control is certainly no exception. For instance, a maximum allowable value of dynamic pressure is usually prescribed for aircraft with supersonic capability. This limit is required to ensure that the vehicle's structural integrity is maintained. Given a typical state-space description of the vehicle dynamics, this limit constitutes an inequality constraint on the vehicle state. Such dynamic pressure bounds are commonly encountered during fuel-optimal climb for supersonic transports[19], for rocket powered launch vehicles such as the U.S. space shuttle[20], and for single-stage-to-orbit air-breathing launch vehicles[21].

State-variable inequality constraints have been studied extensively by researchers in the field of optimal control. First-order necessary conditions for optimality when general functions of the state are constrained have been obtained[22-24]. However, the direct construction of solutions via this set of conditions proves difficult. Moreover, the controllers derived from such traditional formulations of the problem suffer from serious practical flaws. They typically tend to track the hypersurface representing a state-constraint boundary in a finite time, which makes the traditional asymptotic boundary layer theory non-applicable (see below), and they break down whenever a disturbance causes the system to violate an active state-constraint. Accordingly, most practitioners seeking an open-loop control solution rely on direct approaches to optimization that employ penalty functions for satisfaction of state-variable inequality constraints[25]. As a rule however, algorithms employing such methods are computationally intense and slow to converge. Consequently, they are not well-suited for real-time implementation.

From a singular perturbations point of view[26,27], in the absence of a state-variable inequality constraint (i.e. when no constraint is active), the initial boundary-layer solution for the class of systems being considered is an infinite-time process. A solution is sought which asymptotically approaches the reduced solution (solution with $\varepsilon=0$). However, when

a state-constraint is active in the reduced solution, the boundary-layer problem can be of finite-time in the stretched time variable[28,29]. Thus, traditional techniques concerning the asymptotic stability of the boundary-layer system are not applicable, and cannot be used to construct an approximate boundary-layer solution. The presence of an active state-variable inequality constraint also introduces the possibility of discontinuous costate variables at the juncture between constrained and unconstrained arcs. A Valentine transformation can be used to convert the constrained problem to an equivalent unconstrained problem of increased dimension[30]. Smoothness is regained in the process, but at the expense of introducing a singular arc along the state-constraint boundary[30,31] and to little or no advantage when seeking a solution for real-time implementation.

As an alternative, this chapter proposes a complete reformulation of optimal control problems involving active state-variable inequality constraints. Since in practice it is always the asymptotic controllers that have the most desirable properties, maybe the optimization in such problems should be carried out not over the class of all controllers, but only over the class of asymptotic controllers that track a given active state-constraint boundary. It is shown in Section 3.2 that a transformation technique can be used to isolate and describe completely this class of asymptotic controllers. If a minimum over the class of all controllers exists, then the reformulated problem is guaranteed to have an infimum. The results in Section 3.3 suggest however that this infimum for the reformulated problem corresponds to a finite-time controller and is not achieved over the class of all asymptotic controllers. The situation is somewhat reminiscent of H-infinity control theory for linear systems in which one seeks a strictly proper, stabilizing controller to minimize the H-infinity norm of a closed-loop transfer function. The minimum of this norm over all strictly proper, stabilizing controllers does not exist. Its infimum, however, does exist and corresponds to a proper controller. Thus, just as in H-infinity theory, the question arises naturally in the present case as to how one can find an asymptotic controller that somehow approximates this infimum. Although there are no general answers yet, a procedure is presented in Section 3.3 that does supply one with insight at least for a simple example. The procedure leads to a controller that is approximately optimal, asymptotic, but still one-sided.

Finally, if the state-constraint is regarded as a soft constraint, then an example shows that there may exist controllers that are *asymptotic*, *two-sided*, and result in exactly the same optimal value of the performance index corresponding to the original problem, that is, they are practically *optimal*, but at the expense of violating the state-constraint. Such

22

controllers, however, do not correspond to stationary solutions of the optimization problem. Thus, at the present, a systematic procedure for finding them does not exist and remains a topic for future research. Preliminary results on the topic covered in this chapter can be found in Ref. 32.

3.2 Construction of Arbitrary Nonlinear Feedback Control Laws for a Dynamical System, that Track a Given Hypersurface

Consider the dynamical system:

$$\frac{dx}{dt} = f(x,y,u) \quad ; \qquad x(t_0) = x_0 \tag{3.1}$$

$$\frac{dy}{dt} = g(x,y,u) \quad ; \qquad y(t_0) = y_0 \tag{3.2}$$

where x, f are vectors of the same dimension, and y, g and u are scalars. It will be of interest to describe the set C of all piecewise continuous (in time) control laws $u(x(t),y(t),t)$ that track a given hypersurface in the state space of the above system, given by the scalar equation:

$$S(x,y) = 0 \tag{3.3}$$

that is, if $u=u(x,y,t)$ is a specific control law belonging to C, then the system of Eqs. (3.1), (3.2), driven by $u(x,y,t)$ for $t > t_0$ (and assuming that $S(x_0,y_0)$ is not zero) will eventually reach the hypersurface given in Eq. (3.3) and stay on it thereafter. A control law can drive the system onto the hypersurface either in finite time or asymptotically. Accordingly, the set C is the union of two disjoint sets F and A. The set F contains all control laws that track the hypersurface in finite time. The set A contains all control laws that track the hypersurface asymptotically. The purpose in this section is to give a complete description of the sets F and A.

Let Z be the set of all piecewise differentiable, scalar functions of the real variable α, defined and invertible for all α in [0,1], and satisfying the boundary conditions:

$$z(0) = 0 \quad ; \qquad z(1) = -S(x_0,y_0) \tag{3.4}$$

Assume that the range of S is contained in the range of z for all z in Z. Then, consider α as an independent variable and make the transformation from y to α:

$$z(\alpha) + S(x,y) = 0 \qquad (3.5)$$

Differentiating Eq. (3.5) with respect to time and using Eqs. (3.1) and (3.2) results in:

$$\frac{dz}{d\alpha}\frac{d\alpha}{dt} + \frac{\partial S}{\partial x}f(x,y,u) + \frac{\partial S}{\partial y}g(x,y,u) = 0 \qquad (3.6)$$

Now, let $d\alpha/dt$ play the role of a new control, β, by defining:

$$\frac{d\alpha}{dt} = \beta \qquad (3.7)$$

then, Eq. (3.6) becomes:

$$\frac{dz}{d\alpha}\beta + \frac{\partial S}{\partial x}f(x,y,u) + \frac{\partial S}{\partial y}g(x,y,u) = 0 \qquad (3.8)$$

Assume now that the hypersurface given by Eq. (3.3) is *first order* in u, that is, the total time derivative of $S(x,y)$ is explicitly dependent on u. If this is not the case, the results of this section can be generalized to the case where the hypersurface given by Eq. (3.3) is higher order in u. Also, assume that Eq. (3.5) is invertible in y, and that Eq. (3.8) is invertible in u. These assumptions result in the two equations:

$$y = h(x,z) \qquad (3.9)$$

$$u = k\left(x,z,\frac{dz}{d\alpha}\beta\right) \qquad (3.10)$$

for y and u respectively. The system of Eqs. (3.1) and (3.2) has now been transformed through Eqs. (3.5)-(3.10) to the equivalent system:

$$\frac{dx}{dt} = f\left(x,h(x,z(\alpha)),k\left(x,z(\alpha),\frac{dz}{d\alpha}\beta\right)\right) \qquad (3.11)$$

24

$$\frac{d\alpha}{dt} = \beta \qquad\qquad (3.12)$$

with initial conditions $x(t_0)=x_0$ and $\alpha(t_0)=1$.

3.2.1 Finite-Time Tracking

Theorem 3.1. For any given finite time t_f and any function $z(\alpha)$ in Z, there exists a control law $u=u(x,y,t)$ in F that drives the system of Eqs. (3.1) and (3.2) from its initial state at $t=t_0$ onto the hypersurface given by Eq. (3.3) at $t=t_f$ and keeps it on the hypersurface thereafter.

Proof 3.1. Let t_f be a finite time and $z(\alpha)$ be a function in Z. One can use $z(\alpha)$ to obtain the equivalent transformed system of Eqs. (3.11), (3.12). Then, one can use as the control β the function:

$$\beta = -\frac{1}{t_f - t_0} \qquad\qquad \text{for } t_0 < t < t_f \qquad\qquad (3.13)$$

$$\beta = 0 \qquad\qquad \text{for } t_f < t \qquad\qquad (3.14)$$

leading to the time variation for α:

$$\alpha = \frac{t_f - t}{t_f - t_0} \qquad\qquad \text{for } t_0 < t < t_f \qquad\qquad (3.15)$$

$$\alpha = 0 \qquad\qquad \text{for } t_f < t \qquad\qquad (3.16)$$

Thus, α is driven from 1 to 0, in $t_0 < t < t_f$ and stays at zero for $t_f < t$. Accordingly, due to the boundary conditions (Eq. (3.4)) on the function $z(\alpha)$, the original system of Eqs. (3.1), (3.2), is driven from its initial state at $t=t_0$ onto the hypersurface given by Eq. (3.3) in $t_0 < t < t_f$ and stays on the hypersurface for $t_f < t$. The feedback controller $u(x,y,t)$ that will perform this task for the system of Eqs. (3.1), (3.2) can be found from Eq. (3.10). β is given by Eqs. (3.13), (3.14), z is equal to $-S(x,y)$ from Eq. (3.5), and since $z(\alpha)$ is invertible on [0,1], $dz/d\alpha$ can be expressed as a function of z and therefore of $-S(x,y)$ (Q.E.D.). The procedure is best illustrated through an example.

25

Example 1

Consider the system:

$$\frac{dx}{dt} = y - u^2 \quad ; \qquad x(t_0) = x_0 \tag{3.17}$$

$$\frac{dy}{dt} = u \quad ; \qquad y(t_0) = y_0 \tag{3.18}$$

and assume that it is desired to track the straight line:

$$y - 1 = 0 \tag{3.19}$$

in a specified final time t_f. As the function $z(\alpha)$ one can select:

$$z(\alpha) = \left(\frac{1 - y_0}{\ln 2}\right)\ln(1 + \alpha) \tag{3.20}$$

Note that $z(0)=0$, and $z(1)=1-y_0$ as required by Eq. (3.4). From Eq. (3.20) one is led to the transformation:

$$\left(\frac{1 - y_0}{\ln 2}\right)\ln(1 + \alpha) + y - 1 = 0 \tag{3.21}$$

Differentiating Eq. (3.21) with respect to time, one obtains:

$$\left(\frac{1 - y_0}{\ln 2}\right)\left(\frac{\beta}{1 + \alpha}\right) + u = 0 \tag{3.22}$$

resulting in the transformed system:

$$\frac{dx}{dt} = 1 - \left(\frac{1 - y_0}{\ln 2}\right)\ln(1 + \alpha) - \left[\left(\frac{1 - y_0}{\ln 2}\right)\left(\frac{\beta}{1 + \alpha}\right)\right]^2 \tag{3.23}$$

$$\frac{d\alpha}{dt} = \beta \tag{3.24}$$

with initial conditions $x(t_0)=x_0$ and $\alpha(t_0)=1$. Now, if one uses the control β given in Eq. (3.13), then, from Eq. (3.22) one obtains:

26

$$u = \frac{1-y_0}{\ln 2 (t_f - t_0)} \exp\left\{-\ln 2\left(\frac{1-y}{1-y_0}\right)\right\} \tag{3.25}$$

This open-loop control can be shown to drive the system of Eqs. (3.17), (3.18) from its original state at $t=t_0$ onto the line y=1 at $t=t_f$. To obtain a closed-loop (feedback) controller one simply replaces y_0 by y and t_0 by t in Eq. (3.25) to obtain:

$$u = \frac{1-y}{\ln 4 (t_f - t)} \tag{3.26}$$

which again drives the system to y=1 at $t=t_f$.

Theorem 3.2. Let u=u(x,y,t) be any control law in F that drives the system of Eqs. (3.1), (3.2) from its initial state at $t=t_0$ onto the hypersurface Eq. (3.3) at $t=t_f$ and keeps it on the hypersurface thereafter. Then, there exists a function z(α) in Z, such that, when the system of Eqs. (3.1), (3.2) is transformed using z(α) to the system given by Eqs. (3.11), (3.12), the control β for the transformed system corresponding to u(x,y,t) is given by Eqs. (3.13), (3.14).

Proof 3.2. The function z(α) for $0 < \alpha < 1$ is found by solving the system of differential equations:

$$\frac{dx}{d\alpha} = -(t_f - t_0)f(x,y,u(x,y,t)) \tag{3.27}$$

$$-\left(\frac{1}{t_f - t_0}\right)\left(\frac{dz}{d\alpha}\right) = \frac{\partial S}{\partial x} f(x,y,u(x,y,t)) + \frac{\partial S}{\partial y} g(x,y,u(x,y,t)) \tag{3.28}$$

subject to the boundary conditions:

$$x(\alpha = 1) = x_0 \quad ; \qquad z(\alpha = 1) = -S(x_0, y_0) \tag{3.29}$$

where y in Eqs. (3.27), (3.28) is a function of x and z through Eq. (3.9) and t in u(x,y,t) is a function of α through Eq. (3.15), that is,

$$t = t_f - \alpha(t_f - t_0) \tag{3.30}$$

Note that the function $z(\alpha)$ found from the solution of Eqs. (3.27) through (3.29) satisfies Eq. (3.5) for all $t > t_0$ (α and t are related by Eq. (3.15)). Thus, it also satisfies the boundary condition $z(0)=0$, since at $t = t_f$, α and $S(x,y)$ are both equal to zero (Q.E.D.).

Theorems 3.1 and 3.2 indicate that once the control β for the transformed system of Eqs. (3.11), (3.12) is fixed as in Eqs. (3.13), (3.14), there is a complete correspondence between functions in Z and piecewise continuous control laws $u(x,y,t)$ in F that track the hypersurface given by Eq. (3.3) in a finite time t_f. That is, for every element of Z there exists an element of F and, more importantly, for every element of F there exists an element of Z. The correspondence therefore established between F and Z through the selection of β as in Eqs. (3.13), (3.14) is *onto*.

3.2.2 Asymptotic Tracking

Theorem 3.3. For any function $z(\alpha)$ in Z, there exists a control law $u=u(x,y,t)$ in A that drives the system of Eqs. (3.1), (3.2) from its initial state at $t=t_0$ onto the hypersurface given by Eq. (3.3) asymptotically.

Proof 3.3. Let $z(\alpha)$ be a function in Z. One can use $z(\alpha)$ to obtain the equivalent transformed system of Eqs. (3.11), (3.12). Then, using the control β given by:

$$\beta = -\alpha \tag{3.31}$$

leads to the exponential time variation for α:

$$\alpha = e^{-t} \tag{3.32}$$

Thus, α is driven exponentially from 1 to 0. Accordingly, due to the boundary conditions (Eq. (3.4)) on the function $z(\alpha)$, the original system of Eqs. (3.1), (3.2), is driven asymptotically from its initial state at $t=t_0$ onto the hypersurface given by Eq. (3.3). The feedback controller $u(x,y,t)$ that will perform this task for the system of Eqs. (3.1), (3.2) can be found from Eq. (3.10). β is given by Eq. (3.31), z is equal to $-S(x,y)$ from Eq. (3.5) and since $z(\alpha)$ is invertible on [0,1], $dz/d\alpha$ can be expressed as a function of z and therefore of $-S(x,y)$ (Q.E.D.). Again, the procedure can best be illustrated through an example.

Example 2

Consider again the system:

$$\frac{dx}{dt} = y - u^2 \quad ; \qquad x(t_0) = x_0 \tag{3.33}$$

$$\frac{dy}{dt} = u \quad ; \qquad y(t_0) = y_0 \tag{3.34}$$

and assume that one wishes to track asymptotically the straight line:

$$y - 1 = 0 \tag{3.35}$$

As the function $z(\alpha)$ one can again select:

$$z(\alpha) = \left(\frac{1 - y_0}{\ln 2}\right) \ln(1 + \alpha) \tag{3.36}$$

satisfying $z(0)=0$, and $z(1)=1-y_0$ as required by Eq. (3.4). From Eq. (3.36) one is led to the transformation:

$$\left(\frac{1 - y_0}{\ln 2}\right) \ln(1 + \alpha) + y - 1 = 0 \tag{3.37}$$

Differentiating Eq. (3.37) with respect to time one obtains:

$$\left(\frac{1 - y_0}{\ln 2}\right)\left(\frac{\beta}{1 + \alpha}\right) + u = 0 \tag{3.38}$$

resulting in the transformed system:

$$\frac{dx}{dt} = 1 - \left(\frac{1 - y_0}{\ln 2}\right) \ln(1 + \alpha) - \left[\left(\frac{1 - y_0}{\ln 2}\right)\left(\frac{\beta}{1 + \alpha}\right)\right]^2 \tag{3.39}$$

$$\frac{d\alpha}{dt} = \beta \tag{3.40}$$

29

with initial conditions $x(t_0)=x_0$ and $\alpha(t_0)=1$. If now one uses the control β given in Eq. (3.31), then, from Eq. (3.38) one obtains:

$$u = \frac{e^{k(1-y)} - 1}{ke^{k(1-y)}}$$

(3.41)

where k is defined as:

$$k = \frac{\ln 2}{1 - y_0}$$

(3.42)

This open loop control can be shown to drive the system of Eqs. (3.33), (3.34) from its original state at $t=t_0$ asymptotically onto the line $y=1$. To obtain a closed-loop (feedback) controller one simply replaces y_0 by y in Eq. (3.41), to obtain:

$$u = \frac{1-y}{\ln 4}$$

(3.43)

which again drives the system of Eqs. (3.33), (3.34) asymptotically toward $y=1$. Note that as expected, in the asymptotic case u does not depend explicitly on t.

Theorem 3.4. Let $u=u(x,y,t)$ be any control law that drives the system of Eqs. (3.1), (3.2) from its initial state at $t=t_0$ onto the hypersurface given by Eq. (3.3) asymptotically. Then, there exists a function $z(\alpha)$ in Z, such that, when the system of Eqs. (3.1), (3.2) is transformed using $z(\alpha)$ to the system given by Eqs. (3.11), (3.12), the control β for the transformed system corresponding to $u(x,y,t)$ is given by Eq. (3.31).

Proof 3.4. The function $z(\alpha)$ for $0 < \alpha < 1$ is found by solving the system of differential equations:

$$\alpha \frac{dx}{d\alpha} = -f\big(x,y,u(x,y,t)\big)$$

(3.44)

$$\alpha\left(\frac{dz}{d\alpha}\right) = \frac{\partial S}{\partial x}f\big(x,y,u(x,y,t)\big) + \frac{\partial S}{\partial y}g\big(x,y,u(x,y,t)\big)$$

(3.45)

subject to the boundary conditions:

$$x(\alpha = 1) = x_0 \quad ; \qquad z(\alpha = 1) = -S\big(x_0,y_0\big)$$

(3.46)

where y in Eqs. (3.44), (3.45) is a function of x and z through Eq. (3.9), and t in u(x,y,t) is a function of α through Eq. (3.32), that is,

$$t = \ln\left(\frac{1}{\alpha}\right) \tag{3.47}$$

Note that the function $z(\alpha)$ found from the solution of Eqs. (3.44) through (3.46) satisfies Eq. (3.5) for all $t > t_0$ (α and t are related by Eq. (3.32)). Thus, it also satisfies the boundary condition $z(0)=0$, since as t approaches infinity α and $S(x,y)$ both tend to zero (Q.E.D.).

Theorems 3.3 and 3.4 indicate that once the control β for the transformed system of Eqs. (3.11), (3.12) is fixed as in Eq. (3.31), there is a complete correspondence between functions in Z and piecewise continuous control laws u(x,y,t) in A that track the hypersurface given by Eq. (3.3) asymptotically. That is, for every element of Z there exists an element of A and, more importantly, for every element of A there exists an element of Z. The correspondence therefore established between A and Z through the selection of β as in Eq. (3.31) is *onto*.

3.3 Significance for Optimal Control Problems Involving Active State-Variable Inequality Constraints

The ideas presented in Section 3.2 can be appropriately utilized in the study of optimal control problems involving active state-variable inequality constraints. A common feature of such problems is that when a portion of the optimal trajectory rides the hypersurface representing a state constraint boundary, the optimal transition to this hypersurface from an initial point that does not lie on it occurs in finite time. Consequently, the corresponding optimal feedback controllers for such problems, that can be obtained by well-known analytical or numerical methods, suffer from two flaws that tend to eliminate almost completely their practical usefulness. First, such feedback controllers are finite-time, meaning that, for two-time-scale systems traditional asymptotic boundary layer theory is not applicable. Second, if a disturbance throws the system instantaneously toward the prohibited side of the hypersurface, the feedback scheme breaks down and there is no "optimal" way of returning to the hypersurface[28].

Asymptotic controllers on the other hand, capable of tracking from both sides a hypersurface representing a state constraint boundary, presumably won't suffer from either

of the above two flaws. This observation, and the ideas presented in Section 3.2 suggest that once one knows that a portion of the optimal trajectory for a problem rides such a hypersurface, one can change one's point of view and try to optimize the system over all asymptotic controllers capable of tracking that hypersurface from both sides.

Consider therefore that one wishes to minimize the performance index:

$$J = \Phi\big(x(t_f), y(t_f)\big) + \int\limits_{t_0}^{t_f} L(x, y, u)\, dt \qquad (3.48)$$

subject to the dynamical equations:

$$\frac{dx}{dt} = f(x, y, u) \qquad (3.49)$$

$$\frac{dy}{dt} = g(x, y, u) \qquad (3.50)$$

the boundary conditions:

$$x(t_0) = x_0 \;\; ; \quad y(t_0) = y_0 \;\; ; \quad t_0 \text{ fixed} \;\; ; \quad t_f \text{ free} \qquad (3.51)$$

and the state-variable inequality constraint:

$$S(x, y) \le 0 \qquad (3.52)$$

As in Section 3.2, x, f are vectors of the same dimension, and L, S, y, g and u are scalars. Again, it will be assumed that:

$$S(x_0, y_0) < 0 \qquad (3.53)$$

and that the optimal trajectory reaches the hypersurface:

$$S(x, y) = 0 \qquad (3.54)$$

at a finite time $t=t_1$ and stays on it for $t > t_1$. Thus, in order to avoid the problems with the finite-time controllers mentioned above, one would now like to optimize J over the class of all asymptotic controllers, which has already been denoted by A, capable of tracking the hypersurface given by Eq. (3.54) from both sides.

Based on the above observations, a new way of looking into the problem can now be formulated in two steps: In the first step (Section 3.3.1) the optimization is carried out over all asymptotic controllers, but the state constraint is retained. This however would lead at best to an asymptotic controller that is approximately optimal, does not violate the state constraint, but is one-sided, that is, it breaks down on the prohibited side of the constraint boundary. Since this one-sidedness would tend to eliminate the practical usefulness of such a controller, in the second step (Section 3.3.2) the state constraint is discarded, and by means of a simple example it is shown that it is possible to find an asymptotic, two-sided controller that although (unfortunately) violates the state constraint, it results in exactly the same optimal value of the performance index, corresponding to the optimal, finite-time, one-sided controller for the original problem (that does not violate the constraint).

3.3.1 First Reformulation: Optimization over all Asymptotic, One-Sided Controllers

Let z be an arbitrary function in the set of functions Z defined in Section 3.2. The transformation reads:

$$z(\alpha) + S(x,y) = 0 \tag{3.55}$$

with the function $z(\alpha)$ subject to the boundary conditions:

$$z(0) = 0 \quad ; \quad z(1) = -S(x_0, y_0) \tag{3.56}$$

This leads as in Section 3.2 (see Eqs. (3.5) through (3.12)) to:

$$\frac{dz}{d\alpha}\beta + \frac{\partial S}{\partial x}f(x,y,u) + \frac{\partial S}{\partial y}g(x,y,u) = 0 \tag{3.57}$$

and to the transformed system:

$$y = h(x,z) \tag{3.58}$$

$$u = k\left(x, z, \frac{dz}{d\alpha}\beta\right) \tag{3.59}$$

33

$$\frac{dx}{dt} = f\left(x, h(x, z(\alpha)), k\left(x, z(\alpha), \frac{dz}{d\alpha}\beta\right)\right) \qquad (3.60)$$

$$\frac{d\alpha}{dt} = \beta \qquad (3.61)$$

with initial conditions $x(t_0) = x_0$ and $\alpha(t_0) = 1$. The performance index to be minimized assumes the form:

$$J = \Phi\left(x(t_f), h\left(x(t_f), z(\alpha(t_f))\right)\right) + \int_{t_0}^{t_f} L\left(x, h(x, z), k\left(x, z, \frac{dz}{d\alpha}\beta\right)\right) dt \qquad (3.62)$$

As seen in Section 3.2 (Theorems 3.3 and 3.4), once the control β for the transformed system of Eqs. (3.60), (3.61) is fixed at $\beta = -\alpha$, there is a complete correspondence between functions $z(\alpha)$ in Z and piecewise continuous control laws $u(x,y,t)$ in A that track the hypersurface given by Eq. (3.3) asymptotically. That is, for every element of Z there exists an element of A and, more importantly, for every element of A there exists an element of Z. Therefore, to find the "best" asymptotic controller, it is natural to fix the control β at:

$$\beta = -\alpha \qquad (3.63)$$

and to then try to determine the "best" function $z(\alpha)$ in Z that minimizes J. This leads directly to the off-line optimization problem:

Minimize: $\quad J = \Phi\left(x(0), h(x(0), 0)\right) + \int_0^1 \left(\frac{1}{\alpha}\right) L(x, h(x, z), k(x, z, -\alpha v)) d\alpha \qquad (3.64)$

subject to:

$$\frac{dx}{d\alpha} = -\left(\frac{1}{\alpha}\right) f(x, h(x, z), k(x, z, -\alpha v)) \qquad (3.65)$$

$$\frac{dz}{d\alpha} = v \qquad (3.66)$$

34

$$-z(\alpha) \leq 0 \tag{3.67}$$

and to the boundary conditions $x(1)=x_0$, $z(0)=0$, and $z(1)=-S(x_0,y_0)$. Note that the state constraint is still being retained through Eq. (3.67). This point is important, because, if Eq. (3.67) is not imposed, then the problem presumably will not have a solution. One can see from Eq. (3.64) that for every function $z(\alpha)$ in Z that satisfies Eq. (3.67) there corresponds a number $J_1(z)$. Thus, one can define the set of real numbers:

$$J = \{\ J_1(z)\colon z \text{ is in } Z, \text{ and inequality (3.67) is satisfied}\} \tag{3.68}$$

and state the off-line optimization problem, given by Eqs. (3.64) through (3.67), by asking for the minimum of J. Although it is not known at the present if and exactly when such a minimum exists, it is possible to state the following theorem that provides one with an important partial answer:

Theorem 3.5. If the original problem given by Eqs. (3.48) through (3.52), involving an active state variable inequality constraint, has a minimum, then the off-line optimization problem given by Eqs. (3.64) through (3.67) has an infimum.

Proof 4.5. Assume that the problem given by Eqs. (3.48) through (3.52) has a minimum, which will be denoted by J_{min}. This immediately implies that the set J is bounded below by J_{min}, that is, $J_{min} \leq J_1(z)$ for all z in Z. Since any set of real numbers that is bounded below has an infimum, J has an infimum (Q.E.D.).

Example 3

To illustrate the above idea one can apply it to the following problem:

$$\text{Minimize:} \qquad J = \int_0^\infty \left(1 - y + u^2\right)dt \tag{3.69}$$

subject to:

$$\frac{dy}{dt} = u \ ; \qquad y(0) = 0 \tag{3.70}$$

$$y - 1 \leq 0 \tag{3.71}$$

The solution to this problem for $0 < t < 2$ can be shown to be[28]:

$$y = -\frac{t^2}{4} + t \quad ; \qquad u = -\frac{t}{2} + 1 \tag{3.72}$$

leading to the finite-time controller:

$$u = (1 - y)^{1/2} \tag{3.73}$$

Although this controller is optimal, it is clearly useless from a practical point of view since it breaks down when y exceeds 1. It cannot be used to track the line y=1 in the presence of two-sided perturbations about y=1. At t = 2, y reaches the value y = 1. For t > 2, y and u stay constant at 1 and 0 respectively and there is no further contribution to the performance index J. In order to optimize J over all asymptotic controllers that track y = 1 and satisfy Eq. (3.71), one can now use the transformation:

$$z(\alpha) + y - 1 = 0 \tag{3.74}$$

$$z(0) = 0 \quad ; \qquad z(1) = 1 \tag{3.75}$$

which leads to:

$$\frac{dz}{d\alpha} \beta + u = 0 \tag{3.76}$$

and to the transformed optimization problem:

$$\text{Minimize:} \qquad J = \int_0^\infty \left(z(\alpha) + \left(\frac{dz}{d\alpha}\right)^2 \beta^2 \right) dt \tag{3.77}$$

subject to:

$$\frac{d\alpha}{dt} = \beta \quad ; \qquad \alpha(0) = 1 \tag{3.78}$$

$$-z(\alpha) \leq 0 \tag{3.79}$$

Using now the control:

$$\beta = -\alpha \tag{3.80}$$

leads to the off-line optimization problem for the function $z(\alpha)$:

$$\text{Minimize:} \quad J_1 = \int_0^1 \left(\frac{z}{\alpha} + \alpha v^2 \right) d\alpha \tag{3.81}$$

subject to:

$$\frac{dz}{d\alpha} = v \quad ; \quad z(0) = 0 \quad ; \quad z(1) = 1 \tag{3.82}$$

$$-z(\alpha) \le 0 \tag{3.83}$$

The Hamiltonian associated with this problem is:

$$H = \frac{z}{\alpha} + \alpha v^2 + \lambda v - \eta z \tag{3.84}$$

where η is a Lagrange multiplier. This results in the optimality condition for v:

$$v = -\frac{\lambda}{2\alpha} \tag{3.85}$$

and in the costate equation for λ:

$$\frac{d\lambda}{d\alpha} = -\frac{1}{\alpha} + \eta \tag{3.86}$$

The solution for λ is:

$$\lambda = \ln \left| \frac{A}{\alpha} \right| + \eta \alpha \tag{3.87}$$

where A is an integration constant. Combining Eqs. (3.85) and (3.87) with Eq. (3.82) one obtains the differential equation for z:

$$\frac{dz}{d\alpha} = -\left(\frac{1}{2\alpha} \right) \ln \left| \frac{A}{\alpha} \right| - \frac{\eta}{2} \tag{3.88}$$

37

which has the general solution:

$$z = \frac{1}{4}\left(\ln\left|\frac{A}{\alpha}\right|\right)^2 - \frac{\eta\alpha}{2} + B \tag{3.89}$$

B being a second integration constant. A quick inspection now reveals that there are no values of A, B, η, for which the function z(a) given by Eq. (3.89) can satisfy both of the boundary conditions z(0)=0, z(1)=1. Therefore, the off-line optimization problem posed by Eqs. (3.81) through (3.83) has no minimum. As guaranteed however by Theorem 4.5, this problem does have an infimum, since it is bounded below by J_{min}, where J_{min} is the minimum value of the performance index in Eq. (3.69), that is,

$$J_{min} = 2\int_0^2\left(1 + \frac{t^2}{4} - t\right)dt = \frac{4}{3} \tag{3.90}$$

In order to see what kind of controller u the function z(α) found in Eq. (3.89) implies, one can use Eqs. (3.76), (3.80), and (3.88) to find:

$$u = -\frac{1}{2}(t + \ln|A|) - \frac{\eta e^{-t}}{2} \tag{3.91}$$

For $\eta=0$, comparing with Eq. (3.72), it is seen that Eq. (3.91) implies the optimal, finite-time controller found before. Indeed, Eq. (3.91) can be shown to lead to Eq. (3.72) if the boundary conditions y(0)=0 and y(2)=1 are imposed and the equation dy/dt=u is integrated. There is no contradiction however with either Theorems 3.3 or 3.4, since there is no function z in Z corresponding to the finite-time controller u given in Eq. (3.91).

The above result implies that the minimum value of J, J_{min}= 4/3, found in Eq. (3.90) is not only a lower bound of J_1 but the actual infimum itself. This situation is somewhat reminiscent of H-infinity control theory for linear systems in which one seeks a strictly proper, stabilizing controller to minimize the H-infinity norm of a closed-loop transfer function. The minimum of this norm over all strictly proper, stabilizing controllers does not exist. Its infimum does exist, however, and corresponds to a proper controller. Thus, just as in H-infinity theory, the question arises naturally in the present case as to how one can find an asymptotic controller that somehow approximates this infimum. Although there are no general answers yet, a procedure will now be presented that does supply some insight, at least for the above example.

First, one can show using Eq. (3.88), that, for the off-line optimization problem posed by Eqs. (3.81) through (3.83), the following integral ($\eta=0$ when the trajectory does not ride the constraint):

$$\int_0^1 v^2 d\alpha = \int_0^1 \left(\frac{1}{2\alpha}\right)^2 \ln^2\left|\frac{A}{\alpha}\right| d\alpha \tag{3.92}$$

representing the "total energy" stored in the signal $v(\alpha)$, diverges. This suggests that if one imposes the isoperimetric constraint:

$$\int_0^1 v^2 d\alpha = k \tag{3.93}$$

on the off-line optimization problem posed by Eqs. (3.81) through (3.83), where k is a given, finite, strictly positive number, one may have a hope of finding a function $z(\alpha)$ in Z, that is, one that does satisfy the boundary conditions $z(0)=0$, $z(1)=1$, and the state constraint, Eq. (3.83). The Hamiltonian associated with this new problem, posed by Eqs. (3.81) through (3.83), *and* Eq. (3.93) will read:

$$H = \frac{z}{\alpha} + (\mu + \alpha)v^2 + \lambda v - \eta z \tag{3.94}$$

where μ is a constant Lagrange multiplier. For each value of k there corresponds a specific value of μ and vice versa. The corresponding optimality condition for v now becomes:

$$v = -\frac{\lambda}{2(\mu + \alpha)} \tag{3.95}$$

The costate equation for λ remains unchanged as in Eq. (3.86) and leads to the same solution for λ given in Eq. (3.87), while the differential equation for z now reads:

$$\frac{dz}{d\alpha} = -\frac{1}{2(\mu + \alpha)}\ln\left|\frac{A}{\alpha}\right| - \frac{\eta\alpha}{2(\mu + \alpha)} \tag{3.96}$$

With $\eta=0$ Eq. (3.96) leads to the solution:

$$z(\alpha) = -\frac{1}{2} \int_0^\alpha \frac{1}{(\mu + \xi)} \ln\left|\frac{A}{\xi}\right| d\xi \tag{3.97}$$

satisfying the boundary condition $z(0)=0$. The boundary condition $z(1)=1$ is satisfied by the choice of A (as a function of μ) that guarantees that:

$$1 = -\frac{1}{2} \int_0^1 \frac{1}{(\mu + \xi)} \ln\left|\frac{A}{\xi}\right| d\xi \tag{3.98}$$

Finally, the particular value of μ is evaluated from Eq. (3.93) once a value for k has been specified. The state constraint, Eq. (3.83), will still have to be satisfied, but forgetting about that for a moment, it is possible to show that, for nonzero μ, the improper integrals on the right-hand-sides of Eqs. (3.97) and (3.98) do exist. Here, a small indication will be supplied to convince the reader that this is indeed so: Consider the value of k corresponding to the value $\mu=1$. Then, the integral on the right-hand-side of Eq. (3.98) can be evaluated easily[33] and, Eq. (3.98) can be solved for A to yield:

$$\ln|A| = -\frac{(24 + \pi^2)}{12 \ln 2} \tag{3.99}$$

The corresponding asymptotic controller u can be found from Eqs. (3.76), (3.78), (3.80), (3.96), (3.99), and the fact that $\mu=1$. The result is:

$$u = \frac{e^{-t}}{2(1 + e^{-t})} \left(\frac{24 + \pi^2}{12 \ln 2} - t \right) \tag{3.100}$$

It can be shown that this controller drives y asymptotically from $y=0$ at $t=0$ to $y=1$ as t approaches infinity. This fact, however, is already guaranteed by Theorem 3.3. To construct an asymptotic *feedback* controller, one will have to use Eq. (3.100) to integrate the equation $dy/dt=u$. This will lead to an expression for y as a function of t. Elimination of t between this expression and Eq. (3.100) will lead to the desired asymptotic feedback controller. Or, alternatively, one can use the transformation defined by Eq. (3.74) with $z(\alpha)$ supplied by Eq. (3.97) and express α as a function of y. Then, using Eqs. (3.96) and

(3.76) with $\beta = -\alpha$ should result in the same asymptotic feedback controller as before. Although the procedure cannot be carried out analytically for either case, it can be carried out numerically.

It will now be shown that, if one does not impose the state constraint, Eq. (3.67), on the off-line optimization problem, Eqs. (3.64) through (3.67), then this problem may not have a minimum. Indeed, consider again Example 3, and the associated off-line optimization problem without the state constraint, that is, Eqs. (3.81) and (3.82), but not Eq. (3.83). Consider now the control:

$$u(t) = \frac{1}{\beta} \qquad\qquad \text{if } 0 < t < c \qquad\qquad (3.101)$$

$$u(t) = -(b-1)e^{-(t-c)} \qquad\qquad \text{if } c < t \qquad\qquad (3.102)$$

where b is a positive parameter that exceeds 1, and $c = b^2$. This control does violate the state constraint, Eq. (3.71), by driving y (see Eq. (3.70)) from y=0 at t=0 to y=1 as t approaches infinity according to:

$$y(t) = \frac{t}{\beta} \qquad\qquad \text{if } 0 < t < c \qquad\qquad (3.103)$$

$$y(t) = 1 + (b-1)e^{-(t-c)} \qquad\qquad \text{if } c < t \qquad\qquad (3.104)$$

The function $z(\alpha)$ corresponding to Eqs. (3.101) through (3.104) can be found from Eqs. (3.32), (3.47), and (3.74) as:

$$z(\alpha) = 1 + \frac{\ln\alpha}{b} \qquad\qquad \text{if } 0 < \ln(1/\alpha) < c \qquad\qquad (3.105)$$

$$z(\alpha) = -(b-1)e^{c}\alpha \qquad\qquad \text{if } c < \ln(1/\alpha) \qquad\qquad (3.106)$$

Substituting from Eqs. (3.101) through (3.104) into Eq. (3.69), one can evaluate the corresponding value of the performance index as a function of b, which turns out to be:

$$J = -\frac{b^3}{2} + \frac{3b^2}{2} - 2b + \frac{5}{2} \qquad\qquad (3.107)$$

41

From Eq. (3.107) it is seen that as b tends to infinity, J tends to minus infinity, meaning that the problem imposed by Eqs. (3.81) and (3.82) does not have a minimum. Note, however, that there is a value of b, for which the corresponding value of J is *the same* as the optimal value of J (see Eq. (3.90)) for the problem posed by Eqs. (3.69) through (3.71), with the state constraint included! This value of b can be found by solving the cubic polynomial equation:

$$-\frac{b^3}{2} + \frac{3b^2}{2} - 2b + \frac{5}{2} = \frac{4}{3} \tag{3.108}$$

The result is[33]:

$$b = 1 + \sqrt[3]{\frac{1}{6} + \sqrt{\frac{7}{108}}} + \sqrt[3]{\frac{1}{6} - \sqrt{\frac{7}{108}}} \tag{3.109}$$

which is approximately equal to:

$$b = 1.30497 \tag{3.110}$$

The maximum value of y is always equal to b, meaning that, if one regards the constraint given by Eq. (3.71) as a soft constraint, then one can recover the *optimal* value of J with an *asymptotic, two-sided* controller, at the expense of violating the constraint by no more than 0.30497.

3.3.2 Second Reformulation: (Optimal) Asymptotic, Two-Sided Controllers that Violate the State Constraint

The above results hint toward the formulation of the following second off-line optimization problem: One again uses the transformation defined by Eqs. (3.55), (3.56), (3.61), (3.63) and by:

$$\alpha = e^{-(t-t_0)} \quad ; \qquad d\alpha = -\alpha\, dt \tag{3.111}$$

Then, two functions Ψ and M are selected, and the following companion problem is cast:

$$\text{Minimize:} \qquad I = \Psi\big(x(0), h(x(0), 0)\big) + \int_0^1 M(x, z, v) \, d\alpha \qquad (3.112)$$

subject to the isoperimetric constraint (the original performance index now plays the role of an isoperimetric constraint):

$$\Phi\big(x(0), h(x(0), 0)\big) + \int_0^1 \left(\frac{1}{\alpha}\right) L\big(x, h(x, z), k(x, z, -\alpha v)\big) \, d\alpha = J_{min} \qquad (3.113)$$

and the dynamics:

$$\frac{dx}{d\alpha} = -\left(\frac{1}{\alpha}\right) f\big(x, h(x, z), k(x, z, -\alpha v)\big) \qquad (3.114)$$

$$\frac{dz}{d\alpha} = v \qquad (3.115)$$

$$x(1) = x_0 \quad ; \qquad z(0) = 0 \quad ; \qquad z(1) = -S(x_0, y_0) \qquad (3.116)$$

Note that there is no state-variable inequality constraint anymore! Specifically, with this second reformulation one hopes to find controllers that although will violate the given state constraint, will result in the same optimal value of the original performance index, corresponding to the problem posed by Eqs. (3.48) through (3.52), which has been denoted on the right-hand-side of Eq. (3.113) by J_{min}.

3.4 Conclusions

The class of all piecewise continuous (in time) controllers that track a given hypersurface in the state-space of a dynamical system can be split into two disjoint classes. The first class contains all controllers that track the hypersurface in finite-time. The second class contains all controllers that track the hypersurface asymptotically. This splitting of the two classes can be used to reformulate optimal control problems involving active state-

variable inequality constraints, so that, in the *reformulated* problem the optimization is carried out only over the class of asymptotic controllers.

The *original* problem leads to optimal controllers that are finite-time and one-sided. The *reformulated* problem leads to controllers that are approximately optimal, asymptotic, but still one-sided. However, if the state-constraint is regarded as a soft constraint, then one can find controllers that are *asymptotic, two-sided,* and result in the optimal value of the performance index corresponding to the *original* problem. Thus, they are practically *optimal,* but at the expense of violating the state-constraint. From a singular perturbations point of view this suggests that, such controllers can be used in a boundary-layer system, to track the reduced solution corresponding to a specific problem, when this reduced solution happens to ride a state-constraint boundary. However, such controllers do not correspond to stationary solutions of the optimization problem, so at the present, a systematic procedure for finding them does not exist and remains a topic for future research.

CHAPTER IV[*]

Spacecraft Motion under Continuous Thrust

4.1 Introduction and Motivation

Exact analytic solutions are scarce in the field of Space Mechanics, but not as scarce as in other fields. Until most recently[34-36] there have been only *three* cases in this field in which the equations governing the two-dimensional translational motion of a point mass, under the influence of inverse-square gravitational forces, and in the presence or absence of continuous thrust, have been analytically integrated or reduced to quadratures. The first case[37] pertains to Isaac Newton's celebrated solution of the two-body problem and hardly needs any comment. The corresponding motion has been called *Keplerian*, as a tribute to Johannes Kepler and his laws of planetary motion. The second case[38], which is not so well-known, corresponds to Euler's reduction to quadratures of the problem of a point mass moving on a given plane, and in the vicinity of two *fixed*, inverse-square centers of gravitational attraction. Contrary to the first case, the second case has to date largely remained just a mathematical contribution, without any practical applications resulting from it. Both of the above cases relate to the natural motion of a point mass in the absence of thrust. By contrast, the third case relates to the two-body, planar motion of a point mass, under the action of constant radial thrust. The reduction to quadratures corresponding to the third case was first given by Tsien[39], and a more detailed treatment was supplied by Battin[34]. It must be noted here that one can find, in general, many *ad hoc* thrust programs for which the equations of motion can be reduced to quadratures. However, the practical usefulness of the corresponding solutions usually tends to be minimal due to serious flaws, such as the inability to satisfy given boundary conditions, excessively large thrust levels, noneconomical fuel consumption, etc. In fact, the third case happens to be more or less just such a case, and as far as the author knows, it is the *only* such case that has received *some* attention in the literature[34]. The thrust program (constant radial thrust) used by Tsien is quite ad hoc, and accordingly there is little that can be done with it during actual orbital operations. For example, the angular momentum of a vehicle about a planet cannot be changed using radial thrust! The only problem that can be treated using Tsien's solution

[*] This Chapter and the Appendices have been *sole-authored* by Nikos Markopoulos.

45

turns out to be the problem of escape from a circular orbit. Due to the radial character of the thrust such escape usually turns out to be markedly non-optimal[39]. Tsien, being fully aware of these facts, treated also in the same paper the problem of escape from a circular orbit, using constant transverse (horizontal) thrust, and concluded by observing that the latter was much more economical than the former. The equations of motion however cannot be reduced to quadratures for the latter type of thrust.

Tsien's paper turned out to be just one among a series of papers, that appeared during the same period, in which the authors focused primarily on the problem of optimal escape from a circular orbit, and compromised in obtaining only approximate analytic solutions, but at the significant advantage of using more reasonable (and useful) thrust programs. The papers by Benney[40], who assumed tangential thrust, by Lawden[41,42], who determined the optimum thrust direction for minimizing expenditure of rocket propellant, and by Long[43], who studied the possibility of escaping along hyperbolic orbits, are among the notable ones in this series. A recent review written by Lawden[35] supplies an extensive reference list on this subject.

Lawden[41,42] found that, for all practical purposes, optimum thrust is in the flight-path direction, as assumed by Benney[40]. Such thrust will usually be referred to as "tangential" in this chapter. However, as in the solution found by Tsien[39], corresponding to constant transverse thrust, the detailed solutions for the flight path and mass loss obtained by Benney[40] and Lawden[41,42] apply only to cases of large or small thrust. Moreover, in the case of small thrust, the solutions obtained are valid only in the initial and intermediate portions of the escape trajectory. As noted by Lawden[42], the assumptions required to obtain such solutions are invalid in the final portion of the trajectory, as escape speed is approached and the instantaneous or osculating ellipse can no longer be considered close to a circle. More recently, Boltz[36], rather than considering a constant value of the tangential thrust acceleration, assumed that the ratio of the thrust to vehicle weight in orbit is fixed. His approximate analytic solution obtained with this constraint is valid for any constant value of this ratio and describes the motion along the full extent of the escape trajectory.

This chapter shows how to use the tangential thrust assumption, that apparently played a key role in many studies in the past, to propose a continuous thrust program for which the equations of two-dimensional motion of a space vehicle in orbit afford an *exact* analytic solution. To come up with this thrust program, the following important aspect of optimal control theory is utilized: Optimal control formulations are extremely useful not only because they result in control programs that are optimal, but also because they result in

control programs period! For a given problem, a control program representing the absolute optimum can usually be obtained only by solving a two-point boundary value problem by numerical methods. Sometimes however, it turns out to be advantageous to sacrifice (hopefully a small) part of optimality, by means of a reasonable approximation, for the sake of obtaining a control program that is simple enough to afford an analytical description, yet at the same time sophisticated enough to have the ability to steer the system in its state-space in a satisfactory manner. An approximation altering the state equations results in state trajectories that are approximate. An approximation on the other hand altering the costate equations affects only optimality! It results in state trajectories that are *exact*, but nearly-optimal at best!

The optimization problem that will be used to apply the above idea is one that has an analytically most convenient performance index. The problem of minimum-fuel, power-limited transfers between two coplanar (Keplerian) conics comes with a quadratic performance index in the control (thrust acceleration) and has proven in the past to be amenable to analytical treatment. For transfers between arbitrary elliptical orbits this problem has been traditionally attacked using the so-called averaging method[44-51], which is based on the assumption, that, when the duration of transfer is long enough the orbital elements are slowly changing, so that, over any given revolution around a planet their changes can be computed using rates of change averaged over the mean anomaly. This averaging solution provides many useful insights when both the initial and final conics are ellipses of low eccentricity, but, as its underlying assumption implies, its accuracy decreases as the eccentricities of the elliptical orbits increase (and the motion around the planet becomes highly nonuniform with time), and it breaks down when the vehicle does not revolve around the planet, that is, when either the initial, or final conics, or both are hyperbolic. Also, the averaging eliminates any information about the dependence of the solution on the true anomaly. A different approach is clearly needed if one is to improve on the accuracy of the averaging method, and to also account for the cases in which either one or both of the initial/final conics are hyperbolic. Numerical optimizations[44,45,47,49-51] for such problems tend to suggest that there exists a large subclass of power-limited transfers between two coplanar elliptic orbits, corresponding mainly to cases where the changes in orientation and eccentricity are small, for which, as the transfer duration increases, the thrust levels decrease, and the direction of the optimal thrust acceleration tends to coincide more and more with the direction of the tangent to the optimal flight path throughout the transfer. This last observation once again suggests that tangential thrust is the rule rather

than the exception in spaceflight. Although there *exist* cases in which the thrust is markedly nontangential, it seems that such cases arise primarily from a requirement to satisfy given boundary conditions in a prescribed time duration, and only secondarily from optimality.

With this last remark, one can embark on the analysis. The solution of any problem starts *before* its formulation, so, first, in Section 4.2, the relevant equations of motion are written in a *new* state-space format, for which the right-hand-sides of the equations assume quite a simple form, free of highly nonlinear trigonometric or transcendental functions. The proposed thrust program is introduced in Section 4.3, and the corresponding exact analytic solution of the equations of motion is then immediately supplied in Section 4.4. An important quadrature is performed in detail in Section 4.5 taking advantage of the fact that the trajectory equation that was obtained in Section 4.4 is identical in form to the trajectory equation corresponding to Keplerian motion. The fact that the thrust program proposed in Section 4.3 is not ad hoc is documented in Section 4.6, where it is shown that one can obtain this thrust program by using the tangential thrust assumption in *one* costate equation corresponding to the problem of power-limited optimization. This problem of power-limited optimization is formulated in Section 4.6.1, after which the consequences of the tangential thrust assumption are followed in Section 4.6.2. The corresponding transversality conditions are derived from scratch in Section 4.6.3, and they are combined with the tangential thrust assumption in Section 4.6.4. All this leads to the thrust program proposed in Section 4.3, for which the state equations can be solved analytically and exactly, leading to the solution supplied in Section 4.4. Section 4.6 concludes with a preliminary check of the near-optimality of the tangential thrust assumption (in 4.6.5). Section 4.7 casts the boundary conditions in a ready-to-use form. These boundary conditions are manipulated further in the next three sections during the treatment of general transfer and escape problems. Examples are also given in Sections 4.8, 4.9, and 4.10 corresponding to specific transfer and escape problems, in which the existence of particular solutions for such problems is demonstrated for several cases. The existence of one-segment solutions, that is, solutions on which the throttling parameter A (see Nomenclature) has a single value is discussed in Section 4.11, along with some geometric facts pertaining to (one-segment) transfer trajectories. Section 4.12 documents the practically important fact that, using multiple segments, a given coplanar transfer can in principle be performed in an arbitrarily large preassigned duration. Questions about the optimality of the transfer trajectories, both from the point of view of power-limited and constant ejection velocity propulsion systems are discussed in Section 4.13. Section 4.14

constitutes a short deviation from the main subject and supplies a (hopefully reasonable) prediction for the initial values of the costates for the associated rendezvous problem pertaining to power-limited optimization. After a brief summary in Section 4.15, the chapter concludes with some comments in Section 4.16. Preliminary results on the topic presented in this chapter and the Appendices have been published in Ref. 52 (See also Ref. 53).

4.2 Equations of Motion

Written in polar coordinates, the equations of two-dimensional motion for a space vehicle, viewed as a point mass, and moving in the vicinity of an inverse-square gravitational center of attraction (a planet, the sun, etc.) are:

$$\left(\frac{d^2R}{dt^2}\right) - R\left(\frac{d\theta}{dt}\right)^2 = -\left(\frac{\mu}{R^2}\right) + E_R \tag{4.1}$$

$$\frac{d}{dt}\left[R^2\left(\frac{d\theta}{dt}\right)\right] = RE_\theta \tag{4.2}$$

where, R and θ specify the position of the vehicle (see Fig. 4.1), t is the real time, μ is the strength of the inverse-square center, and E_R and E_θ are respectively the sums of the radial (vertical) and transverse (horizontal) components per unit mass of any non-gravitational forces acting on the vehicle. For the purposes of the present work, the only non-gravitational force acting on the vehicle will be the thrust, specified by its components (controls) per unit mass E_R and E_θ.

The goal now is to cast Eqs. (4.1) and (4.2) into a simple state-space form. It turns out to be advantageous for this purpose to define the relevant state variables in such a way that the resulting state equations do not contain any (highly nonlinear) transcendental functions and can be written only in terms of rational functions of the state variables. Although there are many ways of accomplishing this, one simple way is to introduce the angular momentum per unit mass of the vehicle, M, and the vertical component of its velocity X, defined by:

$$M = R^2\left(\frac{d\theta}{dt}\right) \quad ; \quad X = \frac{dR}{dt} \tag{4.3}$$

and use M, X, R, and θ as the governing state variables.

49

It would also be convenient to have the state equations in nondimensional form, so, for this purpose, one can select an arbitrary distance R_s and denote the gravitational acceleration and circular orbital velocity at that distance by g_s and V_s, that is:

$$g_s = \frac{\mu}{R_s^2} \quad ; \quad V_s = \sqrt{g_s R_s} \tag{4.4}$$

By defining now the nondimensional variables:

$$\tau = t\sqrt{\frac{g_s}{R_s}} \quad ; \quad \varepsilon_r = \frac{E_R}{g_s} \quad ; \quad \varepsilon_\theta = \frac{E_\theta}{g_s} \quad ; \quad r = \frac{R}{R_s} \quad ; \quad x = \frac{X}{V_s} \quad ; \quad h = \frac{M}{R_s V_s} \tag{4.5}$$

and using h, x, r, and θ as the new (nondimensional) state variables, one can write Eqs. (4.1) and (4.2) in the following equivalent nondimensional state-space form (see Fig. 4.1):

$$\frac{dh}{d\tau} = r\varepsilon_\theta \tag{4.6}$$

$$\frac{dx}{d\tau} = \left(\frac{h^2 - r}{r^3}\right) + \varepsilon_r \tag{4.7}$$

$$\frac{dr}{d\tau} = x \tag{4.8}$$

$$\frac{d\theta}{d\tau} = \frac{h}{r^2} \tag{4.9}$$

4.3 The Proposed Thrust Program

Consider the thrust (acceleration) program given explicitly by the components:

$$\varepsilon_r = \frac{Ax}{h} \quad ; \quad \varepsilon_\theta = \frac{A}{r} \tag{4.10}$$

where A is an arbitrary constant that will be called the *throttling parameter*. It is straightforward to show that the thrust acceleration corresponding to this program has

magnitude equal to A/(rcosγ) and acts always tangentially to the vehicle's path. Equation (4.10) therefore implies a *special type* of tangential thrust. Also, it is clear that the mechanical energy per unit mass of the vehicle (considered as a point mass) is a strictly increasing function of time for A > 0 and a strictly decreasing function of time for A < 0. When A = 0 there is *no* thrust and the motion is *Keplerian* (see Appendix A). It will be shown in the next section, that Eqs. (4.6) through (4.9) afford an *exact analytic* solution when their right-hand-sides are forced with the thrust (acceleration) components given in Eq. (4.10). This chapter shows how one can come up with this thrust program and use the corresponding exact analytic solution to satisfy boundary conditions for problems of practical interest.

4.4 An Exact Analytic Solution

Substituting the thrust acceleration components proposed in Eq. (4.10) into the right-hand-sides of Eqs. (4.6), (4.7), the state equations assume the form:

$$\frac{dh}{d\tau} = A \tag{4.11}$$

$$\frac{dx}{d\tau} = \left(\frac{h^2 - r}{r^3}\right) + \frac{Ax}{h} \tag{4.12}$$

$$\frac{dr}{d\tau} = x \tag{4.13}$$

$$\frac{d\theta}{d\tau} = \frac{h}{r^2} \tag{4.14}$$

The *exact analytic* solution of the system of Eqs. (4.11) through (4.14) is derived in Appendix B. One can verify easily by direct differentiation that this exact analytic solution is given by the following four quadratures:

$$h = A\tau + h_0 \tag{4.15}$$

51

$$x = \frac{2rA + B\sin(\theta - C)}{h} \tag{4.16}$$

$$r = \frac{h^2}{1 + B\cos(\theta - C)} \tag{4.17}$$

$$\frac{1}{h^2} = \frac{1}{h_0^2} - \int_{\theta_0}^{\theta} \frac{2Ad\theta}{[1 + B\cos(\theta - C)]^2} \tag{4.18}$$

where h_0, B, C, and θ_0 are the four (exact) constants of integration associated with the system of Eqs. (4.11) through (4.14). The procedure carried out in Appendix B also implies the uniqueness of the expressions given in Eqs. (4.15) through (4.18), that is, that every particular solution of the system of Eqs. (4.11) through (4.14) corresponds to a particular set of values for the constants h_0, B, C, and θ_0. Note that the constants h_0 and θ_0 are equal respectively to the initial values (at $\tau=0$) of the angular momentum h, and the argument of latitude θ. Note also that Eq. (4.18) is obtained by combining Eqs. (4.11), (4.14) and using Eq. (4.17) to substitute for r, which leads to (the throttling parameter A is always assumed nonzero):

$$\frac{d\theta}{dh} = \frac{[1 + B\cos(\theta - C)]^2}{Ah^3} \tag{4.19}$$

Equation (4.17), describing the trajectory of the vehicle, is identical in form with the trajectory equation corresponding to two-body Keplerian motion (see Appendix A). Thus, the trajectory equation corresponding to Keplerian motion can be uncovered in the presence of continuous, nonzero thrust!

There is of course an important difference between the two kinds of motion. Keplerian motion takes place in the absence of thrust, and along it the angular momentum h is just a constant. On the other hand, the motion described by Eqs. (4.15) through (4.18) takes place in the presence of continuous tangential thrust (as specified in Eq. (4.10)), and along it h is a linear function of time (see Eq. (4.15)).

Based on the above observation, the explicit integration of Eq. (4.18), that depends strongly on the value of the constant B, will be performed in some detail in the next section by generalizing the concepts of eccentric and hyperbolic anomalies encountered in Keplerian motion. The trajectory described by Eqs. (4.15) through (4.18) will from now on be called the *transfer trajectory*, or just the *transfer*.

4.5 Generalized Eccentric and Hyperbolic Anomalies

4.5.1 Preliminaries

Recall the expression for r given in Eq. (4.17) and denote θ - C by ξ:

$$\xi = \theta - C \tag{4.20}$$

Then, Eq. (4.17) can be written as:

$$r = \frac{h^2}{1 + B\cos\xi} \tag{4.21}$$

The angular momentum h appearing in Eq. (4.21) is the linear function of time given by Eq. (4.15). In order to find the relationship between the time τ and the argument of latitude θ along the transfer trajectory one must integrate equation (4.14). In this case however, since h is a linear function of time, and since the interest is on motion with nonzero A, it is more convenient to find the relationship between h and θ. Then, the relationship between τ and θ can be deduced. Thus, combining the equations:

$$\frac{d\theta}{d\tau} = \frac{h}{r^2} \quad ; \quad \frac{dh}{d\tau} = A \tag{4.22}$$

and using:

$$d\xi = d\theta \quad ; \quad \xi_0 = \theta_0 - C \tag{4.23}$$

one finds after substituting from Eqs. (4.21):

$$\frac{1}{h^2} = \frac{1}{h_0^2} - \int_{\xi_0}^{\xi} \frac{2A\,d\xi}{(1 + B\cos\xi)^2} \tag{4.24}$$

53

The constants B and C appearing in Eq. (4.17) play qualitatively the same role as the eccentricity and orientation constants e and ω do in Keplerian motion[34] (see Appendix A). The vehicle, while on the transfer trajectory, can execute full revolutions around a planet only if B is less than one. B can always be taken as nonnegative by appropriately adjusting the constant C (just as e can always be taken as nonnegative by appropriately adjusting the orientation ω of a conic). Note that escape from a given orbit can be accomplished for *any* value of B, since the angular momentum h, and accordingly the radial distance r can be made to grow without bound if the thrust is kept "on" for a sufficient duration of time.

Based on the above observations, one can call the constants B and C the *generalized eccentricity* and the *generalized orientation* of the transfer trajectory respectively. The constants B and C are *global* characteristics of the transfer trajectory, that is, they are associated with *every* point of the transfer trajectory. If at any point along the transfer the thrust is suddenly reduced to zero, the eccentricity e and orientation ω of the ensuing Keplerian motion are *not* equal to B and C respectively. This follows by equating the expressions for x and r of Eqs. (4.16), (4.17) with the corresponding expressions for x and r of Eq. (A.5) (of Appendix A), valid for Keplerian motion, and by remembering that the throttling parameter A is *nonzero*. Note however, that, for small A, the (Non-Keplerian) constants B and C are *approximately* equal to the (instantaneous Keplerian) constants e and ω.

Carrying the above analogy further facilitates the evaluation of the integral appearing in Eq. (4.24). Traditionally, the corresponding integral for Keplerian motion is evaluated by defining the so-called eccentric and hyperbolic anomalies[34], depending on whether the eccentricity e is less than or greater than one respectively. By analogy, it is possible to evaluate the integral in Eq. (4.24) by defining *generalized* eccentric and hyperbolic anomalies, depending on whether B is less than or greater than one. In the borderline cases in which B=0, or B=1 the evaluation of the integral simply yields[33]:

if B=0, then:
$$\frac{1}{h^2} = \frac{1}{h_0^2} - 2A(\theta - \theta_0) \tag{4.25}$$

if B=1, then:
$$\frac{1}{h^2} = \frac{1}{h_0^2} - A\left[\tan\left(\frac{\xi}{2}\right) - \tan\left(\frac{\xi_0}{2}\right)\right] - \left(\frac{A}{3}\right)\left[\tan^3\left(\frac{\xi}{2}\right) - \tan^3\left(\frac{\xi_0}{2}\right)\right] \tag{4.26}$$

Such borderline cases represent only mathematical but not "real" possibilities, and it is only for reasons of mathematical completeness that one considers them at all. In practice,

when a vehicle is executing an actual transfer, or coasting along a conic, the probability that e or B is exactly equal to any particular value is practically zero. Borderline cases can therefore also be considered as limiting cases, in which the results are first worked out in general (for e or B less than or greater than one) and then the limit is taken in which e or B tends to zero, one etc.

4.5.2 Generalized Eccentric Anomaly

Consider first those transfer trajectories on which $0 < B < 1$. For all these trajectories one can define the *generalized eccentric anomaly* E by:

$$\cos\xi = \frac{\cos E - B}{1 - B\cos E} \quad ; \quad d\xi = \frac{\sqrt{1-B^2}}{1-B\cos E}\,dE \tag{4.27}$$

The expression on the right in Eq. (4.27) relates the differentials $d\xi$ and dE. One can make the convention that E is zero when ξ is zero and vice versa. Then, E goes through π radians exactly when ξ goes through π radians. This means that one can keep track of the number of times a vehicle revolves around a planet (during a given transfer) by just keeping track of E and forgetting about ξ (or θ). Using standard trigonometric identities[33] one can show that:

$$\sin\xi = \frac{\sqrt{1-B^2}\sin E}{1-B\cos E} \quad ; \quad \tan\left(\frac{\xi}{2}\right) = \sqrt{\frac{1+B}{1-B}}\tan\left(\frac{E}{2}\right) \tag{4.28}$$

Also, using Eq. (4.27) one can write the transfer trajectory equation (4.17) as:

$$r = \left(\frac{h^2}{1-B^2}\right)(1 - B\cos E) \tag{4.29}$$

The inverse of expressions in Eqs. (4.27) and (4.28) can be found as:

$$\cos E = \frac{\cos\xi + B}{1 + B\cos\xi} \quad ; \quad dE = \frac{\sqrt{1-B^2}}{1+B\cos\xi}\,d\xi \tag{4.30}$$

$$\sin E = \frac{\sqrt{1-B^2}\sin\xi}{1+B\cos\xi} \quad ; \quad \tan\left(\frac{E}{2}\right) = \sqrt{\frac{1-B}{1+B}}\tan\left(\frac{\xi}{2}\right) \tag{4.31}$$

while the initial and final values of E, E_0 and E_f, are given by:

$$\cos E_0 = \frac{\cos\xi_0 + B}{1+B\cos\xi_0} \quad ; \quad \cos E_f = \frac{\cos\xi_f + B}{1+B\cos\xi_f} \tag{4.32}$$

Eq. (4.24) can then be written as:

$$\frac{1}{h^2} = \frac{1}{h_0^2} - \frac{2A}{\left(1-B^2\right)^{3/2}} \int_{E_0}^{E} (1-B\cos E)dE \tag{4.33}$$

which after a straightforward integration results in:

$$\frac{1}{h^2} = \frac{1}{h_0^2} - \frac{2A\left[E - E_0 - B(\sin E - \sin E_0)\right]}{\left(1-B^2\right)^{3/2}} \tag{4.34}$$

4.5.3 Generalized Hyperbolic Anomaly

For transfer trajectories on which B > 1 one can define the *generalized hyperbolic anomaly* H by:

$$\cos\xi = \frac{B - \cosh H}{B\cosh H - 1} \quad ; \quad d\xi = \frac{\sqrt{B^2 - 1}}{B\cosh H - 1}dH \tag{4.35}$$

The expression on the right in Eq. (4.35) relates the differentials $d\xi$ and dH. One can again make the convention that H is zero when ξ is zero and vice versa. Using standard hyperbolic identities[33] one can show that:

$$\sin\xi = \frac{\sqrt{B^2 - 1}\sinh H}{B\cosh H - 1} \quad ; \quad \tan\left(\frac{\xi}{2}\right) = \sqrt{\frac{B+1}{B-1}}\tanh\left(\frac{H}{2}\right) \tag{4.36}$$

Using Eq. (4.35), the transfer trajectory equation (4.17) can now be written as:

$$r = \left(\frac{h^2}{B^2 - 1}\right)(B\cosh H - 1) \qquad (4.37)$$

The inverse of expressions in Eqs. (4.35) and (4.36) can be found as:

$$\cosh H = \frac{\cos\xi + B}{1 + B\cos\xi} \quad ; \qquad dH = \frac{\sqrt{B^2 - 1}}{1 + B\cos\xi}d\xi \qquad (4.38)$$

$$\sinh H = \frac{\sqrt{B^2 - 1}\sin\xi}{1 + B\cos\xi} \quad ; \qquad \tanh\left(\frac{H}{2}\right) = \sqrt{\frac{B-1}{B+1}}\tan\left(\frac{\xi}{2}\right) \qquad (4.39)$$

while the initial and final values of H, H_0 and H_f, are given by:

$$\cosh H_0 = \frac{\cos\xi_0 + B}{1 + B\cos\xi_0} \quad ; \qquad \cosh H_f = \frac{\cos\xi_f + B}{1 + B\cos\xi_f} \qquad (4.40)$$

Eq. (4.24) can then be written as:

$$\frac{1}{h^2} = \frac{1}{h_0^2} - \frac{2A}{\left(B^2 - 1\right)^{3/2}}\int_{H_0}^{H}(B\cosh H - 1)dH \qquad (4.41)$$

which after a straightforward integration results in:

$$\frac{1}{h^2} = \frac{1}{h_0^2} + \frac{2A\left[H - H_0 - B(\sinh H - \sinh H_0)\right]}{\left(B^2 - 1\right)^{3/2}} \qquad (4.42)$$

4.5.4 Examples of Motion under the Proposed Thrust Program

At this point one can begin to consider some preliminary examples depicting the kind of motion described by the trajectory equation (4.17), in conjunction with Eqs. (4.25), (4.26), (4.34), and (4.42) derived in this section. Figures 4.2 through 4.4 show examples of transfer trajectories (plots of Eq. (4.17)) that start from the perigee of the same initial elliptical orbit and correspond to different values of the throttling parameter A and to

57

different duration τ_f. Figure 4.5 shows a similar case for which the initial conic is a hyperbola. In each figure the final conic, corresponding to the motion that follows after the thrust is turned off at $\tau = \tau_f$, is also plotted. It is seen from Eqs. (4.17), (4.25), (4.26), (4.34), and (4.42) that a vehicle can escape the gravitational field of a planet even along a transfer trajectory for which the generalized eccentricity B is less than one, providing that the thrust is kept "on" for a sufficient duration of time. Note that the distance from the planet r becomes infinite on a transfer trajectory (for any B) *when, and only when* the angular momentum h becomes infinite. This happens when the right-hand-side of the applicable one among Eqs. (4.25), (4.26), (4.34), or (4.42) becomes zero at some θ. Figure 4.4 shows an escape trajectory on which B < 1.

4.6 The Origin of the Thrust Program

In this section a connection will be developed between the thrust program proposed in Section 4.3, and the problem of optimal, power-limited, coplanar motion. It will be shown that, the thrust program proposed in Eq. (4.10) can be obtained by making the tangential thrust assumption and by imposing the transversality conditions in the costate system corresponding to the problem of power-limited, minimum-fuel transfers between two coplanar conics.

A Mayer type formulation of the above problem is the most convenient one, and for this, one will have to add to the system of Eqs. (4.6)-(4.9) the equation governing the performance index:

$$\frac{dJ}{d\tau} = \frac{1}{2}\left(\varepsilon_r^2 + \varepsilon_\theta^2\right) \tag{4.43}$$

The final value of J (at a *fixed* final time τ_f) is a direct (nondimensional) measure of the fuel consumption for power-limited propulsion systems[44-51] (see Appendix C for more details). Note that the variation for the mass of the vehicle during a maneuver is fully taken into account by means of Eq. (4.43) (see Eq. (C.5) of Appendix C).

4.6.1 The State-Costate System for Power-Limited Optimization

The Hamiltonian associated with the system of Eqs. (4.6) - (4.9), and (4.43) is:

$$H = r\varepsilon_\theta P_h + \left(\frac{h^2 - r}{r^3}\right)P_x + \varepsilon_r P_x + x P_r + \frac{h}{r^2}P_\theta + \frac{1}{2}\left(\varepsilon_r^2 + \varepsilon_\theta^2\right)P_J \tag{4.44}$$

58

In order to have minimum fuel consumption one must minimize $J_f - J_0$, or maximize $-J_f + J_0$. The cost J is an ignorable coordinate, meaning that the corresponding costate P_J is *constant* (Specifically, the Hamiltonian does not depend *explicitly* on J). Moreover, examination of the transversality conditions in Section 4.6.3 will further dictate that (see Eq. (4.98)):

$$P_J = -1 \qquad (4.45)$$

With this result, the optimal controls can be found by setting the partial derivatives of H with respect to ε_r, ε_θ in Eq. (4.44) equal to zero. The result is:

$$\varepsilon_r^* = P_x \quad ; \quad \varepsilon_\theta^* = r P_h \qquad (4.46)$$

Substituting these controls back into Eq. (4.44) the Hamiltonian can be written as (using $P_J = -1$):

$$H^* = \frac{1}{2}\left(r^2 P_h^2 + P_x^2\right) + \left(\frac{h^2 - r}{r^3}\right) P_x + x P_r + \frac{h}{r^2} P_\theta \qquad (4.47)$$

Using this expression for the Hamiltonian, the differential equations governing the optimal trajectories can be found from:

$$\frac{ds}{d\tau} = \frac{\partial H^*}{\partial P} \quad ; \quad \frac{dP}{d\tau} = -\frac{\partial H^*}{\partial s} \qquad (4.48)$$

where s and P denote the state and costate vectors respectively. Explicitly, the result is the following tenth order system for the state and costate equations:

$$\frac{dh}{d\tau} = r^2 P_h \qquad (4.49)$$

$$\frac{dx}{d\tau} = \left(\frac{h^2 - r}{r^3}\right) + P_x \qquad (4.50)$$

$$\frac{dr}{d\tau} = x \qquad (4.51)$$

$$\frac{d\theta}{d\tau} = \frac{h}{r^2} \qquad (4.52)$$

59

$$\frac{dJ}{d\tau} = \frac{1}{2}\left(P_x^2 + r^2 P_h^2\right) \qquad (4.53)$$

$$\frac{dP_h}{d\tau} = -\frac{2hP_x}{r^3} - \frac{P_\theta}{r^2} \qquad (4.54)$$

$$\frac{dP_x}{d\tau} = -P_r \qquad (4.55)$$

$$\frac{dP_r}{d\tau} = -rP_h^2 + \frac{3h^2P_x}{r^4} - \frac{2P_x}{r^3} + \frac{2hP_\theta}{r^3} \qquad (4.56)$$

$$\frac{dP_\theta}{d\tau} = 0 \qquad (4.57)$$

$$\frac{dP_J}{d\tau} = 0 \qquad (4.58)$$

Note that Eqs. (4.49) through (4.52) are just the state equations (4.6) through (4.9), with the controls substituted in from Eq. (4.46). It can be verified that this tenth order system has the following three first integrals:

$$H^* = \text{const.} \quad ; \quad P_\theta = \text{const.} \quad ; \quad P_J = \text{const.} = -1 \qquad (4.59)$$

and a fourth integral[48] given by:

$$2rP_r + hP_h - xP_x = 3H^*\tau - 5J + A_4 \qquad (4.60)$$

where A_4 is an integration constant. These four integrals can in principle be used to reduce the order of the system to six, involving the variables h, x, r, θ, P_h, and P_x.

An important point that can be made regarding the state-costate system of Eqs. (4.49) through (4.58) is the relative simplicity of the right-hand-sides of these equations. Note that these equations contain no trigonometric functions. A quick inspection reveals that the number of basic operations (addition, subtraction, multiplication, and division) that need to be performed to compute the right-hand-sides of Eqs. (4.49) through (4.58) is about half times the number of basic operations that need to be performed to compute the right-hand-

sides of the same equations, but written using traditional state variables, like the set (V, γ, r, θ) or the orbital elements. Pursuing this argument further, one can conclude that the computer running time required for the numerical solution of a two-point boundary value problem using Eqs. (4.49) through (4.58) should be about half, compared to the running time required for the numerical solution of the same problem using the traditional state variables (V, γ, r, θ) or the orbital elements.

4.6.2 The Tangential Thrust Assumption and its Implications

One can now pursue the consequences of the assumption that the thrust along an optimal trajectory is approximately tangent to the direction of the optimal flight path. This assumption will be referred to as "the tangential thrust assumption". In terms of the state and costate variables, the tangential thrust assumption means that along an optimal trajectory the relationship:

$$\frac{P_x}{rP_h} = \frac{rx}{h} = \tan\gamma \tag{4.61}$$

is approximately valid. Note that γ is the flight path angle, formed by the path of the vehicle and the local horizontal direction. It will be assumed, as Eq. (4.61) implies, that the tenth order system of Eqs. (4.49)-(4.58) behaves in practice as a ninth order system, meaning that one will have to drop one of these equations out. As it turns out, one can combine Eqs. (4.54) and (4.61) and solve for P_h as a function of the states. Then, P_x can be found by resorting back to Eq. (4.61), and P_r can be found from Eq. (4.55) by differentiating the expression for P_x. Accordingly, one won't need Eq. (4.56), which will be the one equation to be dropped out. Thus, using the tangential thrust assumption, one can replace the system of Eqs. (4.49)-(4.58) by the system:

$$\frac{P_x}{rP_h} = \frac{rx}{h} \tag{4.62}$$

$$\frac{dh}{d\tau} = r^2 P_h \tag{4.63}$$

$$\frac{dx}{d\tau} = \left(\frac{h^2 - r}{r^3}\right) + P_x \tag{4.64}$$

61

$$\frac{dr}{d\tau} = x \tag{4.65}$$

$$\frac{d\theta}{d\tau} = \frac{h}{r^2} \tag{4.66}$$

$$\frac{dJ}{d\tau} = \frac{1}{2}\left(P_x^2 + r^2 P_h^2\right) \tag{4.67}$$

$$\frac{dP_h}{d\tau} = -\frac{2xP_h}{r} - \frac{P_\theta}{r^2} \tag{4.68}$$

$$\frac{dP_x}{d\tau} = -P_r \tag{4.69}$$

$$\frac{dP_\theta}{d\tau} = 0 \tag{4.70}$$

$$\frac{dP_J}{d\tau} = 0 \tag{4.71}$$

Note here that: i) Eq. (4.62) is just the tangential thrust assumption. ii) All the remaining equations (4.63)-(4.71) are the same as the original equations (4.49)-(4.55), and (4.57), (4.58), except equation (4.68), which was obtained from Eq. (4.54) by changing its right-hand side using the tangential thrust assumption. iii) The optimal Hamiltonian H* given in Eq. (4.47), and the constant A_4 defined in Eq. (4.60) are no longer first integrals of Eqs. (4.62)-(4.71). iv) P_θ and P_J are still constant and $P_J = -1$.

One can now show the primary analytical result of this chapter, and also of this report, which can be summarized in the following statement:

For the problem of transfers between two arbitrary conics, if one enforces the transversality conditions exactly, then Eqs. (4.62)-(4.71) can be reduced to quadratures without any further approximations.

By defining the transformation:

$$Q = r^2 P_h \tag{4.72}$$

62

and then, by using Eqs. (4.65), (4.68) one finds that:

$$\frac{dQ}{d\tau} = -P_\theta \qquad (4.73)$$

Since P_θ is constant, the solution of Eq. (4.73) is simply:

$$Q = -P_\theta \tau + A \qquad (4.74)$$

where, A is an integration constant. Combining now Eqs. (4.72), (4.74) and (4.63) one obtains:

$$\frac{dh}{d\tau} = Q = -P_\theta \tau + A \qquad (4.75)$$

the solution of which is:

$$h = -\frac{P_\theta \tau^2}{2} + A\tau + h_0 \qquad (4.76)$$

where, h_0 is another constant of integration, equal to the value of the angular momentum h at time $\tau=0$. Using Eqs. (4.72), (4.62), and then carrying out the differentiation in Eq. (4.69) one can express the costates P_x, P_h, and P_r in terms of the state variables, the time, and the three constants P_θ, A, and h_0 as:

$$P_x = \frac{Qx}{h} \quad ; \quad P_h = \frac{Q}{r^2} \quad ; \quad P_r = \left(\frac{x}{h}\right)P_\theta - \left(\frac{h^2-r}{r^3}\right)\left(\frac{Q}{h}\right) \qquad (4.77)$$

The costate variable P_θ represents the sensitivity of the minimum cost to the initial value of the state component θ. By examining the first variation of the (augmented) cost in Section 4.6.3, it will be shown that for transfers "from" or "to" a circular orbit the *exact* value of P_θ is zero. This is not surprising, since for such problems, due to the initial circular symmetry, the initial value of the state component θ has no effect on the minimum value of the cost. It will also be shown in Sections 4.6.3 and 4.6.4, by enforcing the transversality conditions and by using the expressions for the costates given in Eq. (4.77), that for transfers between two *arbitrary* conics, P_θ is zero *as a direct consequence* of the

tangential thrust assumption. With zero P_θ the variable Q from Eq. (4.75) is just equal to the constant A, and the expressions for the costates given in Eq. (4.77) reduce to:

$$P_x = \frac{Ax}{h} \quad ; \quad P_h = \frac{A}{r^2} \quad ; \quad P_r = -\left(\frac{h^2 - r}{r^3}\right)\left(\frac{A}{h}\right) \qquad (4.78)$$

Using the expressions for P_x and P_h from Eq. (4.78) one can now go back and obtain the corresponding explicit thrust acceleration components, by substituting into Eq. (4.46). The result is:

$$\varepsilon_r = \frac{Ax}{h} \quad ; \quad \varepsilon_\theta = \frac{A}{r} \qquad (4.79)$$

But this is none other then the thrust (acceleration) program proposed in Eq. (4.10)! Therefore, one can state that:

The thrust program proposed in Eq. (4.10) can be obtained by making the tangential thrust assumption in one costate equation and by imposing the transversality conditions for the problem corresponding to power-limited, minimum-fuel, coplanar transfers between two arbitrary conics.

Note that the asterisks have been omitted from ε_r and ε_θ in Eq. (4.79), since these thrust acceleration components are *consequences* of the tangential thrust assumption and can be *near-optimal* at best.

Now that the thrust program is "fixed" and the same as the one proposed in Eq. (4.10), the *exact analytic* solution of the state equations is also "fixed" and the same as the one given in Section 4.4. For $Q = A = $ constant, Eqs. (4.75), (4.76) lead to:

$$\frac{dh}{d\tau} = A \quad ; \quad h = A\tau + h_0 \qquad (4.80)$$

These equations are the same as Eqs. (4.11) and (4.15) of Section 4.4. Using the expression for P_x given in Eq. (4.78), Eqs. (4.64), (4.65) assume the form:

$$\frac{dx}{d\tau} = \left(\frac{h^2 - r}{r^3}\right) + \frac{Ax}{h} \quad ; \quad \frac{dr}{d\tau} = x \qquad (4.81)$$

64

which are the same as Eqs. (4.12), (4.13) of Section 4.4. The solution of Eqs. (4.81) is:

$$x = \frac{2rA + B\sin(\theta - C)}{h} \quad ; \quad r = \frac{h^2}{1 + B\cos(\theta - C)} \qquad (4.82)$$

which is none other than the one given in Eqs. (4.16), (4.17) of Section 4.4. The last state equation that remains to be integrated is Eq. (4.66), which is the same as Eq. (4.14) and can be reduced to quadrature as in Eq. (4.18), or integrated as in Section 4.5.

Denoting by h_f the value of the angular momentum h at the final time τ_f one can write the constant A, playing the role of a *throttling parameter*, and appearing in the linear variation of h (Eqs. (4.15), (4.80)) as:

$$A = \frac{h_f - h_0}{\tau_f} \qquad (4.83)$$

Combining Eqs. (4.79) and (4.83), the two thrust acceleration components along a transfer can be written explicitly as:

$$\varepsilon_r = \frac{(h_f - h_0)x}{\tau_f h} \quad ; \quad \varepsilon_\theta = \frac{(h_f - h_0)}{\tau_f r} \qquad (4.84)$$

By replacing h_0 by h and τ_f by the "time to go" $\tau_f\text{-}\tau$ in Eq. (4.84) one obtains the following explicit, closed-loop, finite-time, *exact* feedback guidance law:

$$\varepsilon_r = \frac{(h_f - h)x}{(\tau_f - \tau)h} \quad ; \quad \varepsilon_\theta = \frac{(h_f - h)}{(\tau_f - \tau)r} \qquad (4.85)$$

During an actual transfer this law will guide a vehicle from the initial conic to the desired final conic, providing that the transfer starts from the "correct" point on the initial conic. Since this happens to be a *finite-time* feedback guidance law, it is bound to suffer from saturation problems (in the presence of disturbances) as the final time $\tau = \tau_f$ is approached. In such a case, the reasonable thing to do would be to switch to the open-loop law of Eq. (4.84) as late as possible on the transfer, but *before* the final time $\tau = \tau_f$ is reached.

As expected, there is a partial loss of controllability that goes along with the tangential thrust assumption, and it will be shown when examining the boundary conditions that, if the initial and final conics do not intersect, then, a *one-segment solution* for a particular transfer problem, that is, a transfer trajectory on which the throttling parameter A has a

single value may in general exist only for *particular* values of the (fixed) final time τ_f. For escape problems on the other hand a solution may exist (in principle) for any value of τ_f because the final value of the angular momentum h_f, or the orientation difference $\omega_f - \omega_0$ between the initial and final conics *may* be left free. A one-segment solution however does not exist, and a (one-segment) transfer trajectory cannot be found, when the initial and final conics intersect (see Theorem 4.1 of Section 4.11, and Appendix F). However, even in such a case, a transfer can still be accomplished using *two* separate transfer trajectories, that is, by first transferring to an intermediate conic (that does not intersect either the initial or the final conic), and then by transferring to the desired final conic (see Sections 4.11, 4.12 for more details).

4.6.3 Derivation of the Transversality Conditions

For transfer or escape problems the state of the vehicle at the initial and final times is only partly specified. Accordingly, the boundary conditions have to be supplemented by the so-called transversality conditions, arising from the requirements of optimality, in order to provide one with enough conditions for a particular solution. The exact form of the transversality conditions will be given in this Section, and then combined with Eq. (4.77) of Section 4.6.4, in order to show the result $P_\theta = 0$, which led to Eq. (4.78) and the thrust program proposed in Eq. (4.10).

There are several methods that can be used to derive the transversality conditions for the problems of interest. The one that will be used here is very straightforward, and it is based on a direct examination of the first variation of the (augmented) performance index. Recall that the performance index is just the negative of the final value of J, that is, $-J_f$. Augmenting this by the dynamics of the problem one obtains the *augmented* performance index I:

$$I = -J_f + \int_{\tau_0}^{\tau_f} P(f - \dot{s}) d\tau \qquad (4.86)$$

The costate (Lagrange multiplier) vector P is a row vector with components P_h, P_x, P_r, P_θ, and P_J. The vector of dynamics f is a column vector with components the right hand sides of Eqs. (4.6)-(4.9) and (4.43). The vector s is also a column vector with components the left-hand sides of Eqs. (4.6)-(4.9) and (4.43). Using the Hamiltonian H=Pf, Eq. (4.86) can be written as:

66

$$I = -J_f + \int_{\tau_0}^{\tau_f} [H(s,P,u) - P\dot{s}]d\tau \qquad (4.87)$$

The components of the control vector u are just the two components of the thrust acceleration, ε_r and ε_θ. The initial time τ_0 and the final time τ_f are always fixed.

Assume now that the value of the augmented performance index I given in Eq. (4.87) is the optimal one, that is, it corresponds to the optimal choice of the control u. Then, if the optimal control is perturbed by a small amount δu to $u+\delta u$, the augmented performance index $\overline{I}$ is correspondingly perturbed to $I+\Delta I$, given by:

$$I + \Delta I = -J_f - \delta J_f + \int_{\tau_0}^{\tau_f} [H(s+\delta s, P, u+\delta u) - P(\dot{s}+\delta\dot{s})]d\tau \qquad (4.88)$$

where, the perturbations in the state components resulting from the perturbation in u have been denoted by δs, and where:

$$\delta\dot{s} = \delta\left(\frac{ds}{d\tau}\right) = \frac{d(\delta s)}{d\tau} \qquad (4.89)$$

From Eqs. (4.87) and (4.88), the *total variation* of I is:

$$\Delta I = -\delta J_f + \int_{\tau_0}^{\tau_f} [\Delta H - P\delta\dot{s}]d\tau \qquad (4.90)$$

The *first variation* of I is that part of ΔI corresponding only to the first order change of H in the small quantities δx, δu:

$$\delta I = -\delta J_f + \int_{\tau_0}^{\tau_f} [\delta H - P\delta\dot{s}]d\tau \qquad (4.91)$$

Integrating the second term in the integral by parts and expressing δH in terms of δs and δu one can write Eq. (4.91) as:

67

$$\delta I = -\delta J_f - P_f \delta s_f + P_0 \delta s_0 + \int_{\tau_0}^{\tau_f} \left[\left(\frac{\partial H}{\partial s} + \dot{P} \right) \delta s + \frac{\partial H}{\partial u} \delta u \right] d\tau \qquad (4.92)$$

where, the subscripts 0 and f were used to denote the values of the costates P and the variations δs at the initial and final time respectively. The natural choice for the costate functions P at this point is:

$$\dot{P} = -\frac{\partial H}{\partial s} \qquad (4.93)$$

based on which δI from Eq. (4.92) can be written as:

$$\delta I = -\delta J_f - P_f \delta s_f + P_0 \delta s_0 + \int_{\tau_0}^{\tau_f} \frac{\partial H}{\partial u} \delta u \, d\tau \qquad (4.94)$$

Since the original choice of u was assumed to be the optimal one, δI should vanish for arbitrary perturbations δu about u. From Eq. (4.94) a necessary condition for this is:

$$\frac{\partial H}{\partial u} = 0 \qquad (4.95)$$

In view of Eq. (4.95) and the requirement that δI be zero, one obtains from Eq. (4.94):

$$\delta I = -\delta J_f - P_f \delta s_f + P_0 \delta s_0 \qquad (4.96)$$

The conditions given by Eqs. (4.93) and (4.95) are necessary for optimality. The explicit form of Eqs. (4.93) and (4.95) has already been obtained in the text. Eq. (4.95) is just the optimality condition used in obtaining Eq. (4.46), while Eq. (4.93) represents the costate equations (4.54)-(4.58). Here, Eq. (4.96) will be further manipulated into a form that will readily yield the transversality conditions for any problem that one wishes to study. First, one can write Eq. (4.96) explicitly, using the components of P and δs at the initial and final times as:

$$\delta I = -\left(1 + P_J\right)\delta J_f - P_{hf}\delta h_f - P_{xf}\delta x_f - P_{rf}\delta r_f - P_\theta \delta \theta_f$$

$$+P_J \delta J_0 + P_{h0} \delta h_0 + P_{x0} \delta x_0 + P_{r0} \delta r_0 + P_\theta \delta \theta_0 \qquad (4.97)$$

The initial value of the cost is zero ($J_0=0$), meaning that $\delta J_0 = 0$. The final value of the cost is free (since the aim in the optimization problem is to find the optimal final value), meaning that:

$$P_J = -1 \qquad (4.98)$$

Note that this proves the result claimed in Eq. (4.45). Now Eq. (4.97) is reduced to:

$$\delta I = P_{h0} \delta h_0 + P_{x0} \delta x_0 + P_{r0} \delta r_0 + P_\theta \delta \theta_0 - P_{hf} \delta h_f - P_{xf} \delta x_f - P_{rf} \delta r_f - P_\theta \delta \theta_f \qquad (4.99)$$

For transfer problems the variations δh, δx, δr, and $\delta \theta$ are not in general independent of each other, neither at the initial nor at the final time. However, in all such problems, the vehicle, before the initial and after the final times is assumed to coast along conics (circles, ellipses, parabolas, or hyperbolas), defined by their orbital elements h_i (angular momentum), e_i (eccentricity), and ω_i (orientation) (i is 0 or f). For all such problems the variables that will be prescribed or left free at the initial or final time are h_i, e_i, ω_i and θ_i. To derive the transversality conditions one will therefore have to cast the remaining part of the first variation of I given in Eq. (4.99) in terms of the independent variations δh_i, δe_i, $\delta \omega_i$, and $\delta \theta_i$ rather than the dependent variations δh_i, δx_i, δr_i, and $\delta \theta_i$. Toward this end one can first observe that at any point along a conic (corresponding to Keplerian motion) the radial distance r and the radial component of the velocity x are given by (see Eq. (A.5) of Appendix A):

$$r = \frac{h^2}{1 + e\cos(\theta - \omega)} \quad ; \qquad x = \frac{e\sin(\theta - \omega)}{h} \qquad (4.100)$$

Differentiating Eq. (4.100) one finds that, to first order, variations in x and r corresponding to small variations δh, δe, $\delta \omega$, and $\delta \theta$ are given by:

$$\delta r = \frac{2r}{h} \delta h - \frac{r(h^2 - r)}{h^2 e} \delta e + \frac{xr^2}{h}(\delta\theta - \delta\omega) \qquad (4.101)$$

$$\delta x = -\frac{x}{h} \delta h + \frac{e^2 r^2 - (h^2 - r)^2}{e x h^2 r^2} \delta e + \frac{(h^2 - r)}{hr}(\delta\theta - \delta\omega) \qquad (4.102)$$

69

Writing these expressions for δx and δr at the initial and final times, one can substitute into Eq. (4.99) and obtain the desired form of the remaining part of δI:

$$\delta I = K_{h0}\delta h_0 - K_{hf}\delta h_f + K_{e0}\delta e_0 - K_{ef}\delta e_f + K_{\theta 0}\delta\theta_0 - K_{\theta f}\delta\theta_f - K_{\omega 0}\delta\omega_0 + K_{\omega f}\delta\omega_f \quad (4.103)$$

where the variables K are defined as:

$$K_h = P_h + \frac{2rP_r - xP_x}{h} \quad ; \quad K_e = \frac{e^2 r^2 - (h^2 - r)^2}{e x h^2 r^2}P_x - \frac{r(h^2 - r)}{e h^2}P_r \quad (4.104.a)$$

$$K_\theta = P_\theta + \frac{h^2 - r}{hr}P_x + \frac{xr^2}{h}P_r \quad ; \quad K_\omega = \frac{h^2 - r}{hr}P_x + \frac{xr^2}{h}P_r \quad (4.104.b)$$

and the additional subscript 0 or f represents corresponding values at the initial or final time.

For any transfer problem of interest Eq. (4.103) can be used to pick the desired transversality conditions at will. First, for all transfer problems the eccentricities of the initial and final conics are always fixed, meaning that, δe_0 and δe_f in Eq. (4.103) will always be zero. Then, whenever one of the six quantities h_0, ω_0, θ_0, h_f, ω_f and θ_f is left free in a problem, the coefficient of the corresponding variation of that quantity in Eq. (4.103) is set equal to zero, resulting in a transversality condition. For example, if for a given problem the angular momentum at the initial and final times is left free, the requirement that $\delta I=0$ results in the two transversality conditions $K_{h0}=K_{hf}=0$. This result has an interesting implication when combined with the fourth integral of motion given in Eq. (4.60). It implies that the constant A_4 is zero, and that the exact optimal cost for all such problems is given by:

$$J_f^* = \frac{3H^*\tau_f}{5} \quad (4.105)$$

In all the (transfer) problems that will be considered here the argument of latitude θ will be free both at the initial and final times. From Eq. (4.103), this means that one will always have at least the two transversality conditions:

$$\text{if } \theta_i \text{ is free, then:} \quad P_\theta + \frac{h_i^2 - r_i}{h_i r_i}P_{xi} + \frac{x_i r_i^2}{h_i}P_{ri} = 0 \quad (4.106)$$

70

where i is 0 or f. Also, the angular momentum of the initial conic will always be specified, meaning that $\delta h_0=0$. Taking the above considerations into account, using Eqs. (4.106), and defining the difference in the orientation between the initial and final conics by Ω:

$$\Omega = \omega_f - \omega_0 \quad ; \quad \delta\Omega = \delta\omega_f - \delta\omega_0 \tag{4.107}$$

one can reduce Eq. (4.103) to (with zero δe_0 and δe_f):

$$\delta I = -\left(P_{hf} + \frac{2r_f P_{rf} - x_f P_{xf}}{h_f}\right)\delta h_f - P_\theta\delta\Omega \tag{4.108}$$

For some of the problems the final value of the angular momentum h will be left free, meaning that, for such problems one will always have the additional transversality condition:

$$\text{if } h_f \text{ is free, then:} \qquad P_{hf} + \frac{2r_f P_{rf} - x_f P_{xf}}{h_f} = 0 \tag{4.109}$$

Finally, for problems in which the orientation difference Ω between the initial and final conics is left free one will also have the transversality condition:

$$\text{if } \Omega \text{ is free then} \qquad P_\theta = 0 \tag{4.110}$$

At the limiting case in which at least one of the eccentricities associated with the initial or final conics tends to zero, this last category of problems includes the very important subclass of transfers from or to a circular orbit. For all the problems in this subclass the *exact optimal* value of P_θ is zero.

In concluding this section one must note that the transversality conditions obtained here were all *exact* and also *necessary* for a (power-limited) trajectory to be *optimal*.

4.6.4 Application of the Transversality Conditions

Sections 4.6.1 and 4.6.3 have supplied the *exact* first-order necessary conditions for optimality for the problem corresponding to power-limited orbital motion. The goal is of course to use the solution uncovered in Section 4.4 and try to satisfy as many first-order conditions as possible. Note that, along a trajectory violating even *a single* first-order condition, the first variation of the (augmented) performance index fails to be *identically*

71

zero. The hope therefore is that, if any first-order condition is violated by the solution uncovered in Section 4.4, the violation will be small, resulting in nearly-optimal trajectories (see also Section 4.6.5 for more on this subject). Thus, this section will combine the results of Sections 4.6.2 and 4.6.3 in order to uncover explicitly the form that the transversality conditions assume under the tangential thrust assumption. As seen in Section 4.6.3, there will always be at least two transversality conditions, given in Eq. (4.106). Thus, substituting for the costates from Eq. (4.77) into Eq. (4.106) one obtains:

$$\left(\frac{r_0^2 V_0^2}{h_0^2}\right) P_\theta = 0 \; ; \qquad \left(\frac{r_f^2 V_f^2}{h_f^2}\right) P_\theta = 0 \qquad (4.111)$$

where V_0, V_f are the (nondimensional) speeds of the vehicle at the initial and final times respectively. Note that, in terms of the state variables h, x, and r, the (nondimensional) speed of the vehicle, V, is given by (see Fig. 4.1):

$$V = \left(x^2 + \frac{h^2}{r^2}\right)^{1/2} \qquad (4.112)$$

Since for obvious reasons the terms within the parentheses cannot be zero at the endpoints of a transfer, Eq. (4.111) implies that the two transversality conditions in Eq. (4.106) can be satisfied by the solution corresponding to the tangential thrust assumption *only* if one selects P_θ as:

$$P_\theta = 0 \qquad (4.113)$$

This result was used as the justification in Section 4.4.3 for reducing Eq. (4.77) to Eq. (4.78). If one now substitutes for the costates from Eq. (4.78), and also takes into account Eq. (4.112), then, Eq. (4.109) assumes the form:

$$\frac{A}{h_f^2}\left(V_f^2 - \frac{2}{r_f}\right) = 0 \qquad (4.114)$$

But on the final conic, the following two well-known[34] relations of Keplerian motion are valid (see Appendix A):

$$V_f^2 - \frac{2}{r_f} = -\frac{1}{a_f} \; ; \qquad h_f^2 = a_f\left(1 - e_f^2\right) \qquad (4.115)$$

a_f in Eq. (4.115) is the semimajor axis of the final conic. If the final conic is an ellipse, then a_f is positive and e_f is between 0 and 1. If the final conic is a hyperbola, then a_f is negative and e_f is greater than 1. If the final conic is a parabola, then a_f is infinite, e_f is 1, and h_f is finite[34]. Substituting from Eq. (4.115) into Eq. (4.114), Eq. (4.109) can now be written as:

$$\frac{A}{h_f^4}\left(e_f^2 - 1\right) = 0 \qquad (4.116)$$

The throttling parameter A cannot be taken equal to zero, since in such a case the thrust is zero and there can be no transfer. Also, the angular momentum of the final conic h_f is always finite. Accordingly, from Eq. (4.116), the only way in which the transversality condition given in Eq. (4.109) can be satisfied by the solution corresponding to the tangential thrust assumption is by selecting the final eccentricity e_f as:

$$e_f = 1 \qquad (4.117)$$

But problems for which $e_f = 1$ are just *escape* problems! Therefore, leaving the final value h_f free, combined with the solution found using the tangential thrust assumption, suggests an escape problem! (from an arbitrary conic).

This section now concludes by summarizing the important results from the present and the last section:

(i) For problems in which the angular momentum at the initial and final times is left free the exact optimal (power-limited) cost is given by Eq. (4.105).

(ii) For all the transfer problems in which either the orientation difference between the initial and final conics is left free or either one of the conics (or both) is circular the exact optimal value of P_θ is zero (see Eq. (4.110)).

(iii) For transfer problems between two arbitrary conics, in which the orientation difference between the conics is fixed, the costate P_θ is also zero, but as a consequence of the tangential thrust assumption (see Eq. (4.113)).

(iv) Leaving the angular momentum at the final time free implies that the eccentricity of the final conic *should* be fixed at 1, and, fixing the eccentricity of the final conic at 1 implies that the angular momentum at the final time *may* be left free (see Eq. (4.117)).

Note that (i) and (ii) are *independent* of the tangential thrust assumption, while (iii) and (iv) are *consequences* of the tangential thrust assumption.

73

4.6.5 How Good is the Tangential Thrust Assumption?

One will sooner or later have to go back and check the validity of the tangential thrust assumption if one is to be able to say anything at all about the possible near-optimality of the thrust program proposed in Eq. (4.10). Recall that the tangential thrust assumption was used in three steps: The first two steps consisted of dropping out Eq. (4.56) representing the costate equation for the radial distance r, and changing the right-hand-side of Eq. (4.54) representing the costate equation for the angular momentum h. This led to the expressions for the costates P_x, P_h, and P_r given in Eq. (4.77). Then, enforcing the transversality conditions (see Sections 4.6.3 and 4.6.4) "fixed" the value of the costate P_θ at zero and simplified the costate expressions for P_x, P_h, and P_r as in Eq. (4.78). A preliminary check of the validity of the tangential thrust assumption should therefore consist of a comparison of the left and right-hand-sides of Eqs. (4.54) and (4.56), with $P_\theta = 0$, and using the expressions for the costates P_x, P_h, and P_r found in Eq. (4.78). Differentiating the expressions for the costates P_x and P_r in Eq. (4.78), and using Eqs. (4.78), and (4.49) through (4.51), one finds that, for $P_\theta = 0$, Eq. (4.54) is always satisfied, while the left and right-hand sides (LHS, RHS) of Eq. (4.56) assume the form:

$$\text{LHS of Eq. (4.56):} \quad -\frac{2Ax}{hr^3}+\frac{3Ahx}{r^4}-\frac{A^2}{r^3}-\frac{A^2}{h^2r^2} \qquad (4.118.a)$$

$$\text{RHS of Eq. (4.56):} \quad -\frac{2Ax}{hr^3}+\frac{3Ahx}{r^4}-\frac{A^2}{r^3} \qquad (4.118.b)$$

Thus, Eq. (4.56) is satisfied only when (A^2/h^2r^2) is zero. In other words, when (A^2/h^2r^2) is very nearly zero, the thrust program proposed in Eq. (4.10) is very nearly optimal (in the power-limited sense), because, in such a case, every single first-order necessary condition, except Eq. (4.56), is satisfied *exactly*, while Eq. (4.56) is satisfied *very nearly*. Note that the term $-(A^2/h^2r^2)$ causing the disagreement in Eq. (4.118.a) is *second order* in the throttling parameter A compared to the remaining terms. Since the throttling parameter A is inversely proportional to the transfer duration (see Eq. (4.83)), for long duration transfers this term is negligible, the optimal thrust is approximately tangential, and the thrust program proposed in Eq. (4.10) is practically optimal! The result in Eq. (4.118) also suggests that the assumption that the optimal thrust is approximately tangent to the optimal flight path is more consistent with transfers that are performed far away from a planet and on which the average levels of the magnitude of the angular momentum remain high. This observation is clearly in agreement with one's intuition.

As the duration of transferring between two given conics tends to infinity, and the thrust levels go to zero (see Eq. (4.83)), the solution supplied in Section 4.4, corresponding to the thrust program proposed in Eq. (4.10), *asymptotically* tends to the *optimal* solution for power-limited transfers. In fact, in such a case, both the optimal solution and the solution of Section 4.4 tend to Keplerian motion, for which the cost is zero! Note that it has been well-established in the literature, that, for power-limited transfers between two given conics the *optimal* cost is inversely proportional to the transfer duration[44-51]. Assuming that the angular momentum h_0, the eccentricity e_0, and the orientation ω_0 of the initial conic are always *fixed*, and that a transfer is performed using a *one-segment* transfer trajectory, that is, a trajectory on which the throttling parameter A has a *single* value, one can distinguish between the following three classes of transfers in conjunction with the near-optimality of the thrust program proposed in Eq. (4.10) and the corresponding exact analytic solution given in Section 4.4 (see Sections 4.7 through 4.12 for a justification):

(i) For "pure" transfer problems the shape, size, and orientation of the final conic are always of interest. This means that the angular momentum h_f, the eccentricity e_f, and the orientation ω_f of the final conic are always *fixed*. For such problems, due to the loss of controllability suffered because of the tangential thrust assumption, the duration of (a one-segment) transfer cannot be preassigned. Solutions exist only for a finite set of values of the transfer duration. Accordingly, one is not free to perform the (one-segment) transfer in arbitrarily large time intervals, using arbitrarily small thrust levels. Once the initial and final conics are *fixed*, the minimum amount of fuel that is required to perform a one-segment transfer using the thrust program proposed in Eq. (4.10) is also *fixed*.

(ii) An important exception in case (i) corresponds to the subclass of transfers between two coplanar circular orbits. This turns out to be an interesting singular case (see Section 4.8). If both the initial and final conics are circles, then, one-segment transfer solutions between the conics do not exist. However, if the eccentricity of the final conic is slightly off zero, then there exists a very large number of solutions! Specifically, as the eccentricity of the final conic tends to zero and the final conic tends to a perfect circle, the number of possible solutions increases without bound, and one can in such a case find solutions corresponding to arbitrarily large transfer durations! Thus, in this case the amount of fuel required for a transfer can (in principle) be reduced by as much as desired (within the operating limits of the power-limited propulsion system), as long as one picks the solution corresponding to a "large enough" transfer duration.

(iii) Escape problems are a special kind of transfer problem in which the interest is in escaping the gravitational field of a planet. Accordingly, the size of the final parabolic trajectory is of little importance and one can now get away (*in practice*) by specifying only the eccentricity ($e_f = 1$) of the final parabolic trajectory and by leaving its angular momentum h_f free. Because of this, one can now freely *preassign* the duration of transferring to the final parabola, and thus, for such problems, one can (in principle) make the amount of the required fuel very small by picking a large enough transfer duration. A variation on these problems is the one for which the angular momentum of the final parabola is specified, but its orientation ω_f is left free. This situation is not as practical as the previous one because there is usually a need to specify the orientation ω_f and exit (for example) a planet's sphere of influence with a heliocentric speed having a preassigned direction. A very interesting property of the thrust program proposed in Section 4.3 is the fact that the corresponding exact analytic solution of Section 4.4 satisfies the corresponding transversality condition for both of the above cases. This was shown in some detail in Section 4.6.4.

It will be shown in Section 4.12, that the difficulty in preassigning large transfer durations, associated with one-segment transfers, can be bypassed by allowing multiple-segment transfers, that is, transfers composed of a finite number of segments, on each one of which the throttling parameter A assumes a specific value. If multiple-segment transfers are allowed, then one can in principle still use the thrust program proposed in Eq. (4.10) and preassign arbitrarily large durations for each *individual* segment of a transfer between *any two* given coplanar conics! This result is of great practical importance, because it implies that if one is willing to compromise with respect to the transfer duration and "wait longer" one can still reduce the fuel consumption to very small levels using a power-limited propulsion system and the guidance corresponding to the exact analytic solution of Section 4.4 (see Section 4.12 for more details).

4.7 Boundary Conditions

The boundary conditions for any transfer problem arise from the requirement that the state of the vehicle be continuous at the initial and final times. A "split second" before the initial time $\tau = 0$ the vehicle coasts along a Keplerian conic, specified by its orbital elements h_0, e_0, and ω_0. A "split" second after $\tau = 0$ the thrust is turned on, and the vehicle is on the

transfer trajectory, specified by its integration constants A, B, and C. Similarly, a "split second" before the final time $\tau = \tau_f$ the thrust is turned off, and a "split" second after $\tau = \tau_f$ the vehicle coasts along a Keplerian conic, specified by its orbital elements h_f, e_f, and ω_f. Combining Eqs. (4.16), (4.17), describing the transfer trajectory, and Eq. (A.5), describing a Keplerian conic (see Appendix A), one finds that the following conditions should be satisfied at $\tau = 0$ and $\tau = \tau_f$:

$$r_0 = \frac{h_0^2}{1 + e_0 \cos(\theta_0 - \omega_0)} = \frac{h_0^2}{1 + B\cos(\theta_0 - C)} \qquad (4.119)$$

$$x_0 = \frac{e_0 \sin(\theta_0 - \omega_0)}{h_0} = \frac{2r_0 A + B\sin(\theta_0 - C)}{h_0} \qquad (4.120)$$

$$r_f = \frac{h_f^2}{1 + e_f \cos(\theta_f - \omega_f)} = \frac{h_f^2}{1 + B\cos(\theta_f - C)} \qquad (4.121)$$

$$x_f = \frac{e_f \sin(\theta_f - \omega_f)}{h_f} = \frac{2r_f A + B\sin(\theta_f - C)}{h_f} \qquad (4.122)$$

In addition, one always has the explicit expression for the throttling parameter A:

$$A = \frac{h_f - h_0}{\tau_f} \qquad (4.123)$$

found in Eq. (4.83) from the requirement that $h = h_0$ at $\tau = 0$, and $h = h_f$ at $\tau = \tau_f$.

The final condition arises from the requirement that at the final time $\tau = \tau_f$, one among Eqs. (4.25), (4.26), (4.34), and (4.42) of Section 4.5, relating h with θ along the transfer trajectory, should be satisfied. Only one among these equations applies along a particular transfer, according to whether B=0, B=1, 0<B<1, or B>1 respectively. Note that (see Section 4.5) there is a one-to-one correspondence between the generalized eccentric or hyperbolic anomalies E or H, and the argument of latitude θ or ξ, where $\xi = \theta$-C. Note also, that the generalized hyperbolic anomaly has been denoted by H, since there is no danger of confusion with the Hamiltonian H given in Eq. (4.44) which does not play an important

77

role in this chapter. The conditions given in Eqs. (4.119) through (4.123) can only specify the final values E_f, or θ_f up to a multiple of 2π, that is, one can write:

$$E_f = E_{fP} + 2k\pi \; ; \quad \theta_f = \theta_{fP} + 2k\pi \qquad (4.124)$$

where $k=0,1,2,3,4,...$etc, and E_{fP} and θ_{fP} are between 0 and 2π. Using Eq. (4.124), one can write Eqs. (4.25), (4.26), (4.34), and (4.42) of Section 4.5 at the final time $\tau=\tau_f$ in a *unified* fashion as:

(i) For B=0
$$\frac{\tau_f(h_f + h_0)}{4\pi h_0^2 h_f^2} - \frac{1}{2\pi}(\theta_{fP} - \theta_0) = k \qquad (4.125.a)$$

(ii) For 0<B<1
$$\frac{\tau_f(h_f + h_0)b}{4\pi h_0^2 h_f^2} + \frac{B(\sin E_{fP} - \sin E_0) - (E_{fP} - E_0)}{2\pi} = k \qquad (4.125.b)$$

(iii) For B=1
$$\frac{\tau_f(h_f + h_0)}{4\pi h_0^2 h_f^2} - \frac{(y_f^3 - y_0^3) + 3(y_f - y_0)}{12\pi} = 0 \qquad (4.125.c)$$

(iv) For B>1
$$\frac{\tau_f(h_f + h_0)b}{4\pi h_0^2 h_f^2} - \frac{B(\sin H_f - \sin H_0) - (H_f - H_0)}{2\pi} = 0 \qquad (4.125.d)$$

where, b in Eqs. (4.125.b) and (4.125.d) is defined respectively as:

$$b = (1 - B^2)^{3/2} \quad \text{or} \quad b = (B^2 - 1)^{3/2} \qquad (4.126)$$

and y_f, y_0 in Eq. (4.125.c) are defined as:

$$y_f = \tan\left(\frac{\xi_f}{2}\right); \quad y_0 = \tan\left(\frac{\xi_0}{2}\right) \qquad (4.127)$$

Note that k in Eqs. (4.125.a), (4.125.b) is a nonnegative integer, related directly to the number of revolutions around the planet during the transfer. For the case in which B is less than one, among all the particular solutions satisfying Eqs. (4.119) through (4.123)

only the ones for which the left-hand-side of Eqs. (4.125.a) or (4.125.b) is a nonnegative integer are acceptable. It is clear from Eqs. (4.125) that the time of transfer τ_f and the number of revolutions around the planet during the transfer are intimately connected with each other.

4.8 Transfer from a Circular Orbit to an Arbitrary Conic

For this class of problems the quantities that are *fixed* at the initial and final times are h_0, e_0, h_f, e_f, and ω_f (ω_0 is not defined). The initial conic is assumed to be a circle, meaning that the initial eccentricity is zero. With no loss of generality, due to the circular symmetry of the initial conic, one can assume that the orientation of the final conic is zero. It will also be assumed that h_f is different than h_0. Explicitly, one has:

$$e_0 = 0 \; ; \quad \omega_f = 0 \; ; \quad h_f \neq h_0 \tag{4.128}$$

Taking the above into account, and according to whether h_f is greater or less than h_0, Eqs. (4.119), (4.120) yield:

$$A > 0: \quad r_0 = h_0^2 \; ; \quad \theta_0 - C = -\frac{\pi}{2} \; ; \quad B = 2h_0^2 A \tag{4.129.a}$$

$$A < 0: \quad r_0 = h_0^2 \; ; \quad \theta_0 - C = \frac{\pi}{2} \; ; \quad B = -2h_0^2 A \tag{4.129.b}$$

Using Eqs. (4.129) into Eqs. (4.121), (4.122) one obtains, for both positive or negative A, the conditions:

$$e_f \cos\theta_f = 2h_0^2 A \sin(\theta_f - \theta_0) \tag{4.130}$$

$$e_f \sin\theta_f = 2r_f A - 2h_0^2 A \cos(\theta_f - \theta_0) \tag{4.131}$$

Note that a solution does not exist if $e_f = 0$, that is, if the final conic is also a circular orbit. It will therefore be assumed that $e_f > 0$. The singular case $e_f = 0$ will have to be treated as a limiting case in which e_f is taken as very small. Eqs. (4.130), (4.131) can be combined and solved for the sine and the cosine of θ_f:

$$\sin\theta_f = \frac{2A\left(h_f^2 - h_0^2 e_f \cos\theta_0\right)\left(e_f + 2h_0^2 A\sin\theta_0\right)}{\left(e_f + 2h_0^2 A\sin\theta_0\right)^2 + 4h_0^4 A^2 \cos^2\theta_0} \tag{4.132}$$

$$\cos\theta_f = \frac{2A\left(h_f^2 - h_0^2 e_f \cos\theta_0\right)\left(2h_0^2 A\cos\theta_0\right)}{\left(e_f + 2h_0^2 A\sin\theta_0\right)^2 + 4h_0^4 A^2 \cos^2\theta_0} \tag{4.133}$$

Using now the trigonometric identity:

$$\sin^2\theta_f + \cos^2\theta_f = 1 \tag{4.134}$$

and substituting from Eqs. (4.132), (4.133) into Eq. (4.134) one obtains a condition for the starting value of the argument of latitude θ_0 on the initial circular orbit. Using standard trigonometric identities[33], this condition can be put in the form of a fourth order polynomial equation:

$$b_4 y^4 + b_3 y^3 + b_2 y^2 + b_1 y + b_0 = 0 \tag{4.135}$$

where the unknown y is defined as:

$$y = \tan\left(\frac{\theta_0}{2}\right) \tag{4.136}$$

The coefficients of Eq. (4.135) are given explicitly in Appendix D. Note that, due to the identity expressed in Eq. (4.134), the expressions for the sine and the cosine of θ_f given in Eqs. (4.132) and (4.133) can be considerably simplified and written as:

$$\sin\theta_f = \frac{\left(e_f / 2A\right) + h_0^2 \sin\theta_0}{h_f^2 - h_0^2 e_f \cos\theta_0} \tag{4.137}$$

$$\cos\theta_f = \frac{h_0^2 \cos\theta_0}{h_f^2 - h_0^2 e_f \cos\theta_0} \tag{4.138}$$

The solution methodology for a given problem proceeds in the following fashion: One assumes a value for the final time τ_f and evaluates A from Eq. (4.123), and B from Eq. (4.129). B cannot be zero. Then, solving the polynomial equation (4.135) one finds all the

real roots y, and determines the corresponding starting points θ_0 on the initial circular orbit. Any such θ_0 can be taken (at first) with no loss of generality to be between 0 and 2π, that is, $0 \leq \theta_0 < 2\pi$. For every such θ_0, Eqs. (4.137), (4.138) fix the corresponding θ_f up to a multiple of 2π. That is, $\theta_f = \theta_{fp} + 2k\pi$, with $0 \leq \theta_{fp} < 2\pi$, and k=0,1,2,3,...etc. If $B \geq 1$, then k=0 and one checks whether the left-hand-side of Eq. (4.125.c or d) is zero. If B<1, then one checks whether the left-hand-side of Eq. (4.125.b) is equal to zero or a positive integer. If not, one repeats the procedure with a new value of τ_f. Therefore, one way of finding all the possible solutions for a given problem is to plot the left-hand-side of Eq. (4.125) as a function of τ_f, and for all the real roots of Eq. (4.135). The values of τ_f (for 0<B<1) for which this plot intersects any positive integer (k=1,2,3,...), plus the values of τ_f (for B>0) for which it intersects zero (k=0) represent the candidate solutions to a given problem. For k=0 the starting point on the initial circular orbit is either θ_0, or θ_0-2π. Each such candidate value of τ_f is a *real* solution *only if* the transition from the starting point to the final point can be made without going through a value of θ at which the angular momentum h, evaluated through the applicable one among Eqs. (4.25), (4.26), (4.34), and (4.42), becomes infinite. For each such value of τ_f representing a real solution the corresponding value of k fixes both the value of θ_f and the number of full revolutions around the planet during the transfer. The transfer problem is then completely solved, that is, everything related to the transfer can be easily calculated.

One may argue that the problem with the above procedure is that, to find all the possible solutions, one will have to plot Eq. (4.125) for τ_f between 0 and ∞! However, after working on specific problems for a while, it becomes apparent that, except for the case of transfers between a circular and a very nearly circular orbit, the interval of values of τ_f for which Eq. (4.135) has real roots is very limited. However, it has not been proven in this chapter that solutions for much higher values of τ_f do not exist, and this topic may deserve some further consideration in the future. An example of a transfer between a circular and a very nearly circular (e_f=0.05) orbit is given in Figs. 4.6 and 4.7. From Fig. 4.6 it is seen that there are 9 solutions for this example. The actual transfer (Eq. (4.17)) corresponding to the solution with k=10 is plotted in Fig. 4.7. It is interesting to remark here that if one starts reducing the eccentricity of the final orbit toward zero, then, both the number of solutions and the corresponding transfer durations greatly increase. This fact is vividly depicted in Figs. 4.8 through 4.11, for which e_f is equal respectively to 0.01, 0.005, 0.001, and 0.0005. Since h_f is still equal to 2, Figs. 4.8 through 4.11 basically correspond to (practically) the same transfer problem defined in Fig. 4.6. Thus, in practice,

for the case of transfers between two coplanar circular orbits, by playing around with the (very small) value of e_f one can find (one-segment) transfer solutions of arbitrarily large transfer duration. This result has important practical implications from the point of view of power-limited optimality and fuel consumption and more will be said on it in Section 4.12. The case of transferring between two coplanar circular orbits, along with a complete mathematical description of what happens as e_f tends to zero, is given in Appendix D. Note that when $e_f = 0$ Eq. (4.135) has no real solution. In fact, when e_f is *exactly* equal to zero, to satisfy this polynomial equation one must perform the transfer in infinite time using zero thrust. The case with $e_f = 0$ is thus clearly a singular case. Figures 4.12 through 4.17 supply three examples of transfers (Eq. (4.17)) to elliptic orbits of low and high eccentricities and to a hyperbolic conic. It appears that, as the eccentricity of the final conic increases, the number of (one-segment) solutions decreases (very fast), but does not go to zero. As long as the final conic does not intersect the initial conic (see Section 4.11) there always seems to be at least one (one-segment) solution.

4.9 Escape from a Circular Orbit

Escape problems are just a special case of transfer problem, in which the primary aim is to escape from the gravitational attraction of a planet[34]. This can be done by transferring to an open conic for which the eccentricity e_f is greater than or equal to one[34]. For $e_f > 1$ the vehicle escapes with finite speed at infinity[34]. For $e_f = 1$ the vehicle escapes with zero speed at infinity[34]. Accordingly, from an energy point of view, the cheapest way to escape is by transferring to a conic for which $e_f = 1$. The actual final value h_f of the angular momentum of the vehicle is not important and can be left free. Then, as was seen in Section 4.6.4, as long as $e_f = 1$, the corresponding transversality condition (Eqs. (4.109), (4.116)) is automatically satisfied. Thus, for an escape problem from a circular orbit, it will be assumed that the quantities that are *fixed* at the initial and final times are h_0, e_0, $e_f = 1$, and $\omega_f = 0$; ω_0 is not defined, while h_f is left free. The important difference between such problems and the transfer problems considered in Section 4.8 is that now, solutions may exist (in principle) for *any* value of τ_f. This is so, because the free final value of the angular momentum h_f now plays (technically) the same role that the time of transfer τ_f played in Section 4.8. Physically, escape can be achieved at any desired final time by appropriately selecting the constant A, so that the mechanical energy (per unit mass) of the system is increased at the correct (mean) rate. Thus, the solution methodology for a given escape

82

problem is basically identical to the one given in Section 4.8. The difference is that instead of plotting the left-hand-side of Eq. (4.125) as a function of τ_f, one now plots it as a function of h_f. Figure 4.18 supplies the plot of the left-hand-side of Eq. (4.125) for such an escape problem. The transfer trajectory (Eq. (4.17)) corresponding to point S in Fig. 4.18, with k=3, is plotted in Fig. 4.19, along with the initial (circular) and the final (parabolic) conic.

4.10 Transfer Between two Arbitrary Conics, and Escape from an Elliptic Orbit

The more general problems relating to transfers between two arbitrary conics and to escape from an elliptic orbit can be treated basically in exactly the same way as the corresponding problems of Sections 4.8 and 4.9. However, the corresponding algebra is considerably more involved.

For this class of problems the quantities that are *always fixed* at $\tau=0$ and at $\tau=\tau_f$ are respectively h_0, e_0, ω_0, and e_f. For transfer problems h_f and ω_f are also fixed, and (one-segment) solutions exist only for particular values of τ_f. For escape problems the initial conic is assumed to be an ellipse ($e_0<1$), h_f is free, $e_f=1$, and (one-segment) solutions (in principle) exist for any value of τ_f. With no loss of generality one can always assume that $\omega_0=0$, that is, the orientation of the initial conic is zero. From Eqs. (4.119) through (4.122) one then obtains:

$$e_0 \cos\theta_0 = B\cos(\theta_0 - C) \tag{4.139}$$

$$e_0 \sin\theta_0 = 2r_0 A + B\sin(\theta_0 - C) \tag{4.140}$$

$$e_f \cos(\theta_f - \omega_f) = B\cos(\theta_f - C) \tag{4.141}$$

$$e_f \sin(\theta_f - \omega_f) = 2r_f A + B\sin(\theta_f - C) \tag{4.142}$$

From Eqs. (4.139) and (4.141) B can be expressed as:

83

$$B = \frac{e_0 \cos\theta_0}{\cos(\theta_0 - C)} = \frac{e_f \cos(\theta_f - \omega_f)}{\cos(\theta_f - C)} \qquad (4.143)$$

With no loss of generality one may assume that $0 \le C < 2\pi$. The equality on the right in Eq. (4.143) can be solved for the tangent of C to yield:

$$\tan C = \frac{e_0 \cos\theta_0 \cos\theta_f - e_f \cos(\theta_f - \omega_f)\cos\theta_0}{e_f \cos(\theta_f - \omega_f)\sin\theta_0 - e_0 \cos\theta_0 \sin\theta_f} \qquad (4.144)$$

Equation (4.144) supplies two roots for C in $0 \le C < 2\pi$. The possible solution(s) for C are the one(s) for which B is nonnegative. The remaining steps are algebraically quite intense. First, substituting from Eqs. (4.143), (4.144) into Eqs. (4.139)-(4.142) one can solve for the sine and the cosine of θ_f as:

$$\sin\theta_f = \frac{N_1}{N_3} \quad ; \quad \cos\theta_f = \frac{N_2}{N_3} \qquad (4.145)$$

where the quantities N_1, N_2, and N_3 are given by:

$$N_1 = 2h_0^2 A \sin\theta_0 + (1 + e_0 \cos\theta_0)(e_f \cos\omega_f - e_0) \qquad (4.146)$$

$$N_2 = 2h_0^2 A \cos\theta_0 - (1 + e_0 \cos\theta_0)e_f \sin\omega_f \qquad (4.147)$$

$$N_3 = (2h_f^2 A + e_0 e_f \sin\omega_f)(1 + e_0 \cos\theta_0) - 2h_0^2 A e_f \cos(\theta_0 - \omega_f) \qquad (4.148)$$

Then, using the trigonometric identity:

$$\sin^2\theta_f + \cos^2\theta_f = 1 \qquad (4.149)$$

and substituting from Eqs. (4.145)-(4.148) into Eq. (4.149) results in a condition for the starting point θ_0 on the initial conic. Using standard trigonometric identities[33], this condition can again (see Eq. (4.135)) be put in the form of a fourth order polynomial equation:

$$b_4 y^4 + b_3 y^3 + b_2 y^2 + b_1 y + b_0 = 0 \qquad (4.150)$$

84

C-2

where the unknown y is (see Eq. (4.136)) defined as:

$$y = \tan\left(\frac{\theta_0}{2}\right) \qquad (4.151)$$

The coefficients of Eq. (4.150) are given explicitly in Appendix E.

Note that for $e_0 = \omega_f = 0$ the results of the present section reduce to the corresponding results of Section 4.8, valid for transfers and escapes from a circular orbit.

The solution methodology for a given transfer or escape problem is more or less identical to the one given at the end of Section 4.8, with the analogies involved being too obvious to go through in detail once again. The left-hand-side of Eq. (4.125) can always be plotted as a function of τ_f or h_f to determine the candidate solutions. However, due to the well-defined orientation difference between the initial and final conics, there arises in this case another possibility for escape problems that is worth exploring. If one chooses to leave this orientation difference free, then one may consider escape problems with fixed τ_f and h_f. Recall that in such a case the *exact optimal* value of P_θ is zero (see Eq. (4.110)), that is, P_θ is not zero just because of the tangential thrust assumption. For escape problems in which ω_f is left free the candidate solutions are determined by plotting the left-hand-side of Eq. (4.125) as a function of ω_f, and only for $0 \le \omega_f < 2\pi$.

A transfer example between two elliptic orbits, involving no orientation change, is supplied in Figs. 4.20, 4.21. One must note here that for transfers between two coplanar elliptic orbits having the same orientation the number of (one-segment) solutions and the corresponding transfer durations greatly increase as the final eccentricity e_f approaches the initial eccentricity e_0. This situation is similar to the one corresponding to transfers between two coplanar circular orbits (see Section 4.8), and is depicted clearly in Figs. 4.22, 4.23. The solution search conducted in Figs. 4.22, 4.23 corresponds practically to the *same* transfer problem. An actual transfer corresponding to either Fig. 4.22 or Fig. 4.23 is not shown. Figures 4.24, 4.25 supply a transfer example between two elliptic orbits, involving a large orientation change. Figures 4.26, 4.27 supply a transfer example from an elliptic orbit to a hyperbolic trajectory, while Figs. 4.28, 4.29 supply a transfer example between two hyperbolic trajectories. The jump of magnitude 1.0 that appears whenever the left-hand-side of Eq. (4.125) is plotted is due to the fact that all such plots are done with $0 \le \theta_0 < 2\pi$, and $0 \le \theta_{fp} < 2\pi$. A maneuver such as the one given in Fig. 4.29 could play an important role during a planetary encounter, in which, having control over the vector of

85

heliocentric velocity of a vehicle at the exit of a planet's sphere of influence (Jupiter for example) is most desirable for setting up the next (planetary) encounter (with Saturn, Uranus, Neptune, etc.).

Figures 4.30 and 4.31 supply two solutions for an escape problem from an elliptic orbit for which the orientation of the final parabolic trajectory is left free. The solution that is cheaper, both in the power-limited and the constant ejection velocity sense, is the one given in Fig. 4.30, corresponding to $\omega_f \approx 0$ (see Table 4.1, Section 4.13). Note that the plot of the left-hand-side of Eq. (4.125) as a function of ω_f is not shown for this problem.

This section concludes on the note that, as long as the final conic does not intersect the initial conic, there always seems to be at least one (one-segment) solution for the corresponding (transfer or escape) problem.

4.11 Existence of One-Segment Solutions, and some Geometric Considerations

The search in the previous three sections was for *one-segment solutions* to given transfer or escape problems, that is, trajectories on which the throttling parameter A had a *single* value. An *n-segment solution* (n=1,2,3,...) will henceforth denote a trajectory on which the value of A switches n-1 times in $0 < \tau < \tau_f$. Note that there is really no reason to refer to escape problems explicitly, since escape problems are just a special kind of transfer problem. Thus, for simplicity, one-segment solutions will henceforth be referred to just as "transfers", or as "one-segment transfers". Before discussing the existence of such transfers it will be helpful to adopt some notational conventions. For any transfer problem the word "from" will always be associated with the initial conic (at the initial time) and the word "to" with the final conic (at the final time). The quadruplet (h,e,ω,θ) will be used to denote a (Keplerian) conic with orbital constants h, e, and ω, with θ fixing the point of departure "from" or arrival "to" the conic. If the conic is a circle the second entry will be zero and the third entry will be a dash. Sometimes the fourth entry may be omitted and a conic be denoted by the triplet (h,e,ω). Similarly, a one-segment transfer with constants $A \neq 0$, B, C, and time duration $\tau_f > 0$, will be denoted by the quadruplet (A,B,C,τ_f), or by the triplet (A,B,C).

Let now P be any point on a transfer trajectory (A,B,C), and let h, x, r, θ be the state components at P. If the thrust were suddenly turned off at P, the motion that would follow after P would be Keplerian. The orbital elements of this Keplerian motion define the so-

86

called[34] *instantaneous conic* (h,e,ω) at P. One can also define the *associated conic* at P to be the conic (h,B,C). The associated conic (h$_0$,B,C) at τ=0 will be called the *initial associated conic* and the associated conic (h$_f$,B,C) at τ=τ$_f$ will be called the *final associated conic*. Figures 4.32 and 4.33 show the initial (AC0) and final (ACf) associated conics for the transfer examples given in Figs. 4.21 and 4.25.

It is now possible to supply a few lemmas, related to the geometry of motion and the existence of one-segment transfers. It will henceforth be tacitly assumed that the motion along any transfer is performed under the thrust program proposed in this chapter (Eq. (4.10)), and that the initial and final conics are *different*. A detailed proof for a lemma will be supplied only when absolutely necessary. The proof of the following four lemmas is elementary.

Lemma 4.1. A one-segment transfer trajectory (A,B,C,τ$_f$) can never intersect itself.

Lemma 4.2. If (A,B,C,τ$_f$) is a transfer from conic (h$_0$,e$_0$,ω$_0$,θ$_0$) to conic (h$_f$,e$_f$,ω$_f$,θ$_f$), then (A,B,C,τ$_f$) is also a transfer from conic (-h$_f$,e$_f$,ω$_f$,θ$_f$) to conic (-h$_0$,e$_0$,ω$_0$,θ$_0$).

Lemma 4.3. If a vehicle takes off at τ = 0 from a point K of a circular orbit (h$_0$,0,-,θ$_0$) along a one-segment transfer trajectory (A > 0,B,C,τ$_f$), and if at time τ > 0 the vehicle is at point L, then, the distance KL is equal to (e/2A), where e is the eccentricity of the instantaneous conic at L (see Fig. 4.34).

Lemma 4.4. Consider a vehicle that takes off at τ = 0 from a conic (h$_0$,e$_0$,ω$_0$,θ$_0$) along a one-segment transfer trajectory (A > 0,B,C,τ$_f$), and draw a vector with origin at the center of the planet, of magnitude (B/2A) and direction C-(π/2). Let K be the endpoint of this vector. Then,

(i) If M is the point of departure of the vehicle from conic (h$_0$,e$_0$,ω$_0$,θ$_0$), then the distance MK is equal to (e$_0$/2A) (see Fig. 4.35).

(ii) If at time τ > 0 the vehicle is at point L, then the distance KL is equal to (e/2A), where e is the eccentricity of the instantaneous conic at L (see Fig. 4.35).

The proof for Lemma 4.1 is obtained by considering the trajectory equation (Eq. (4.17)). The proof for Lemma 4.2 is obtained by considering Eqs. (4.119)-(4.122). The proof for Lemmas 4.3 and 4.4 is obtained by considering Eqs. (4.130), (4.131), (4.139)-(4.142), dropping the subscript f from Eqs. (4.141), (4.142), and using the law of cosines[33].

Lemma 4.5. A one-segment transfer (A,B,C,τ_f) from conic $(h_0,e_0,\omega_0,\theta_0)$ to conic $(h_f,e_f,\omega_f,\theta_f)$ does not exist if at least one among the following two equalities is valid:

$$h_0 = h_f \; ; \quad \frac{h_0^2}{1-e_0^2} = \frac{h_f^2}{1-e_f^2} \tag{4.152}$$

Proof 4.5. If the equality on the left is valid then A=0 and the motion is Keplerian. If the equality on the right is valid then the orbital energy of the two conics is the same[34] (see Eqs. (A.7), (A.9)), contradicting the fact that for nonzero A the orbital energy either increases or decreases (strictly monotonically) on a one-segment trajectory (Q.E.D.).

Note that if at least one among the equalities given in Eq. (4.152) is true, then the initial and final conics *intersect*. This fact, combined with one's previous experience with specific examples, leads one to suspect that Lemma 4.5 is most probably a particular case of a more general result: One-segment solutions actually don't exist when the initial and final conics intersect. For example, consider the problem of transfer between two hyperbolic conics (see Fig. 4.36) having the same eccentricities, different (but both positive) angular momenta, and opposite orientations $(\omega_f = \omega_0 - \pi)$. It appears that it is impossible to construct a one-segment transfer trajectory that joins these two conics. Due to the tangential character of the thrust, the vehicle, approaching from leg a of the initial hyperbola cannot transfer to leg d of the final hyperbola unless it executes at least one full revolution around the planet. But this implies an initial capture, energy loss, and a negative value of A. The subsequent transfer to leg d of the final hyperbola implies a final escape, energy gain, and a positive value of A.

Lemma 4.6. The instantaneous conic (h,e,ω) and the associated conic (h,B,C) (at the same instant) have always two and only two points in common. At any instant of time along a transfer (A,B,C,τ_f) the vehicle occupies one of those two points and has velocity that is tangential to the instantaneous conic.

Proof 4.6. (h,e,ω) and (h,B,C) are two conics having the same angular momentum but *different* eccentricities and orientations (Q.E.D.).

The following lemma can be proved by considering Eq. (4.17).

Lemma 4.7. A one-segment transfer (A,B,C,τ_f) from conic $(h_0,e_0,\omega_0,\theta_0)$ to conic $(h_f,e_f,\omega_f,\theta_f)$ has no common points with either the initial, (h_0,B,C), or the final, (h_f,B,C), associated conic for $0 < \tau < \tau_f$.

A fact that is intuitively obvious, but the proof of which is not trivial, is provided by the lemma that follows.

88

Lemma 4.8. Let (A,B,C,τ_f) be a one-segment transfer from conic $(h_0,e_0,\omega_0,\theta_0)$ to conic $(h_f,e_f,\omega_f,\theta_f)$, and let τ_1 and $\tau_1+d\tau$ be two infinitesimally separated time instants in $0<\tau<\tau_f$. Then, the instantaneous conic $(h_1,e_1,\omega_1,\theta_1)$, and the instantaneous conic $(h_1+\Delta h,e_1+\Delta e,\omega_1+\Delta\omega,\theta_1+\Delta\theta)$, associated with the transfer trajectory at the instants τ_1 and $\tau_1+d\tau$ respectively, can have at most one common point.

Proof 4.8. The trajectory equations corresponding to the two instantaneous conics are given by:

$$r = \frac{h_1^2}{1+e_1\cos(\theta-\omega_1)} \tag{4.153}$$

$$r = \frac{(h_1+\Delta h)^2}{1+(e_1+\Delta e)\cos(\theta-\omega_1-\Delta\omega)} \tag{4.154}$$

To first order in $d\tau$ the changes in the orbital elements h_1, e_1, and ω_1 can be found as[34]:

$$\Delta h = Ad\tau \tag{4.155}$$

$$\Delta e = \frac{2A[e_1+\cos(\theta_1-\omega_1)]}{h_1}d\tau \tag{4.156}$$

$$\Delta\omega = \frac{2A\sin(\theta_1-\omega_1)}{e_1h_1}d\tau \tag{4.157}$$

Equating the right-hand-sides of Eqs. (4.153), (4.154), using Eqs. (4.155)-(4.157), and expanding in Taylor series the terms $\sin(\Delta\omega)$ and $\cos(\Delta\omega)$ one finds that to first order in $d\tau$ the following equality must be valid:

$$[\cos(\theta-\theta_1)-1]d\tau = 0 \tag{4.158}$$

for *arbitrary*, but infinitesimally small $d\tau$. This implies that the two conics can have at most one common point, corresponding to $\theta=\theta_1$ in $0\le\theta<2\pi$ just as the lemma claims (Q.E.D.).

Along a one-segment transfer trajectory the mechanical energy and angular momentum (per unit mass) associated with the instantaneous conic either increase $(A > 0)$

or decrease $(A < 0)$ strictly monotonically with time. Thus, Lemma 4.8 implies the lemma that follows, which is basically a companion to Lemma 4.7.

Lemma 4.9. A one-segment transfer (A,B,C,τ_f) from conic $(h_0,e_0,\omega_0,\theta_0)$ to conic $(h_f,e_f,\omega_f,\theta_f)$ has no common points with either $(h_0,e_0,\omega_0,\theta_0)$ or $(h_f,e_f,\omega_f,\theta_f)$ for $0 < \tau < \tau_f$.

Lemmas 4.7 and 4.8 suggest that for $A > 0$ a one-segment transfer trajectory always stays "outside" the initial and the initial associated conics, and "inside" the final and the final associated conics. Analogous observations can be made also for $A < 0$. When the initial and final conics do not intersect the allowable space for the transfer trajectory has the shape of a "ring" (see Figs. 4.32, 4.33). However, as the initial and final conics come closer and closer toward intersecting each other, this allowable space is constrained considerably (see Fig. 4.33), and after the intersection it is cut-off, that is, it looses its "ring" character.

The above considerations, and in particular Lemmas 4.7, 4.8, and 4.9, point toward the following underlying theorem:

Theorem 4.1. Consider the problem of transferring from conic $(h_0,e_0,\omega_0,\theta_0)$ to conic $(h_f,e_f,\omega_f,\theta_f)$ using the thrust program proposed in Eq. (4.10) and the corresponding exact analytic solution of Section 4.4. Then,

(i) If $(h_0,e_0,\omega_0,\theta_0)$ and $(h_f,e_f,\omega_f,\theta_f)$ have more than one common point (that is, if they intersect), then a one-segment transfer solution does not exist.

(ii) If $(h_0,e_0,\omega_0,\theta_0)$ and $(h_f,e_f,\omega_f,\theta_f)$ have only one common point (a point of tangency) then there exists at most *a single impulsive* one-segment transfer solution, performed at the point of tangency of the two conics, for which A is infinitely large, τ_f is infinitely small, and $A\tau_f$ is finite and equal to h_f-h_0.

The proof of Theorem 4.1 is rather lengthy and is given in Appendix F *without* using any of Lemmas 4.7, 4.8, or 4.9. In fact, the proof given in Appendix F can also be considered to be an indirect proof for Lemmas 4.8 and 4.9.

Before closing this section one can also state the following conjecture, that the author feels is true, having to do with the existence of one-segment and two-segment solutions.

Conjecture. Consider the problem of transferring from conic $(h_0,e_0,\omega_0,\theta_0)$ to conic $(h_f,e_f,\omega_f,\theta_f)$ using the thrust program proposed in Eq. (4.10) and the corresponding exact analytic solution of Section 4.4. Then,

(i) A two-segment transfer solution always exists.

(ii) A one-segment transfer solution (A,B,C,τ_f) with finite A and $\tau_f > 0$ exists if and only if $(h_0,e_0,\omega_0,\theta_0)$ and $(h_f,e_f,\omega_f,\theta_f)$ have no common point.

Note that in case (i) above the selection of the intermediate instantaneous conic at the point where the switching of the value of A occurs is not unique but will most probably have to be decided on the basis of optimality. Figures 4.37 and 4.38 supply two examples of two and three-segment transfers respectively. Figure 4.37 corresponds to a situation similar to the one given in Fig. 4.36. In Fig. 4.38 there is an intermediate transfer segment, KS, which is shown with dotted line, which corresponds to zero thrust (A=0) and Keplerian motion along a circular orbit.

4.12 When is it Possible to Preassign Arbitrarily Large Transfer Durations?

If multiple-segment transfers are allowed, the answer to the above question is: *Always*. Before expanding on this issue however, and explaining its practical importance, it is insightful to make a few comments concerning the behavior of the thrust acceleration along a one-segment transfer. Recall that the angular momentum of the vehicle is given by $h = rV\cos\gamma$, where, V is the speed of the vehicle, given by Eq. (A.8) in Appendix A. Using the components given in Eq. (4.10), the thrust acceleration corresponding to the proposed (tangential) thrust program can be written as:

$$\epsilon = \sqrt{\epsilon_r^2 + \epsilon_\theta^2} = \frac{AV}{h} = \frac{A}{r\cos\gamma} \tag{4.159}$$

Squaring and differentiating the right-hand-side of Eq. (4.159), and then using Eqs. (4.11) through (4.14), the first and second time derivatives of $(\epsilon^2/2)$ can be found as:

$$\frac{d}{d\tau}\left(\frac{\epsilon^2}{2}\right) = -\frac{A^2 x}{h^2 r^2} \quad ; \quad \left[\frac{d^2}{d\tau^2}\left(\frac{\epsilon^2}{2}\right)\right]_{x=0} = -\frac{A^2 \dot{x}}{h^2 r^2} \tag{4.160}$$

where, the second derivative was evaluated at the points where x is zero. From Eq. (4.160) one can conclude that the thrust acceleration has a (local) maximum at the successive perigees and a local minimum at the successive apogees of an (osculating) one-segment transfer trajectory. Figures 4.39 and 4.40 supply the variation of $(\epsilon^2/2)$ with τ and θ respectively for the transfer example of Fig. 4.2. Note how the variation in Fig. 4.39 resembles a series of impulses delivered at the successive perigees of the (osculating) transfer trajectory.

Using Eq. (159), and the expression for A found in Eq. (4.83), the power-limited cost associated with a one-segment transfer can be written as:

91

$$J_{PL} = \frac{1}{2} \int_0^{\tau_f} \varepsilon^2 d\tau = \frac{A^2}{2} \int_0^{\tau_f} \frac{d\tau}{r^2 \cos^2 \gamma} = \frac{(h_f - h_0)^2}{2\tau_f^2} \int_0^{\tau_f} \frac{d\tau}{r^2 \cos^2 \gamma} \qquad (4.161)$$

This expression can be further manipulated into:

$$J_{PL} = \frac{(h_f - h_0)^2}{2\tau_f} \times \left(\text{average value of } \frac{1}{r^2 \cos^2 \gamma} \text{ along the transfer} \right) \qquad (4.162)$$

The average value of $(1/r^2\cos^2\gamma)$ along a one-segment transfer remains a well-behaved quantity as the duration of transfer τ_f tends to infinity. Thus, as τ_f tends to infinity, the power-limited cost associated with a one-segment transfer tends to zero. This behavior compares well with the behavior of the *optimal* cost, since it is well-known[42-51], that the *optimal* power-limited cost for a given transfer problem is inversely proportional to the transfer duration, and tends to zero as the transfer duration tends to infinity. For a multiple-segment transfer the power-limited cost is given by a summation of terms similar to the one appearing on the right-hand-side of Eq. (4.162). Thus, for a multiple-segment transfer, if it is still possible to preassign large durations for each *individual* segment, then, the total fuel consumption can still be made very small, but at the expense of waiting longer for completing the (overall) transfer. Thus, whether it is possible to preassign arbitrarily large transfer durations or not is an important practical issue. By recalling the results of Sections 4.6.5, and 4.8 through 4.10, one can now distinguish between the following three cases:

(i) **Escape problems:** For all such problems it is possible to use a one-segment transfer trajectory. Because the final value of the angular momentum h_f is left free, the time duration τ_f for transferring to the final parabolic trajectory can in principle be freely preassigned. As this time duration tends to infinity the one-segment transfer and the corresponding power-limited cost asymptotically tend to the optimal transfer and the optimal power-limited cost respectively.

(ii) **Transfer between two coplanar circular orbits:** For this problem it is still possible to use a one-segment transfer trajectory. A small transfer duration τ_f in this case does not exist. However, a large transfer duration τ_f can still be preassigned (see Section 4.8 and Appendix D). Again, as this time duration tends to infinity this one-segment transfer and the corresponding power-limited cost asymptotically tend to the optimal transfer and the optimal power-limited cost respectively.

(iii) Transfer between two arbitrary conics: For this problem it is not in general possible to use a one-segment transfer trajectory. However, it is in principle possible to perform the overall transfer using a multiple-segment transfer trajectory, for which one can still preassign arbitrarily large durations for each segment. For example, a vehicle can first transfer to an intermediate closed orbit in time τ_{f1}, and then, after coasting for some time τ_{f2} on this intermediate closed orbit, it can transfer to the desired final conic in time τ_{f3}, where, the sum of τ_{f1}, τ_{f2}, and τ_{f3} is equal to τ_f. The fact that the angular momentum, the eccentricity, and the orientation of the intermediate closed orbit may be left free is what makes it possible to preassign arbitrarily large durations τ_{f1} and τ_{f3}. This of course is not the only way to perform a transfer between two arbitrary conics in an arbitrarily large duration, and, with a little imagination, the reader can come up with some more ways for himself.

4.13 Optimality of the Trajectories

In this section, hints will be provided, suggesting that there should be cases in which the (tangential) thrust program proposed in this report (see Eqs. (4.10), (4.159)) results in sufficiently optimal trajectories, both for power-limited (PL) and constant ejection velocity (CEV) systems.

The thrust program was obtained by using the tangential thrust assumption in the problem corresponding to minimum-fuel PL transfers. Numerical optimizations[44,45,47,49-51] for such problems tend to suggest strongly, that there exists a large subclass of PL transfers between two coplanar elliptic orbits, corresponding mainly to cases where the changes in orientation and eccentricity are small, for which, as the duration of transfer increases, the thrust levels decrease, and the direction of the optimal thrust acceleration tends more or less to coincide with the direction of the tangent to the optimal flight path throughout the transfer. This leads one to expect that this thrust program (Eqs. (4.10), (4.159)) should turn out to be sufficiently optimal for at least some of these cases. An important subclass of such problems is the one corresponding to transfers between two circular orbits, and in this class, as was seen in Section 4.8, this thrust program is capable of resulting in solutions of very large duration. Also, as was seen in Sections 4.9 and 4.10, for escape problems from an arbitrary elliptical orbit, if one leaves either the angular momentum h_f, or the orientation ω_f of the final parabolic trajectory free, then one has the freedom to *preassign* the duration of the maneuver, making the thrust levels as small as one

wishes. To summarize, it appears that the best starting point for evaluating the performance of the thrust program (Eqs. (4.10), (4.159)) in the PL sense is to compare the exact optimal PL cost with the PL cost corresponding to the thrust program given in Eqs. (4.10), (4.159), first, for long duration escape problems from an arbitrary elliptical orbit, then, for long duration transfers between two coplanar circular orbits, and then, for transfers between two coplanar, nonintersecting elliptical orbits having the same orientation.

Based primarily on the results of Section 4.6.5, one could go as far as to conjecture here that, for power-limited, long duration (more than three or four revolutions around the planet) escape problems, and for long duration transfers between two coplanar circular orbits, the exact analytic solution of Section 4.4 must be very close to the *exact optimal* solution.

A really interesting question is the optimality of the thrust program given in Eqs. (4.10), (4.159) with regard to *other* than power-limited propulsion systems. The costs corresponding to PL and CEV systems along any maneuver lasting for a time duration τ_f are given respectively by[46,48]:

$$J_{PL} = \int_0^{\tau_f} \frac{\varepsilon^2}{2} d\tau \quad ; \qquad J_{CEV} = \int_0^{\tau_f} \varepsilon \, d\tau \qquad (4.163)$$

Table 4.1 supplies the PL and CEV costs for all the transfer trajectories given in the examples, as well as the corresponding initial and final values of the (nondimensional) thrust acceleration (Eq. (4.159)) ε_0 and ε_f for each trajectory. These costs were obtained by numerically evaluating the integrals in Eq. (4.163) along the (exact analytic) trajectories using a Simpson's Multiple-Segment 1/3 routine[54].

The PL cost in Table 4.1 is given for any future comparisons with the optimal costs corresponding to the exact optimal PL transfers. The CEV cost is given because it will now be compared with the cost corresponding to Hohmann (HM) and Biparabolic (BP) transfers[34,48] between the same initial and final conics for some of the examples. The Hohmann transfer is basic in the theory of impulsive transfers[34,48] and for coplanar orbits having the same orientation is performed (see Fig. 4.41) via two impulsive, tangential speed changes (ΔV's) at the perigee of the initial orbit and the apogee of the final orbit[34,48]. The perigee and apogee of an HM transfer orbit thus coincide with the perigee of the initial and the apogee of the final orbit, respectively. The BP transfer (see Fig. 4.42) is performed

Table 4.1 PL and CEV costs along the transfers

Transfer	ε_0	ε_f	J_{PL}	J_{CEV}
Fig. 4.2	5.9500e-3	2.9355e-3	1.5369e-4	1.2861e-1
Fig. 4.3	2.5500e-2	9.6038e-3	7.3223e-4	1.6795e-1
Fig. 4.4	5.9500e-2	7.0071e-3	3.9537e-3	4.1077e-1
Fig. 4.5	1.5610e-2	2.4088e-2	3.7966e-3	3.0343e-1
Fig. 4.7	6.1139e-3	1.5127e-3	8.9225e-4	5.0001e-1
Fig. 4.13	3.6210e-2	9.0432e-3	5.4860e-3	5.0993e-1
Fig. 4.15	1.0542e-1	5.5871e-2	1.7064e-2	3.9424e-1
Fig. 4.17	1.0131e-1	3.4644e-2	2.0457e-2	5.9559e-1
Fig. 4.19	2.9601e-2	2.6492e-3	5.0593e-3	7.8669e-1
Fig. 4.21	5.9693e-3	1.9951e-3	1.4626e-4	1.6022e-1
Fig. 4.25	7.7549e-3	1.1576e-3	3.0947e-4	1.7577e-1
Fig. 4.27	7.2092e-3	6.4353e-3	2.6292e-3	4.5698e-1
Fig. 4.29	2.8987e-2	3.4832e-2	1.3490e-2	8.1437e-1
Fig. 4.30	5.0729e-3	1.3587e-3	5.7875e-4	3.7680e-1
Fig. 4.31	1.5905e-2	7.4914e-4	6.4252e-4	3.7963e-1
Fig. 4.37	1.5000e-1	7.6719e-2	6.7975e-2	1.1451e+0
Fig. 4.38	9.8358e-3	5.7974e-3	1.6055e-3	4.7716e-1

by transferring to an (outgoing) parabola with an impulsive, tangential ΔV at the perigee of the initial orbit, then transferring to an (incoming) parabola at infinite distance from the planet (which takes zero cost) and then transferring to the final orbit with an impulsive, tangential ΔV applied at the perigee of the final orbit[48]. The BP transfer is only of theoretical importance because it takes infinite time to perform. Due to the impulsive character of the thrust, from Eq. (4.163), the cost for a HM or BP transfer is just the sum of the two impulsive speed changes required to perform the transfer. Table 4.2 compares the HM and BP costs for the transfers corresponding to Figs. 4.7, 4.13, 4.15, 4.21, and 4.38 with the CEV cost corresponding to the present thrust program (second column), which is reproduced from Table 4.1. For Figs. 4.7, 4.13, 4.15, and 4.21 the HM cost is the minimum CEV cost possible[48] and one can see that the cost corresponding to the present thrust program is about 10 to 20 percent more than the HM cost for Figs. 4.7, 4.13, and 4.15, 120 percent more for Fig. 4.21, but mostly less than the BP cost, except for Fig. 4.21. For Fig. 4.38 the BP cost is the minimum CEV cost possible[48] and, instead of the

HM cost, Table 4.2 supplies the symmetric AD cost which corresponds to the sum of two impulsive, tangential ΔV's, the first accelerating, the second decelerating, applied at the apogees of the initial and final elliptic orbits respectively. The transfer trajectory in this case is a circular orbit. This symmetric AD transfer, contrary to the BP transfer, is quite a practical one[48], and one can see from Table 4.2 that the cost corresponding to the present thrust program for Fig. 4.38 is about 10 percent more than the corresponding symmetric AD cost.

Table 4.2 Hohmann and Biparabolic CEV costs*

Transfer	Present J_{CEV}	Hohmann	Biparabolic
Fig. 4.7	5.0001e-1	4.4868e-1	6.2132e-1
Fig. 4.13	5.0993e-1	4.2351e-1	5.6080e-1
Fig. 4.15	3.9424e-1	3.5130e-1	5.1015e-1
Fig. 4.21	1.6022e-1	7.3568e-2	9.8042e-2
Fig. 4.38	4.7716e-1	4.3246e-1*	9.8718e-2

The above comparisons were supplied with the hope that they may convince some investigators that the near-optimality of the proposed thrust program in the CEV sense may deserve some further consideration.

4.14 The Rendezvous Problem

This last section constitutes a small deviation from the main subject (of transfers) and discusses the possibility of using the results of Section 4.6.2 for predicting the initial values of the costates corresponding to the problem of power-limited, minimum-fuel, coplanar rendezvous. For these problems the position of the vehicle on the initial and final conics is *fixed*. This is equivalent to specifying the state of the vehicle at the initial and final times completely, that is, the quantities h_0, x_0, r_0, θ_0, h_f, x_f, r_f, and θ_f, are fixed. Thus, for this problem, there are no transversality conditions, and the value of the (constant) costate P_θ is in general not zero, since the initial position of the vehicle can be expected to have an effect on the optimal value of the cost. The tangential thrust assumption was (mathematically at least) *consistent* with the transfer and escape problems, because, although the order of the original system of state-costate equations was reduced by *one*, *two* transversality conditions were satisfied by fixing the value of *one* constant of

integration (namely P_θ) at zero. The tangential thrust assumption is, however, *inconsistent* with the rendezvous problem, since the eight boundary conditions are in general completely arbitrary, and one cannot expect to satisfy all of them simultaneously with fewer than eight constants of integration. However, one can assume, that if the duration of the maneuver is long, then the optimal thrust for the most part of the trajectory (away from the endpoints) is approximately tangential, and that for such long duration problems, the initial position of the vehicle probably has *little* effect on the optimal value of the cost. This means that one can combine Eq. (4.78), which was obtained using the tangential thrust assumption and zero P_θ, with Eq. (4.83), and predict the initial values of the costates:

$$P_{x0} = \frac{x_0(h_f - h_0)}{h_0 \tau_f} \quad ; \quad P_{h0} = \frac{(h_f - h_0)}{r_0^2 \tau_f} \tag{4.164}$$

$$P_{r0} = -\left(\frac{h_0^2 - r_0}{r_0^3}\right)\left(\frac{h_f - h_0}{h_0 \tau_f}\right) \quad ; \quad P_\theta = 0 \tag{4.165}$$

These expressions for the costates may be used as reasonable guesses during a numerical optimization scheme aiming at the exact optimal solution of such problems.

4.15 Summary

This chapter has documented a case in which a mathematical model representing a meaningful physical system affords a closed-form solution. Recall that Keplerian two-body motion that takes place in the absence of thrust gives rise to a trajectory equation describing a conic (section). It was shown in the present chapter that the same trajectory equation (Eq. (4.17)) can be uncovered even in the presence of (a particular form of) nonzero, continuous thrusting terms. The difference is that in the former type of motion the angular momentum is a constant, while in the latter type of motion it is a linear function of time, with slope equal to a throttling parameter. Moreover, the corresponding thrusting terms are not really ad hoc, but arise from the optimization problem corresponding to power-limited, minimum-fuel, coplanar orbital motion. The assumption of tangential thrust plays a remarkable catalytic role in this problem, since it allows one to change the right-hand-side of only *one* costate equation (which affects *only* optimality), eliminate completely the costates by expressing them as functions of the states and a throttling parameter, and obtain the thrust

program for which the equations of motion can be solved *exactly* and *analytically*. It has been demonstrated in this chapter that it is, in principle, possible to solve arbitrary (coplanar) transfer and escape problems using this solution, for which one can preassign arbitrarily large durations. Transfers between two conics that intersect cannot be performed using a one-segment transfer trajectory. They can always be performed however using multiple-segment transfer trajectories, although the corresponding procedure is not unique. Hints were also given in the chapter suggesting that there should be cases in which the thrust program results in sufficiently optimal trajectories, both for power-limited and constant ejection velocity propulsion systems.

4.16 Concluding Remarks

Although the coverage in this chapter appears to be rather extensive, the work done is far from being complete. Above all, how the thrust program will perform in *each* and *every* particular case is far from having been documented, or even understood. Of primary interest for the future would be a more complete investigation of the transfer and escape problems studied above, and especially of the near-optimality of the thrust program in a general setting. It appears that, both Keplerian motion (zero thrust), and the kind of Non-Keplerian motion (nonzero thrust) documented in this chapter afford a common mathematical description. Physically, however, and philosophically, there is a significant difference between the two kinds of motion. Keplerian motion is guided by *Nature*, and requires no human effort. It represents a fundamental behavior of Nature. The kind of motion uncovered in this chapter on the other hand will have to be guided by *humans*, and there is nothing fundamental about it. This brings in a host of practical problems that need to be taken care of before a vehicle can actually be made to trace a path corresponding to such motion. With no misconceptions about this point, the main purpose of the present chapter on the practical side, was only to demonstrate, beyond a reasonable doubt, that the analytical results presented here may be of some help during actual planetocentric or heliocentric orbital operations. Thus, this report presents this thrust program and the corresponding exact analytic solution of the governing equations of motion, with the hope that its complete features will be more extensively investigated, its near-optimal or non-optimal aspects as relate to different types of propulsion fully uncovered, and its full domain of practical applicability, if any, clearly identified.

CHAPTER V

Conclusions and Recommendations

The research in this report concentrated in three areas related to aircraft and spacecraft trajectory optimization and optimal guidance. Specifically, the attention was focused on the areas of unconstrained and constrained aircraft energy-state modeling and spacecraft motion under continuous thrust.

5.1 Aircraft Unconstrained Energy-State Modeling

The research in the area of aircraft unconstrained energy-state modeling has uncovered a systematic procedure for identifying the singular perturbation parameter in the differential equations of motion governing both conventional (subsonic-supersonic, flat Earth) and transatmospheric (hypersonic, spherical Earth) flight. A set of arbitrary scaling constants was used during the procedure to nondimensionalize all the variables of interest. Then, aided by a useful choice of the scaling constants, the conclusion was reached that two-time-scale behavior of the corresponding aircraft can be expected when the maximum longitudinal load factor during a maneuver remains sufficiently less than one. The important point was the validity of this statement regardless of the performance index being optimized. This explicit identification of the singular perturbation parameter also explained the past successes of singular perturbation treatments of aircraft energy climbs.

A possible extension of this work would be a similar investigation of the existence of conditions under which the aforementioned differential equations exhibit three-time-scale behavior. It is straightforward to extend the procedure used in the second chapter by introducing *two* singular perturbation parameters instead of one, of which, one may be designated as ε_1 and the other as ε_2. A useful choice for the scaling constants, combined with the values of these singular perturbation parameters, would then serve again as a means to uncover conditions under which three-time-scale behavior can be expected. For example, one could use such a procedure to investigate under what conditions, if any, are the energy, altitude, and flight-path angle dynamics of aircraft separated from each other, giving rise to three-time-scale behavior. Since it is well-known that usually the altitude and

flight-path angle dynamics are highly coupled, such a study would be of *some* importance if it succeeded in uncovering the underlying reason for this coupling in terms of explicit physical parameters, or in predicting the existence of possible cases for which the coupling is absent, giving rise to three-time-scale behavior.

5.2 Aircraft State-Constrained Energy-State Modeling

The research in the area of aircraft state-constrained energy-state modeling has so far shown that a transformation technique can be used to isolate and describe completely the class of asymptotic controllers that track a given state-constraint boundary. This result provided the incentive for proposing a reformulation for optimal control problems involving active state-variable inequality constraints, so that, in the reformulated problem the optimization is carried out only over the class of asymptotic controllers. The original problem leads to optimal controllers that are finite-time and one-sided. The reformulated problem leads to controllers that are approximately optimal, asymptotic, but still one-sided. If however the state constraint is regarded as a soft constraint, then one can find controllers that are *asymptotic, two-sided*, and result in the *same* optimal value of the performance index corresponding to the *original* problem, that is, they are practically *optimal*, but at the expense of violating the state constraint. From a singular perturbations point of view this suggests that such controllers can be used in a boundary-layer system, to track the reduced solution corresponding to a specific problem, when this reduced solution happens to ride a state-constraint boundary. However, such controllers do not correspond to stationary solutions of the optimization problem, so at the present, a systematic procedure for finding them does not exist.

This last remark also suggests the primary recommendation for future research with regard to this area. Although a procedure *was* introduced in Section 3.3.2 that would presumably result in controllers that are asymptotic and two-sided, it is still not clear how to pick the two functions Ψ and M (see Section 3.3.2) when formulating the related companion problem. If a meaningful way of picking these functions can be found, this formulation can be applied to supersonic or hypersonic energy climbs, for which part of the trajectory lies on a state-constraint boundary representing a constant value of dynamic pressure, aerodynamic heating rate etc. The resulting controllers will be nonlinear, practically optimal, asymptotic, and capable of tracking such boundaries from both sides. A first step toward this direction would be to try to find (by trial and error) an asymptotic,

two-sided controller, that for a simple model representing an aircraft energy climb will guide a vehicle along a constant dynamic pressure constraint boundary, and will result in the same optimal value of the performance index (minimum time for example) corresponding to the problem in which the dynamic pressure constraint is explicitly imposed.

5.3 Spacecraft Motion under Continuous Thrust

In the area of spacecraft motion under continuous thrust the primary result of this report has been a generalization of the *exact analytic* solution of the orbital equations of motion corresponding to Keplerian two-body motion (that takes place in the absence of thrust) to a type of motion performed under a special kind of continuous thrust. The most significant result of this report is most probably the fact that the trajectory equations corresponding to the two types of motion have identical form. The difference is that, in Keplerian motion the angular momentum is a constant, while in the type of motion uncovered in this report it is a linear function of time, with slope equal to a throttling parameter. A very important aspect of this work was the fact that the thrust program used for the exact analytic solution of the equations of motion was not really ad hoc, but arose from the optimization problem corresponding to power-limited, minimum-fuel, coplanar orbital motion. It has been demonstrated in the fourth chapter that it is in principle possible to solve arbitrary (coplanar) transfer and escape problems using this solution, for which one can preassign arbitrarily large durations. Transfers between two conics that intersect cannot be performed using a one-segment transfer trajectory. They can always be performed, however, using multiple-segment transfer trajectories, although the corresponding procedure is not unique. Hints were also given in the fourth chapter suggesting the existence of cases for which the thrust program results in sufficiently optimal trajectories, both for power-limited and constant ejection velocity propulsion systems.

There are several suggestions for future research in this area. First, one may try to establish the near-optimality or non-optimality of the exact analytic solution uncovered in Section 4.4 in a full setting, by evaluating the *exact optimal* cost for a given maneuver and by comparing it to the cost corresponding to this exact analytic solution.

For power-limited propulsion systems the above would be a rather formidable task, since it would require repeated numerical solution of two-point boundary value problems

for evaluating the power-limited optimal trajectories between many pairs of conics, and the corresponding (exact optimal) costs. At this point however, this task appears to be more significant in a mathematical, rather than in a practical sense, because, as argued upon in Section 4.12, the time duration for any type of (coplanar) escape or transfer problem, using the proposed thrust program, can be preassigned to be arbitrarily large. This implies (see Section 4.12) that the corresponding fuel consumption can (in principle) be made arbitrarily small if one is willing to compromise with regard to the time duration it takes to perform such a maneuver! Such a situation may appear as overly restrictive but it really isn't! Balancing the fuel consumption for a maneuver against the time it takes to perform the maneuver is nothing new in spaceflight. The Hohmann transfer, which has been routinely used during the past thirty years in actual orbital operations, is a good example. Once the initial and final elliptical orbits are *fixed*, the time duration for a Hohmann transfer is *fixed* and cannot be preassigned! The Bielliptic transfer, which in practice can be used as an approximation to the Biparabolic transfer, represents just another such example, in which "reducing the fuel consumption further" means that one "has to wait longer" for completing the transfer.

For constant ejection velocity propulsion systems the situation may be somewhat easier to deal with, since there are many cases of transfers for which the optimal constant ejection velocity cost, impulsive in character, can be calculated with relative ease.

Another recommendation for future research would be a continuation of the work started here on the existence or non-existence of one-segment solutions. Theorem 4.1 of Section 4.11 started at first as a conjecture, and then was rigorously proven in Appendix F. Similarly, one now has the conjecture on the existence of one or two-segment solutions given at the end of Section 4.11 that awaits to be shown true or false.

Still other possible recommendations for future research would include an extension of the work to the case of three-dimensional motion, and a regular perturbations point of view of the solution uncovered in Sections 4.3 and 4.4. Although three-dimensional transfers cannot be performed by using exclusively tangential thrust, the set of state variables introduced in Section 4.2 can be generalized to the case of three-dimensional motion, after which, the three-dimensional power-limited optimization problem can be cast, and the structure of the corresponding costate equations examined. Viewing the solution uncovered in Sections 4.3 and 4.4 as the lowest order solution of the state-costate equations corresponding to a regular perturbation expansion would first require the nontrivial task involving a clear identification of a regular perturbation parameter.

APPENDIX A

Main Features of Two-Body Keplerian Motion

This Appendix is supplied for a direct comparison between the main features of Keplerian motion, that takes place in the absence of thrust, and the motion uncovered in Section 4.4, that takes place in the presence of continuous thrust, specified by the thrust acceleration components proposed in Eq. (4.10).

The term "two-body Keplerian motion" refers to the translational motion that a space vehicle (considered as a point mass) executes in the vicinity of a spherical, homogeneous planet, in the absence of any thrusting forces. The only force acting on the vehicle during such motion is the inverse-square gravity from the planet. This translational motion is confined to a plane, and is fully described by Eqs. (4.6)-(4.9), with the thrust components ε_r and ε_θ set equal to zero:

$$\frac{dh}{d\tau} = 0 \tag{A.1}$$

$$\frac{dx}{d\tau} = \frac{h^2 - r}{r^3} \tag{A.2}$$

$$\frac{dr}{d\tau} = x \tag{A.3}$$

$$\frac{d\theta}{d\tau} = \frac{h}{r^2} \tag{A.4}$$

The solution of the differential equations describing such motion was first given, of course, by Isaac Newton[37], and in terms of the variables used in Eqs. (A.1) through (A.4) can be summarized as:

$$h = \text{const.} \quad ; \quad x = \frac{e\sin(\theta - \omega)}{h} \quad ; \quad r = \frac{h^2}{1 + e\cos(\theta - \omega)} \tag{A.5}$$

103

In Eq. (A.5) e and ω are two integration constants, and the angular momentum h, which stays constant, plays the role of a third integration constant. The fourth integration constant relates the time τ to the argument of latitude θ and can be uncovered by using the expression for r from Eq. (A.5) and reducing Eq. (A.4) to a quadrature:

$$\tau = \int \frac{h^3 \, d\theta}{\left[1 + e\cos(\theta - \omega)\right]^2} + \text{const.} \qquad (A.6)$$

According to the trajectory equation for r given in Eq. (A.5), the motion takes place along a conic[34]. The constant e is just the eccentricity of the conic. For e = 0 or 0 < e < 1 the conic is respectively a circle or an ellipse, and the corresponding trajectory is closed and usually called an orbit. For e = 1 or e > 1 the conic is respectively a parabola or a hyperbola, and the corresponding trajectory is open[34]. The evaluation of the integral in Eq. (A.6) depends strongly on whether e is less than or greater than one, or equal to zero or one. The constant ω represents the orientation of the conic. If one imagines a vector pointing from the center of the planet toward the point on the conic where r is a minimum (the perigee), then ω is just the angle, measured anticlockwise, from the fixed direction in space (where all the latitude angles are measured from - see Fig. 4.1) to that vector[34].

An important parameter associated with a conic is its semimajor axis a. The semimajor axis is a direct measure of the mechanical (kinetic plus potential) energy per unit mass of the vehicle[34]. Because the inverse-square gravity field generated by the planet is conservative the mechanical energy per unit mass of the vehicle stays constant during the motion[34]. Specifically, this mechanical energy is related to the semimajor axis a by the well-known energy integral[34]:

$$V^2 - \frac{2}{r} = -\frac{1}{a} \qquad (A.7)$$

In Eq. (A.7) V is the speed of the vehicle, which in terms of the state variables used in Eqs. (A.1) through (A.4) is given by:

$$V^2 = x^2 + \frac{h^2}{r^2} \qquad (A.8)$$

The semimajor axis a is related to the angular momentum h and the eccentricity e through[34]:

104

$$h^2 = a\left(1 - e^2\right) \tag{A.9}$$

When the conic is a circle or an ellipse e is less than one and a is positive. Specifically, when e is zero the conic is a circle and a is just the radius of the circle. When the conic is a hyperbola e is greater than one and a is negative. When the conic is a parabola e is equal to one and a is infinite[34] (but the angular momentum h is always finite).

APPENDIX B

Derivation of the Exact Analytic Solution
of the System of Eqs. (4.11) - (4.14)

The development in this Appendix is valid for nonzero A (the case with zero A corresponds to Keplerian motion and was summarized in Appendix A). The solution of Eq. (4.11) is obviously the linear variation for the angular momentum h supplied in Eq. (4.15). Consider now the system of Eqs. (4.12), (4.13), and define the transformation:

$$w = \frac{h}{A} \quad ; \quad \frac{dw}{d\tau} = \frac{1}{A}\left(\frac{dh}{d\tau}\right) = \frac{1}{A}A = 1 \tag{B.1}$$

Using w rather than τ as the independent variable, this system assumes the form:

$$\frac{dx}{dw} = \frac{A^2w^2 - r}{r^3} + \frac{x}{w} \tag{B.2}$$

$$\frac{dr}{dw} = x \tag{B.3}$$

By switching from the variable x to a new variable P, defined by:

$$P = \frac{x}{w} \tag{B.4}$$

the system of Eqs. (B.2), (B.3) can be written as:

$$\frac{dP}{dw} = \frac{A^2w^2 - r}{wr^3} \tag{B.5}$$

$$\frac{dr}{dw} = wP \tag{B.6}$$

One can now define two new variables K and z, by:

$$K = \frac{1}{w^2} \quad ; \quad z = \frac{r}{w^2} \tag{B.7}$$

Replacing r by z, and using z as the independent variable, the system of Eqs. (B.5), (B.6) transforms into:

$$\frac{dP}{dz} = \frac{(z - A^2)K^2}{(2z - P)z^3} \tag{B.8}$$

$$\frac{dK}{dz} = \frac{2K}{2z - P} \tag{B.9}$$

Finally, using the transformation:

$$S = \frac{2K}{2z - P} \tag{B.10}$$

the system of Eqs. (B.8), (B.9) assumes the analytically soluble form:

$$\frac{dS}{dz} = \left(\frac{z - A^2}{4z^3}\right)S^3 \tag{B.11}$$

$$\frac{dK}{dz} = S \tag{B.12}$$

The general solution of Eq. (B.11) can be found by a simple integration[33]. The result is:

$$S^2 = \frac{4z^2}{Dz^2 + 2z - A^2} \tag{B.13}$$

where D is an integration constant. Using this result, Eq. (B.12) can be written as:

$$\left(\frac{dK}{dz}\right)^2 = \frac{4z^2}{Dz^2 + 2z - A^2} \tag{B.14}$$

More will be said about Eq. (B.14) at the end of this Appendix. First, Eq. (4.14) in the main text can be rewritten as a simple quadrature:

$$\theta = \int \left(\frac{h}{r^2} \right) d\tau + F \qquad (B.15)$$

where F is an integration constant. Tracing the transformations back, Eq. (B.15) can further be written as:

$$\theta = \pm \int \left(\frac{A}{z\sqrt{Dz^2 + 2z - A^2}} \right) dz + F \qquad (B.16)$$

Note that the double sign in front of the integral is due to the fact that *both* signs have been kept when taking the square root of S in Eq. (B.13). Evaluation of the integral[33] in Eq. (B.16) for *any* value of D, and for nonzero A (zero A corresponds to Keplerian motion) leads, *for both signs*, to the expression:

$$z = \frac{A^2}{1 + B\cos(\theta - C)} \qquad (B.17)$$

where B is a *nonnegative* constant defined by:

$$B = \sqrt{1 + DA^2} \qquad (B.18)$$

and C is a constant which can be written always as a linear function of the constant F. Since z is just equal to rA^2/h^2, Eq. (B.17) can be written as:

$$r = \frac{h^2}{1 + B\cos(\theta - C)} \qquad (B.19)$$

which just happens to be the transfer trajectory equation, Eq. (4.17). Differentiating Eq. (B.19) one can easily find the corresponding expression for x given in Eq. (4.16).

The last equation that remains to be integrated is Eq. (B.14). However, a simple inspection reveals that this integration has in fact been already carried out (in disguise) in Section 4.5 of the main text, by defining more useful variables, such as the generalized eccentric and hyperbolic anomalies, etc. There is therefore no need to integrate Eq. (B.14). This completes the exact analytic solution of Eqs. (4.11) through (4.14).

APPENDIX C

Power-Limited Propulsion Systems

Power-Limited propulsion systems basically correspond to electric propulsion, and generate thrust by accelerating particles through an electromagnetic or electrostatic field[46,48,51]. There is usually a propellant feeding mechanism that supplies the particles, and an electrical generator that generates the electric field that accelerates the particles. The primary characteristic of such systems is that the above two mechanisms operate (ideally) independently of each other. For example[51], if a nuclear reactor heats a working fluid, as in an electrothermal device, changing the operating temperature of the reactor regulates the mass flow rate of the particles -dm/dt. If a solar cell accelerates ions, as in an electrostatic device, changing the operating voltage of the cell controls the ejection speed of the ions c. Thus, it is possible in principle to modify both the ejection speed c and the mass flow rate -dm/dt, and therefore to control *independently* the thrust T *and* the power P, given by the expressions:

$$T = -\frac{dm}{dt}c \quad ; \quad P = -\frac{1}{2}\left(\frac{dm}{dt}\right)c^2 \tag{C.1}$$

The above expressions can be obtained by considering the state of the vehicle *and* the propellant at times t and t+dt, and by performing a momentum and energy balance. That the power in Eq. (C.1) is indeed the power supplied by a power-limited thruster can be further argued upon as follows. The power P supplied by such a thruster can be written as[46,48]:

$$P = UI \tag{C.2}$$

where U is the *beam voltage* and I is the *beam current*. If a particle of mass m, charge q, and negligible initial velocity is accelerated through a potential difference U it acquires cinetic energy equal to (mc²/2), where c is the ejection speed. Accordingly, the following two relations are valid:

$$Uq = \frac{mc^2}{2} \quad ; \quad I = \left(\frac{q}{m}\right)\left(-\frac{dm}{dt}\right) \tag{C.3}$$

109

Substituting from Eq. (C.3) into Eq. (C.2), one obtains the expression for the power given in Eq. (C.1). As the name implies, the power that can be supplied by such propulsion systems is limited, that is, there is a maximum level of power P_{max} that cannot be exceeded[48,51]. In the T vs (-dm/dt) operating domain constant power is represented by the parabola:

$$T = \sqrt{2P\left(-\frac{dm}{dt}\right)} \qquad (C.4)$$

The two relations in Eq. (C.1) lead to:

$$\frac{1}{m_f} - \frac{1}{m_0} = \int_{t_0}^{t_f} \frac{\alpha^2}{2P} dt \qquad (C.5)$$

where $\alpha = T/m$ is the thrust acceleration, given by:

$$\alpha^2 = E_R^2 + E_\theta^2 \qquad (C.6)$$

The initial mass m_0 is given, and in order to minimize the fuel consumption one must maximize the final mass m_f. Therefore, it is required to operate with maximum power $P = P_{max}$ during the entire maneuver, which leads to the minimization of the quadratic performance index:

$$K = \frac{1}{2} \int_{t_0}^{t_f} \alpha^2 dt \qquad (C.7)$$

In practice[48], there is usually a minimum ejection speed c_{min} and a maximum mass flow rate $(-dm/dt)_{max}$. These constraints however need not be taken into account explicitly during a formulation of the corresponding optimal control problem, since by selecting the time duration for a maneuver appropriately one can ensure that these limits are not violated. The primary reason that one can usually do this is the fact that the optimal thrust acceleration levels and the optimal cost K_{min} are inversely proportional to the time duration of a maneuver.

110

Nondimensionalizing α and K as (see Eqs. (4.4) and (4.5)):

$$J_f = \frac{K}{g_s V_s} \quad ; \quad \varepsilon = \frac{\alpha}{g_s} \quad ; \quad \varepsilon^2 = \varepsilon_r^2 + \varepsilon_\theta^2 \qquad (C.8)$$

where J_f represents the final value of the variable J (the initial value of J can be taken as zero), leads to Eq. (4.43), describing the time evolution of the cost J(t) along a maneuver.

APPENDIX D

Coefficients of Polynomial Eq. (4.135), and an Explicit Solution for Transfers Between Coplanar Circular Orbits

The coefficients of the fourth order polynomial equation (4.135) are given by the following expressions:

$$b_4 = e_f^2 + 4h_0^4 A^2(1 - e_f^2) - 4h_f^4 A^2 - 8h_0^2 h_f^2 A^2 e_f \tag{D.1}$$

$$b_3 = b_1 = 8h_0^2 A e_f \tag{D.2}$$

$$b_2 = 2\left[e_f^2 + 4h_0^4 A^2(1 + e_f^2) - 4h_f^4 A^2\right] \tag{D.3}$$

$$b_0 = e_f^2 + 4h_0^4 A^2(1 - e_f^2) - 4h_f^4 A^2 + 8h_0^2 h_f^2 A^2 e_f \tag{D.4}$$

D.1 Long Duration Transfers Between two Coplanar Circular Orbits

Consider the case in which the final orbit is circular, that is, $e_f = 0$. In such a case the polynomial Eq. (4.135) has no real roots, and can be satisfied only if A is zero. But when A is zero the motion is Keplerian and (assuming that the initial and final circular orbits are different) there can be no transfer. Thus, mathematically, the case with $e_f = 0$ is a singular case. In practice however, the transfer between two circular orbits *can* be performed by selecting a very small e_f. This immediately implies that the time duration for such a transfer will be large, that is, for the problem of transferring between two coplanar circular orbits long duration is implied if one uses the thrust program proposed in Eq. (4.10) and the corresponding exact analytic solution of Section 4.4. Small e_f implies large τ_f and small A. Thus, keeping only the lowest order terms in A and e_f, the coefficients given in Eqs. (D.1) through (D.4) assume the form:

112

$$b_4 = \frac{b_2}{2} = b_0 = k_1 = e_f^2 + 4\left(h_0^4 - h_f^4\right)A^2 \quad ; \qquad b_3 = b_1 = k_2 = 8h_0^2 A e_f \qquad (D.5)$$

and now, the quartic polynomial Eq. (4.135) can be simplified as:

$$k_1 y^4 + k_2 y^3 + 2k_1 y^2 + k_2 y + k_1 = 0 \qquad (D.6)$$

Equation (D.6) can be easily factored as:

$$\left(y^2 + 1\right)\left(k_1 y^2 + k_2 y + k_1\right) = 0 \qquad (D.7)$$

from which one concludes that in such a case there can be at most two real solutions for y, and this happens only when the discriminant:

$$\Delta_1 = k_2^2 - 4k_1^2 \qquad (D.8)$$

is nonnegative. Substituting from Eq. (D.5) into Eq. (D.8), this condition can be stated explicitly as:

$$\Delta_1 = -4\left[16\left(h_0^4 - h_f^4\right)^2 A^4 - 8\left(h_0^4 + h_f^4\right)A^2 e_f^2 + e_f^4\right] \geq 0 \qquad (D.9)$$

Whenever the above condition is satisfied there are two real roots for y, corresponding to the initial value θ_0 of θ, which determine the starting point on the initial circular orbit. These two real roots are given by:

$$y_{1,2} = \frac{-k_2 \pm \sqrt{k_2^2 - 4k_1^2}}{2k_1} \qquad (D.10)$$

For a given (small) e_f, real solutions for y exist only for $\tau_{f1} < \tau_f < \tau_{f2}$, where τ_{f1} and τ_{f2} are the two values of the final time τ_f for which Δ_1 becomes zero. Figures 4.6 and 4.8 through 4.11 depict this situation very clearly. Using the expression supplied in Eq. (D.9), and assuming that the angular momenta h_0 and h_f of the initial and final circular orbits are always strictly positive, the two values τ_{f1} and τ_{f2} can be found as:

(i)   For $h_f > h_0$ and $A > 0$:

$$\tau_{f1} = \frac{2\left(h_f^2 - h_0^2\right)\left(h_f - h_0\right)}{e_f} \quad ; \qquad \tau_{f2} = \frac{2\left(h_f^2 + h_0^2\right)\left(h_f - h_0\right)}{e_f} \qquad (D.11.a)$$

113

(ii) For $h_f < h_0$ and $A < 0$:

$$\tau_{f1} = \frac{2(h_0^2 - h_f^2)(h_0 - h_f)}{e_f} \quad ; \quad \tau_{f2} = \frac{2(h_0^2 + h_f^2)(h_0 - h_f)}{e_f} \qquad \text{(D.11.b)}$$

Equation (D.11.a) is in complete agreement with the situation depicted in Figs. 4.6, and 4.8 through 4.11. With $h_0 = 1$ and $h_f = 2$, one obtains from Eq. (D.11.a) $\tau_{f1} = 6/e_f$ and $\tau_{f2} = 10/e_f$. With $e_f = 0.05$ these relations yield $\tau_{f1} = 120$ and $\tau_{f2} = 200$, in complete agreement with Fig. 4.6. Similar results can be validated for Figs. 4.8 through 4.11.

If now one preassigns a (large) value for the transfer duration τ_f, in order to make the final eccentricity as small as possible, one should obviously choose the (double) root for y corresponding to τ_{f1}. Thus, in such a case, the final eccentricity e_f and the corresponding value of the throttling parameter A are given by:

$$e_f = \frac{2(h_f^2 - h_0^2)(h_f - h_0)}{\tau_f} \quad ; \quad A = \frac{h_f - h_0}{\tau_f} = \frac{e_f}{2(h_f^2 - h_0^2)} \qquad \text{(D.12)}$$

Using this expression for A, and keeping in mind that Δ_1 is zero, the (double) root for y from Eq. (D.10) can be found as:

$$y = -\frac{k_2}{2k_1} = 1 \qquad \text{(D.13)}$$

Since y is equal to $\tan(\theta_0/2)$ (see Eq. (4.136)), the initial value of the argument of latitude is simply:

$$\theta_0 = \frac{\pi}{2} \qquad \text{(D.14)}$$

The final value of the argument of latitude can be found substituting the above results for A and θ_0 into Eqs. (4.137) and (4.138). The result is:

$$\theta_f = \theta_{fP} + 2k\pi \quad ; \quad \theta_{fP} = \frac{\pi}{2} \qquad \text{(D.15)}$$

Now, what about (the integer) k? k fixes the number of revolutions about the planet during the transfer. The value of k is the one for which Eq. (4.125.b) is satisfied. For (long

114

duration) transfers between two coplanar circular orbits Eq. (4.125) decouples from the rest of the problem. Using Eqs. (4.129) and (D.12), the generalized eccentricity of the transfer trajectory is:

$$B = \pm \frac{h_0^2 e_f}{h_f^2 - h_0^2} \qquad (D.16)$$

Using now Eqs. (D.14) through (D.16), and (4.126) one concludes from Eq. (4.125.b) that k is:

$$k = \frac{\tau_f (h_f + h_0)}{4 \pi h_0^2 h_f^2} \left[1 - \frac{h_0^4 e_f^2}{(h_f^2 - h_0^2)^2} \right]^{3/2} \qquad (D.17)$$

Any nonnegative integer value of k is acceptable. Thus, for large τ_f, if τ_f is arbitrarily preassigned, then, Eq. (D.17) is approximately satisfied. In fact, by playing around with the values of τ_f and e_f, connected through Eq. (D.12), one can satisfy Eq. (D.17) exactly, that is, one can make Eq. (D.17) result in an integer value for k. For very large τ_f one can also simplify Eq. (D.17) as:

$$k \approx \frac{\tau_f (h_f + h_0)}{4 \pi h_0^2 h_f^2} \qquad (D.18)$$

D.2 Summary

To summarize, consider the problem of transferring from an initial circular orbit ($e_0 = 0$) with angular momentum h_0 to a final coplanar circular orbit ($e_f = 0$) with angular momentum h_f, using the thrust program proposed in Eq. (4.10) and the corresponding exact analytic solution supplied in Section 4.4. The solution can be summarized as follows:

(a) One preassigns a large transfer duration τ_f.

(b) Eq. (D.12) then fixes the final (small) eccentricity e_f and the throttling parameter A to be used for the transfer.

(c) The value of the right-hand-side of Eq. (D.17), truncated to the nearest integer, supplies the number of revolutions k about the planet during the transfer. By selecting τ_f appropriately one can satisfy Eq. (D.17) *exactly* by making its right-hand-side come out equal to an integer.

115

(d) The transfer starts and ends at the same argument of latitude after k full revolutions about the planet.

(e) The generalized eccentricity and orientation constants B and C of the transfer trajectory are given by Eq. (4.129).

(f) The transfer trajectory is given by Eqs. (4.17) or (4.29), where the angular momentum depends on the generalized eccentric anomaly E through Eq. (4.34).

(g) If τ_f is large enough, further simplifications are obtained by considering B as being approximately equal to zero. In this case the transfer trajectory is simply $r = h^2$, while the angular momentum h along the transfer is given by Eq. (4.25). Thus, for large enough τ_f one obtains the following spiral, representing the one-segment transfer trajectory:

$$r = h^2 = \frac{h_0^2}{1 - 2 A h_0^2 (\theta - \theta_0)} \tag{D.19}$$

(h) Also, when τ_f is large enough and B can be approximated by zero, the power-limited cost along the transfer is approximately given by Eq. (G.19.c) of Appendix G:

$$J_{PL} = \left(\frac{h_f - h_0}{6 \tau_f} \right) \left(\frac{1}{h_0^3} - \frac{1}{h_f^3} \right) \tag{D.20}$$

This expression for the power-limited cost compares well with the *exact optimal* power-limited cost supplied in Table 5.7 of Ref. 51. Based primarily on the results of this Appendix, and of Section 4.6.5, one could conjecture that for long duration transfers between two coplanar circular orbits the solution delineated in steps (a) through (h) above is the optimal power-limited solution, and the cost given in Eq. (D.20) is the optimal power-limited cost for all practical purposes.

116

APPENDIX E

Coefficients of Polynomial Eq. (4.150)

The coefficients of the fourth order polynomial equation (4.150) are given by the following expressions:

$$b_4 = (1 - e_0)^2 (e_0^2 + e_f^2 - 2e_0 e_f \cos \omega_f)$$

$$-(1 - e_0)^2 (2h_f^2 A + e_0 e_f \sin \omega_f)^2 + 4h_0^4 A^2 (1 - e_f^2 \cos^2 \omega_f)$$

$$+2h_0^2 A e_f (1 - e_0)(2 \sin \omega_f - 4h_f^2 A \cos \omega_f - e_0 e_f \sin 2\omega_f) \qquad (E.1)$$

$$\frac{b_3}{2} = 4h_0^2 A (1 - e_0)(e_f \cos \omega_f - e_0) + 4h_0^4 A^2 e_f^2 \sin 2\omega_f$$

$$+4h_0^2 A e_f (1 - e_0)(2h_f^2 A + e_0 e_f \sin \omega_f) \sin \omega_f \qquad (E.2)$$

$$\frac{b_2}{2} = (1 - e_0^2)(e_0^2 + e_f^2 - 2e_0 e_f \cos \omega_f) - (1 - e_0^2)(2h_f^2 A + e_0 e_f \sin \omega_f)^2$$

$$+2h_0^2 A e_0 e_f (2 \sin \omega_f - 4h_f^2 A \cos \omega_f - e_0 e_f \sin 2\omega_f)$$

$$+4h_0^4 A^2 (1 + e_f^2 \cos^2 \omega_f - 2e_f^2 \sin^2 \omega_f) \qquad (E.3)$$

$$\frac{b_1}{2} = 4h_0^2 A(1+e_0)(e_f \cos\omega_f - e_0) - 4h_0^4 A^2 e_f^2 \sin 2\omega_f$$

$$+4h_0^2 Ae_f(1+e_0)(2h_f^2 A + e_0 e_f \sin\omega_f)\sin\omega_f \tag{E.4}$$

$$b_0 = (1+e_0)^2(e_0^2 + e_f^2 - 2e_0 e_f \cos\omega_f)$$

$$-(1+e_0)^2(2h_f^2 A + e_0 e_f \sin\omega_f)^2 + 4h_0^4 A^2(1 - e_f^2 \cos^2\omega_f)$$

$$-2h_0^2 Ae_f(1+e_0)(2\sin\omega_f - 4h_f^2 A\cos\omega_f - e_0 e_f \sin 2\omega_f) \tag{E.5}$$

Note that for $e_0 = \omega_f = 0$ the expressions in Eqs. (E.1) through (E.5) reduce to the corresponding expressions given in Eqs. (D.1) through (D.4), valid for transfer and escape problems from a circular orbit.

118

APPENDIX F

Proof of Theorem 4.1, Section 4.11

This Appendix supplies the detailed proof of Theorem 4.1 (page 89) of Section 4.11, which is reproduced here for convenience to the reader:

Theorem 4.1. Consider the problem of transferring from conic $(h_0, e_0, \omega_0, \theta_0)$ to conic $(h_f, e_f, \omega_f, \theta_f)$ using the thrust program proposed in Eq. (4.10) and the corresponding exact analytic solution of Section 4.4. Then,

(i) If $(h_0, e_0, \omega_0, \theta_0)$ and $(h_f, e_f, \omega_f, \theta_f)$ have more than one common point (that is, if they intersect), then a one-segment transfer solution does not exist.

(ii) If $(h_0, e_0, \omega_0, \theta_0)$ and $(h_f, e_f, \omega_f, \theta_f)$ have only one common point (a point of tangency) then there exists at most *a single impulsive* one-segment transfer solution, performed at the point of tangency of the two conics, for which A is infinitely large, τ_f is infinitely small, and $A\tau_f$ is finite and equal to $h_f - h_0$.

Proof 4.1. Since only the relative (and not the absolute) orientation of the two conics on the plane affects the problem, there is no loss of generality in taking ω_0 as zero. First, one can show part (i) using contradiction. Assume that, contrary to the claim made in the theorem, the initial and final conics intersect and a one-segment transfer trajectory (A, B, C, τ_f) joining the conics with $\tau_f > 0$ does exist. Then, by equating the right-hand-sides of the trajectory equations:

$$r = \frac{h_0^2}{1 + e_0 \cos\theta} \quad ; \quad r = \frac{h_f^2}{1 + e_f \cos(\theta - \omega_f)} \tag{F.1}$$

corresponding to the two conics, one obtains the equation:

$$h_f^2 - h_0^2 + \left(h_f^2 e_0 - h_0^2 e_f \cos\omega_f\right)\cos\theta - h_0^2 e_f \sin\omega_f \sin\theta = 0 \tag{F.2}$$

Using now the definition for y, and the identities[33]:

$$y = \tan\left(\frac{\theta}{2}\right) \quad ; \quad \sin\theta = \frac{2y}{1 + y^2} \quad ; \quad \cos\theta = \frac{1 - y^2}{1 + y^2} \tag{F.3}$$

119

Eq. (F.1) can be manipulated into the form:

$$a_2 y^2 + 2a_1 y + a_0 = 0 \qquad (F.4)$$

where the quantities a_2, a_1, and a_0 are given by:

$$a_2 = h_f^2(1 - e_0) - h_0^2(1 - e_f \cos\omega_f) \; ; \quad a_1 = -h_0^2 e_f \sin\omega_f \; ; \quad a_0 = h_f^2(1 + e_0) - h_0^2(1 + e_f \cos\omega_f)$$

$$(F.5)$$

Equation (F.4) is a quadratic polynomial equation in the unknown y (corresponding to θ), and since by assumption the initial and final conics intersect, it should have *at least one* real solution. Accordingly, the discriminant Δ of Eq. (F.4), given by:

$$\Delta = a_1^2 - a_2 a_0 \qquad (F.6)$$

should be nonnegative. Substituting from Eq. (F.5), this necessary condition can be written explicitly as:

$$\Delta = h_f^4(e_0^2 - 1) + h_0^4(e_f^2 - 1) + 2h_0^2 h_f^2(1 - e_0 e_f \cos\omega_f) \geq 0 \qquad (F.7)$$

Keeping in mind that the initial and final conics have a *common focus*, one can now conclude that:

(i) If the initial and final conics have only *one* point in common (a point of tangency), Δ should be zero, resulting in *one* real solution for y (of multiplicity two).

(ii) If the initial and final conics have *two* points in common (that is, if they intersect), Δ should be strictly positive, resulting in *two* distinct real solutions for y.

(iii) Two (different) conics (with a common focus) can have *no more than two* points in common.

Since by assumption a one-segment transfer trajectory (A,B,C,τ_f), with $\tau_f > 0$, joining the initial and final conics exists, the quantities appearing in Eq. (F.7) are all dependent on the characteristics A, B, C, and $\tau_f > 0$ of this one-segment transfer trajectory, through the boundary conditions given in the main text by Eqs. (4.139) through (4.142) and also through one among Eqs. (4.25), (4.26), (4.34), or (4.42), written at the final time τ_f. To prove the theorem one must uncover this dependence explicitly and show that Δ is strictly negative, contradicting the necessary condition given in Eq. (F.7). With this in mind, one can first use the definitions:

120

$$\xi_0 = \theta_0 - C \quad ; \qquad \xi_f = \theta_f - C \tag{F.8}$$

and write Eqs. (4.141), (4.142) as:

$$e_f \cos(\xi_f + C - \omega_f) = B \cos \xi_f \tag{F.9}$$

$$e_f \sin(\xi_f + C - \omega_f) = 2r_f A + B \sin \xi_f \tag{F.10}$$

Now, Eqs. (F.9) and (F.10) can be solved for $e_f \sin \omega_f$, $e_f \cos \omega_f$, and the square of e_f to yield:

$$e_f \sin \omega_f = B \sin C - 2r_f A \cos(\xi_f + C) \tag{F.11}$$

$$e_f \cos \omega_f = B \cos C + 2r_f A \sin(\xi_f + C) \tag{F.12}$$

$$e_f^2 = B^2 + 4A^2 r_f^2 + 4ABr_f \sin \xi_f \tag{F.13}$$

Using Eqs. (F.12), (F.13), and the definitions:

$$p_0 = h_0^2 \quad ; \qquad p_f = h_f^2 \tag{F.14}$$

one can write the discriminant Δ given in Eq. (F.7) as:

$$\Delta = p_f^2(e_0^2 - 1) + p_0^2(B^2 - 1) + 2p_0 p_f + 4ABp_0^2 r_f \sin \xi_f - 2B(e_0 \cos C)p_0 p_f$$

$$+ 4A^2 p_0^2 r_f^2 - 4A(e_0 \cos C)p_0 p_f r_f \sin \xi_f - 4A(e_0 \sin C)p_0 p_f r_f \cos \xi_f \tag{F.15}$$

In an analogous manner, one can write Eqs. (4.139), (4.140) as:

$$e_0 \cos(\xi_0 + C) = B \cos \xi_0 \tag{F.16}$$

$$e_0 \sin(\xi_0 + C) = 2r_0 A + B \sin \xi_0 \tag{F.17}$$

and solve Eqs. (F.16) and (F.17) for $e_0 \sin C$, $e_0 \cos C$, and the square of e_0 to obtain:

$$e_0 \sin C = 2r_0 A \cos \xi_0 \qquad (F.18)$$

$$e_0 \cos C = B + 2r_0 A \sin \xi_0 \qquad (F.19)$$

$$e_0^2 = B^2 + 4A^2 r_0^2 + 4AB r_0 \sin \xi_0 \qquad (F.20)$$

Using Eqs. (F.18) through (F.20), one can further write the discriminant Δ given in Eq. (F.15) as:

$$\Delta = (p_f - p_0)^2 (B^2 - 1) + 4A^2 \left(p_f^2 r_0^2 + p_0^2 r_f^2 - 2p_0 p_f r_0 r_f \cos(\xi_f - \xi_0) \right)$$

$$+ 4AB(p_f - p_0)(p_f r_0 \sin \xi_0 - p_0 r_f \sin \xi_f) \qquad (F.21)$$

Note that the radial distances r_0 and r_f at the initial and final times can be expressed more explicitly using the trajectory equation (Eq. (4.21)) and the definitions given in Eq. (F.14) as:

$$r_0 = \frac{p_0}{1 + B \cos \xi_0} \qquad ; \qquad r_f = \frac{p_f}{1 + B \cos \xi_f} \qquad (F.22)$$

To proceed further with the proof one must now express more explicitly the six quantities r_0, r_f, $r_0 \sin \xi_0$, $r_0 \cos \xi_0$, $r_f \sin \xi_f$, and $r_f \cos \xi_f$. This step however depends strongly on whether the generalized eccentricity B of the transfer trajectory is zero, one, between zero and one, or greater than one. One therefore has to consider the following four possible cases:

F.1 First case: B = 0

In this case, from Eqs. (4.139) and (4.140) one can deduce the following two possibilities for the starting point θ_0 on the initial conic:

$$\text{if } A > 0 \text{ then } \theta_0 = \frac{\pi}{2} \qquad ; \qquad \text{if } A < 0 \text{ then } \theta_0 = -\frac{\pi}{2} \qquad (F.23)$$

122

From Eq. (F.22), with B = 0 one obtains:

$$r_0 = p_0 \quad ; \qquad r_f = p_f \qquad (F.24)$$

Also, one can define the change $\Delta\theta$ or $\Delta\xi$ in the argument of latitude during the one-segment transfer as:

$$\Delta\theta = \theta_f - \theta_0 = \theta_f - C + C - \theta_0 = \xi_f - \xi_0 = \Delta\xi \qquad (F.25)$$

Note that, since the transfer duration is strictly positive, that is, $\tau_f > 0$, one must necessarily have $\Delta\theta > 0$ for the transfer. Along such a one-segment transfer, with B = 0, Eq. (4.25) is valid. Using the definitions given in Eqs. (F.14) and (F.25), one can write Eq. (4.25) at the final time τ_f as:

$$\frac{1}{p_f} = \frac{1}{p_0} - 2A\Delta\theta \qquad (F.26)$$

By defining the quantity D as:

$$D = 1 - 2Ap_0\Delta\theta \qquad (F.27)$$

p_f can be written from Eq. (F.26) as:

$$p_f = \frac{p_0}{D} \qquad (F.28)$$

The last step consists of substituting from Eqs. (F.24) and (F.28) into the expression for Δ given in Eq. (F.21). With B = 0, and for both possibilities given in Eq. (F.23), one can write the result as:

$$\Delta = -\frac{16A^2 h_0^8}{D^2}\left[\left(\frac{\Delta\theta}{2}\right)^2 - \sin^2\left(\frac{\Delta\theta}{2}\right)\right] \qquad (F.29)$$

For $\Delta\theta > 0$ the following inequality is always valid:

$$\frac{\Delta\theta}{2} > \sin\left(\frac{\Delta\theta}{2}\right) \qquad (F.30)$$

123

Accordingly, from Eq. (F.29), the discriminant Δ must be strictly negative ($\Delta < 0$), contradicting the necessary condition $\Delta \geq 0$ found in Eq. (F.7). This concludes the proof of part (i) for $B = 0$.

F.2 Second case: $B = 1$

In this case, to facilitate the algebra, one can again define the two quantities:

$$y_0 = \tan\left(\frac{\xi_0}{2}\right) \quad ; \quad y_f = \tan\left(\frac{\xi_f}{2}\right) \tag{F.31}$$

Using Eq. (F.31), and some standard trigonometric identities[33], one can express the six quantities r_0, r_f, $r_0\sin\xi_0$, $r_0\cos\xi_0$, $r_f\sin\xi_f$, and $r_f\cos\xi_f$ as (recall that $B = 1$):

$$r_0 = \frac{p_0(1+y_0^2)}{2} \quad ; \quad r_0\sin\xi_0 = p_0 y_0 \quad ; \quad r_0\cos\xi_0 = \frac{p_0(1-y_0^2)}{2} \tag{F.32}$$

$$r_f = \frac{p_f(1+y_f^2)}{2} \quad ; \quad r_f\sin\xi_f = p_f y_f \quad ; \quad r_f\cos\xi_f = \frac{p_f(1-y_f^2)}{2} \tag{F.33}$$

Along such a one-segment transfer, with $B = 1$, Eq. (4.26) is valid. Using the definitions given in Eqs. (F.14) and (F.31), one can write Eq. (4.26) at the final time τ_f as:

$$\frac{1}{p_f} = \frac{1}{p_0} - A(y_f - y_0) - \frac{A}{3}(y_f^3 - y_0^3) \tag{F.34}$$

By defining the quantity D as:

$$D = 3 - Ap_0(y_f - y_0)(3 + y_f^2 + y_f y_0 + y_0^2) \tag{F.35}$$

p_f can be written from Eq. (F.34) as:

$$p_f = \frac{3p_0}{D} \tag{F.36}$$

The last step consists of substituting from Eqs. (F.32), (F.33) and (F.36) into the expression for Δ given in Eq. (F.21). With $B = 1$, one can write the result as:

$$\Delta = -\frac{3A^2 h_0^8}{D^2}\left[\tan\left(\frac{\xi_f}{2}\right) - \tan\left(\frac{\xi_0}{2}\right)\right]^4 \tag{F.37}$$

For $B = 1$, a full revolution around the planet during a one-segment transfer is not possible, because θ, or ξ go through a value at which r becomes infinite, as can be seen from Eq. (4.21). Thus, along such a transfer $0 < \xi_f - \xi_0 < 2\pi$, and the following statement is always true:

$$\tan\left(\frac{\xi_f}{2}\right) \neq \tan\left(\frac{\xi_0}{2}\right) \tag{F.38}$$

Accordingly, from Eq. (F.37), the discriminant Δ must be strictly negative ($\Delta < 0$), contradicting the necessary condition $\Delta \geq 0$ found in Eq. (F.7). This concludes the proof of part (i) for $B = 1$.

F.3 Third case: $0 < B < 1$

In this case, the generalized eccentric anomaly E, introduced in Section 4.5.2, rather than θ or ξ, is the "natural" angular coordinate to use in the expression for Δ. By defining the quantities:

$$b = \left(1 - B^2\right)^{3/2} \quad ; \quad \Delta E = E_f - E_0 \tag{F.39}$$

and using the results of Section 4.5.2, one can express the six quantities r_0, r_f, $r_0\sin\xi_0$, $r_0\cos\xi_0$, $r_f\sin\xi_f$, and $r_f\cos\xi_f$ as:

$$r_0 = \frac{p_0\left(1 - B\cos E_0\right)}{b^{2/3}} \quad ; \quad r_0\sin\xi_0 = \frac{p_0\sin E_0}{b^{1/3}} \quad ; \quad r_0\cos\xi_0 = \frac{p_0\left(\cos E_0 - B\right)}{b^{2/3}} \tag{F.40}$$

$$r_f = \frac{p_f\left(1 - B\cos E_f\right)}{b^{2/3}} \quad ; \quad r_f\sin\xi_f = \frac{p_f\sin E_f}{b^{1/3}} \quad ; \quad r_f\cos\xi_f = \frac{p_f\left(\cos E_f - B\right)}{b^{2/3}} \tag{F.41}$$

Along such a one-segment transfer, with $0 < B < 1$, Eq. (4.34) is valid. Using the definitions given in Eqs. (F.14) and (F.39), one can write Eq. (4.34) at the final time τ_f as:

125

$$\frac{1}{p_f} = \frac{1}{p_0} - \frac{2A\left[\Delta E - B(\sin E_f - \sin E_0)\right]}{b} \qquad (F.42)$$

By defining the quantity D as:

$$D = b - 2Ap_0\left[\Delta E - B(\sin E_f - \sin E_0)\right] \qquad (F.43)$$

p_f can be written from Eq. (F.42) as:

$$p_f = \frac{b\,p_0}{D} \qquad (F.44)$$

The last step consists of substituting from Eqs. (F.40), (F.41) and (F.44) into the expression for Δ given in Eq. (F.21). One can write the result as:

$$\Delta = -\frac{16A^2 h_0^8 (1 - B^2)}{D^2}\left[\left(\frac{\Delta E}{2}\right)^2 - \sin^2\left(\frac{\Delta E}{2}\right)\right] \qquad (F.45)$$

Since the transfer duration is strictly positive, that is, $\tau_f > 0$, it must necessarily be true that $\Delta\theta = \theta_f - \theta_0 > 0$, which in turn implies that $\Delta\xi = \xi_f - \xi_0 > 0$ and $\Delta E > 0$. Moreover, for $\Delta E > 0$ the following inequality is always valid:

$$\frac{\Delta E}{2} > \sin\left(\frac{\Delta E}{2}\right) \qquad (F.46)$$

Accordingly, from Eq. (F.45), the discriminant Δ must be strictly negative ($\Delta < 0$), contradicting the necessary condition $\Delta \geq 0$ found in Eq. (F.7). This concludes the proof of part (i) for $0 < B < 1$.

F.4 Fourth case: B > 1

In this case, the generalized hyperbolic anomaly H, introduced in Section 4.5.3, rather than θ or ξ, is the "natural" coordinate to use in the expression for Δ. By defining the quantities:

$$b = (B^2 - 1)^{3/2} \quad ; \qquad \Delta H = H_f - H_0 \qquad (F.47)$$

126

and using the results of Section 4.5.3, one can express the six quantities r_0, r_f, $r_0 \sin\xi_0$, $r_0 \cos\xi_0$, $r_f \sin\xi_f$, and $r_f \cos\xi_f$ as:

$$r_0 = \frac{p_0(B\cosh H_0 - 1)}{b^{2/3}} \quad ; \quad r_0 \sin\xi_0 = \frac{p_0 \sinh H_0}{b^{1/3}} \quad ; \quad r_0 \cos\xi_0 = \frac{p_0(B - \cosh H_0)}{b^{2/3}} \quad \text{(F.48)}$$

$$r_f = \frac{p_f(B\cosh H_f - 1)}{b^{2/3}} \quad ; \quad r_f \sin\xi_f = \frac{p_f \sinh H_f}{b^{1/3}} \quad ; \quad r_f \cos\xi_f = \frac{p_f(B - \cosh H_f)}{b^{2/3}} \quad \text{(F.49)}$$

Along such a one-segment transfer, with $B > 1$, Eq. (4.42) is valid. Using the definitions given in Eqs. (F.14) and (F.47), one can write Eq. (4.42) at the final time τ_f as:

$$\frac{1}{p_f} = \frac{1}{p_0} + \frac{2A[\Delta H - B(\sinh H_f - \sinh H_0)]}{b} \quad \text{(F.50)}$$

By defining the quantity D as:

$$D = b + 2Ap_0[\Delta H - B(\sinh H_f - \sinh H_0)] \quad \text{(F.51)}$$

p_f can be written from Eq. (F.50) as:

$$p_f = \frac{bp_0}{D} \quad \text{(F.52)}$$

The last step consists of substituting from Eqs. (F.48), (F.49) and (F.52) into the expression for Δ given in Eq. (F.21). One can write the result as:

$$\Delta = -\frac{16A^2 h_0^8(B^2 - 1)}{D^2}\left[\sinh^2\left(\frac{\Delta H}{2}\right) - \left(\frac{\Delta H}{2}\right)^2\right] \quad \text{(F.53)}$$

Since the transfer duration is strictly positive, that is, $\tau_f > 0$, it must necessarily be true that $\Delta\theta = \theta_f - \theta_0 > 0$, which in turn implies that $\Delta\xi = \xi_f - \xi_0 > 0$ and $\Delta H > 0$. Moreover, for $\Delta H > 0$ the following inequality is always valid:

$$\sinh\left(\frac{\Delta H}{2}\right) > \frac{\Delta H}{2} \quad \text{(F.54)}$$

Accordingly, from Eq. (F.53), the discriminant Δ must be strictly negative ($\Delta < 0$), contradicting the necessary condition $\Delta \geq 0$ found in Eq. (F.7). This concludes the proof of part (i) for $B > 1$.

At this point, the proof of part (i) of Theorem 4.1 is complete. Now that part (i) has been proven, the validity of part (ii) becomes intuitively obvious, and can be argued for in the following way: First, assuming that the initial and final conics are tangent to each other, one will have to agree that the existence of an impulsive transfer solution at the point of tangency is obvious. All one has to do for such an impulsive transfer is use the correct amount of $\varepsilon\tau_f$ at the point of tangency (with ε infinitely large, τ_f infinitely small, and $\varepsilon\tau_f$ finite) and change the speed of the vehicle (tangentially to both conics) by the desired amount (ΔV). That there can be no other impulsive transfer is also obvious, since the orbital speeds associated with the two conics at the point of tangency are *unique*, resulting in a *unique* ΔV requirement. Thus, the only thing that is left to complete the proof for part (ii) is to show that there can be no finite time (nonimpulsive) transfer in such a case. But this is again (almost) obvious, since, for a finite time transfer, the discriminant Δ found in Eqs. (F.29), (F.37), (F.45), and (F.53) is strictly negative, contradicting the requirement that it be zero (see Eq. (F.7)), coming from the assumption that the initial and final conics have *one* common point.

Q. E. D.

APPENDIX G

Explicit Expressions for the Power-Limited Cost
Along a One-Segment Transfer Trajectory

In this Appendix the goal is to obtain a workable approximation for the power-limited cost associated with a one-segment transfer trajectory, valid in the limit of long transfer duration and very low thrust (small throttling parameter A). Recall the expression for the (nondimensional) speed of the vehicle given by Eq. (A.8) in Appendix A. Differentiating this expression and 1/r with respect to time, and using Eqs. (4.11) through (4.13) one obtains :

$$\frac{dV}{d\tau} = \frac{AV}{h} - \frac{x}{Vr^2} \quad ; \quad \frac{d}{d\tau}\left(\frac{1}{r}\right) = -\frac{x}{r^2} \qquad (G.1)$$

Let now S be the (nondimensional) mechanical energy (kinetic plus potential) of the vehicle. Explicitly, S is:

$$S = \frac{V^2}{2} - \frac{1}{r} \qquad (G.2)$$

Using Eq. (G.1), and substituting for the thrust acceleration program from Eq. (4.159), the time derivative of S can be found as:

$$\frac{dS}{d\tau} = \frac{AV^2}{h} = \varepsilon V \qquad (G.3)$$

Equation (G.3) expresses a familiar result. It simply states that the work done per unit time by the thrust program proposed in Eq. (4.10) is equal to the time rate of change of the mechanical energy of the vehicle. Along a (one-segment) transfer trajectory dh = Adτ, so that Eq. (G.3) can be rewritten as:

$$dS = \left(\frac{V^2}{h}\right)dh \qquad (G.4)$$

129

The power-limited cost associated with a (one-segment) transfer is given by:

$$J_{PL} = \int_0^{\tau_f} \frac{\varepsilon^2}{2} d\tau = \frac{1}{2} \int_0^{\tau_f} \frac{A^2 V^2}{h^2} d\tau = \frac{A}{2} \int_{h_0}^{h_f} \frac{V^2}{h^2} dh \qquad (G.5)$$

and, using Eq. (G.4), it assumes the form:

$$J_{PL} = \frac{A}{2} \int_{S_0}^{S_f} \frac{dS}{h} \qquad (G.6)$$

Integrating by parts in Eq. (G.6) one obtains:

$$J_{PL} = \frac{A}{2} \left(\frac{S_f}{h_f} - \frac{S_0}{h_0} \right) + \frac{A}{2} \int_{h_0}^{h_f} \frac{S dh}{h^2} \qquad (G.7)$$

and, substituting from Eq. (G.2), J_{PL} can be written as:

$$J_{PL} = \frac{A}{2} \left(\frac{S_f}{h_f} - \frac{S_0}{h_0} \right) + \frac{A}{4} \int_{h_0}^{h_f} \frac{V^2 dh}{h^2} - \frac{A}{2} \int_{h_0}^{h_f} \frac{dh}{r h^2} \qquad (G.8)$$

Using the definition of J_{PL} given in Eq. (G.5), one can further simplify Eq. (G.8) as:

$$J_{PL} = A \left(\frac{S_f}{h_f} - \frac{S_0}{h_0} \right) - A \int_{h_0}^{h_f} \frac{dh}{r h^2} \qquad (G.9)$$

From Eqs. (A.7) and (G.2) S is equal to $-1/(2a)$, where, a is the instantaneous semimajor axis along the transfer trajectory. Combining this with Eq. (A.9), one obtains:

$$S = - \frac{1}{2a} = \frac{e^2 - 1}{2h^2} \qquad (G.10)$$

where of course e and h are the (instantaneous) eccentricity and angular momentum along the transfer trajectory respectively. Using Eq. (G.10), one can write Eq. (G.9) as:

130

$$J_{PL} = \frac{A}{2}\left(\frac{e_f^2 - 1}{h_f^3} - \frac{e_0^2 - 1}{h_0^3}\right) - A\int_{h_0}^{h_f}\frac{dh}{r\,h^2} \qquad (G.11)$$

Consider now a (one-segment) transfer trajectory on which B is zero. On such a transfer trajectory r is equal to h^2 (see Eq. (4.17)), and Eq. (G.11) becomes:

$$\text{if } B = 0, \text{ then:} \quad J_{PL} = \frac{A}{2}\left(\frac{e_f^2 - 1}{h_f^3} - \frac{e_0^2 - 1}{h_0^3}\right) - A\int_{h_0}^{h_f}\frac{dh}{h^4} \qquad (G.12)$$

which after a simple integration results in:

$$\text{if } B = 0, \text{ then:} \quad J_{PL} = \frac{A}{6}\left(\frac{3e_f^2 - 1}{h_f^3} - \frac{3e_0^2 - 1}{h_0^3}\right) \qquad (G.13)$$

When B is nonzero things are more complicated. With $\xi = \theta - C$ (see Eq. (4.20)), and $d\xi = d\theta$, one can now use Eqs. (4.11) and (4.14) and write Eq. (G.11) as:

$$J_{PL} = \frac{A}{2}\left(\frac{e_f^2 - 1}{h_f^3} - \frac{e_0^2 - 1}{h_0^3}\right) - A^2\int_{\xi_0}^{\xi_f}\frac{r\,d\xi}{h^3} \qquad (G.14)$$

When B=1, one can introduce the variable $y = \tan(\xi/2)$, and, noting that:

$$d\xi = \frac{2dy}{\left(1 + y^2\right)} \quad ; \quad r = \frac{h^2}{1 + B\cos\xi} = \frac{h^2}{1 + \cos\xi} = \frac{h^2\left(1 + y^2\right)}{2} \qquad (G.15)$$

one can substitute in Eq. (G.14) and write the power-limited cost as:

$$\text{if } B = 1, \text{ then:} \qquad J_{PL} = \frac{A}{2}\left(\frac{e_f^2 - 1}{h_f^3} - \frac{e_0^2 - 1}{h_0^3}\right) - A^2\int_{y_0}^{y_f}\frac{dy}{h} \qquad (G.16)$$

Similarly, when $0 < B < 1$, or $B > 1$, one can introduce respectively the generalized eccentric and hyperbolic anomalies, use the results of Sections 4.5.2 and 4.5.3, and write the power-limited cost as:

131

$$\text{if } 0 < B < 1, \text{ then:} \quad J_{PL} = \frac{A}{2}\left(\frac{e_f^2-1}{h_f^3} - \frac{e_0^2-1}{h_0^3}\right) - \frac{A^2}{\sqrt{1-B^2}}\int_{E_0}^{E_f}\frac{dE}{h} \qquad (G.17)$$

$$\text{if } B > 1, \text{ then:} \quad J_{PL} = \frac{A}{2}\left(\frac{e_f^2-1}{h_f^3} - \frac{e_0^2-1}{h_0^3}\right) - \frac{A^2}{\sqrt{B^2-1}}\int_{H_0}^{H_f}\frac{dH}{h} \qquad (G.18)$$

Although the expression for the power-limited cost found in Eq. (G.13) is exact only when B=0, this expression is also approximately valid when B is small:

$$\text{if } B \approx 0, \text{ then:} \quad J_{PL} \approx \left(\frac{h_f-h_0}{6\tau_f}\right)\left(\frac{3e_f^2-1}{h_f^3} - \frac{3e_0^2-1}{h_0^3}\right) \qquad (G.19.a)$$

For transfers from a circular orbit (see Section 4.8) e_0 is zero, and if e_f is not very large, then B is quite close to zero (see Figs. 4.7, 4.13, 4.15, 4.17, and 4.19). In this case Eq. (G.19.a) assumes the form:

$$\text{if } e_0 = 0, B \approx 0, \text{ then:} \quad J_{PL} \approx \left(\frac{h_f-h_0}{6\tau_f}\right)\left(\frac{1}{h_0^3} + \frac{3e_f^2-1}{h_f^3}\right) \qquad (G.19.b)$$

Transfers between two coplanar circular orbits (see Appendix D) correspond to the limiting case of very small e_f. On such transfers B is indeed very small (see Fig. 4.7), and in this case Eq. (G.19.b) assumes the form:

$$\text{if } e_0 = e_f = 0, B \approx 0, \text{ then:} \quad J_{PL} \approx \left(\frac{h_f-h_0}{6\tau_f}\right)\left(\frac{1}{h_0^3} - \frac{1}{h_f^3}\right) \qquad (G.19.c)$$

The validity of the approximation expressed in Eq. (G.19) is checked in Table G.1 that follows, by comparing the power-limited cost evaluated from Eq. (G.19.b) with the exact power-limited cost (see Table 4.1) for some of the transfers (the ones from a circular orbit). The second and third columns of Table G.1 supply the throttling parameter A and the generalized eccentricity B for the corresponding transfer. The approximate power-limited cost, evaluated from Eq. (G.19.b), is given in the fourth column, and it is compared with the exact power-limited cost given in the fifth column, reproduced from the fourth column of Table 4.1.

Table G.1 Approximate power-limited cost using Eq. (G.19)

Transfer	A	B	J_{PL} (Eq. (G.19))	J_{PL} (Table 4.1)
Fig. 4.7	6.1139e-3	1.2228e-2	8.9257e-4	8.9225e-4
Fig. 4.13	3.6210e-2	7.2420e-2	5.5579e-3	5.4860e-3
Fig. 4.15	1.0542e-1	2.1084e-1	2.0017e-2	1.7064e-2
Fig. 4.17	1.0131e-1	2.0261e-1	2.2436e-2	2.0457e-2
Fig. 4.19	2.9601e-2	5.9202e-2	5.0924e-3	5.0593e-3

It is apparent from Table G.1 that the approximation expressed by Eq. (G.19.b) is indeed valid for low thrust levels (small A) and small B. Thus, for transfers from a circular to a nearly circular orbit, since both A and B are small, Eq. (G.19.b) is valid. For low-thrust transfers however from an arbitrary conic, B in general need not be small (see Fig. 4.2 for example), and Eq. (G.19) needs to be corrected. For the cases in which $0 < B < 1$, or $B > 1$, this correction can be obtained by noting that Eqs. (4.34) and (4.42), supplying the dependence of the angular momentum h on the generalized eccentric and hyperbolic anomalies E and H respectively, can be approximated as:

$$\text{small A, } 0 < B < 1: \qquad \frac{1}{h^2} \approx \frac{1}{h_0^2} - \frac{2A(E - E_0)}{(1 - B^2)^{3/2}} \qquad (G.20)$$

$$\text{small A, } B > 1: \qquad \frac{1}{h^2} \approx \frac{1}{h_0^2} + \frac{2A(H - H_0)}{(B^2 - 1)^{3/2}} \qquad (G.21)$$

Now, substituting from Eqs. (G.20) and (G.21) into Eq. (G.17) and (G.18) respectively, one obtains for *both* of the above cases the approximate expression:

$$\text{if A is small enough, then: } \quad J_{PL} \approx \left(\frac{h_f - h_0}{6\tau_f} \right) \left(\frac{3e_f^2 - 2B^2 - 1}{h_f^3} - \frac{3e_0^2 - 2B^2 - 1}{h_0^3} \right) \qquad (G.22)$$

Note that Eq. (G.19) corresponds to a special case in Eq. (G.22), for which B=0. By a continuity argument it is also obvious that the approximation expressed in Eq. (G.22) should also be valid when B=1. Thus, Eq. (G.22) is a single, general approximation, valid for low-thrust, long duration, one-segment transfers.

133

One must be careful however when using Eq. (G.22), because, for the case in which both the initial and final conics are noncircular, low-thrust, long duration, one-segment transfers between the conics may not exist. It appears that, when $0 < B < 1$, Eq. (G.22) is valid for low-thrust, many revolution, one-segment transfers, that is, transfers on which E_f-E_0 is large. When on the other hand $B > 1$, Eq. (G.22) is most probably valid for low-thrust, one-segment transfers on which H_f-H_0 is small. This condition seems to be necessary if the term $-B(\sinh H-\sinh H_0)$ that was omitted when writing down Eq. (G.21) is to be unimportant along a transfer. Table G.2 that follows supplies all the cases of transfers among the examples, for which the power-limited cost evaluated from Eq. (G.22) (fourth column) compares well with the exact power-limited cost (fifth column) associated with the same one-segment transfer.

Table G.2 Approximate power-limited cost using Eq. (G.22)

Transfer	A	B	J_{PL} (Eq. (G.22))	J_{PL} (Table 4.1)
Fig. 4.2	3.5000e-3	7.0000e-1	1.5969e-4	1.5369e-4
Fig. 4.4	3.5000e-2	7.0120e-1	3.9261e-3	3.9537e-3
Fig. 4.7	6.1139e-3	1.2228e-2	8.9283e-4	8.9225e-4
Fig. 4.13	3.6210e-2	7.2420e-2	5.6132e-3	5.4860e-3
Fig. 4.19	2.9601e-2	5.9202e-2	5.1264e-3	5.0593e-3

For the cases of course in which $B > 0$ and the approximation supplied by Eq. (G.22) is not good one can always evaluate the power-limited cost associated with a one-segment transfer trajectory using the exact expressions given by Eqs. (G.16) through (G.18).

APPENDIX H

Comparison Between Keplerian Motion and the Motion Uncovered in Section 4.4

$\mathbf{K}$eplerian conics corresponding to Keplerian motion (see Appendix A), and two-dimensional transfer trajectories, corresponding to the motion uncovered in Section 4.4, have in this report been unified into a single descriptive scheme, exemplified by a common trajectory equation. This Appendix supplies an elementary comparison of the two types of motion, which can be summarized as in Table H.1 that follows.

Table H.1 Comparison between Keplerian motion and Present motion

Type of motion:	Keplerian	Present (Section 4.4)
Thrust acceleration:	$\varepsilon = 0$	$\varepsilon = \dfrac{A}{r\cos\gamma}$ (tangential)
Angular momentum:	$h = h_0 = $ constant	$h = A\tau + h_0$
Trajectory equation:	$r = \dfrac{h^2}{1 + e\cos(\theta - \omega)}$	$r = \dfrac{h^2}{1 + e\cos(\theta - \omega)}$

In Keplerian motion the thrust acceleration is zero and the angular momentum of the vehicle (considered as a point mass) about the planet is constant. In the type of motion uncovered in Section 4.4 the thrust acceleration is tangential and equal to $A/(r\cos\gamma)$, where A is a constant (the throttling parameter), and the angular momentum of the vehicle about the planet is a linear function of time. For both types of motion the trajectory equation has the same identical form! Just as Keplerian motion, the motion uncovered in Section 4.4 corresponds to an *exact analytic* solution of the equations of motion. Note that the generalized eccentricity and orientation constants B and C of a transfer trajectory have in Table H.1 been denoted as e and ω respectively, to make clear the analogy with the eccentricity and orientation constants corresponding to Keplerian motion. The reader is advised to compare Table H.1 with Table I.1 (page 139) of Appendix I.

135

APPENDIX I

The Keplerian Class of Thrust Programs

Let Q be an *arbitrary, explicit, differentiable* function of the nondimensional time variable τ. For any such function Q one can form the thrust program given explicitly by the components:

$$\varepsilon_r = \frac{xQ}{h} + \frac{2r\dot{Q}}{h} \quad ; \qquad \varepsilon_\theta = \frac{Q}{r} \tag{I.1}$$

where the dot denotes differentiation with respect to τ. Q will be called the *throttling function*. Note that when Q is a constant, say equal to a *throttling parameter* A, one obtains from Eq. (I.1) the thrust program proposed in Eq. (4.10) of Section 4.3 in the main text. The totality of thrust programs defined by Eq. (I.1) will be given the name the *Keplerian class*. The Keplerian class is a rather privileged class of thrust programs, because for all its members the corresponding equations of motion afford a rather simple *exact analytic* solution. Specifically, if the right-hand-sides of Eqs. (4.6), (4.7) are forced with the components of the thrust acceleration vector given in Eq. (I.1), then the *exact* solution of Eqs. (4.6) through (4.9) is given by the following four quadratures:

$$h = h_0 + \int_0^\tau Q\, d\tau \tag{I.2}$$

$$x = \frac{2rQ + B\sin(\theta - C)}{h} \tag{I.3}$$

$$r = \frac{h^2}{1 + B\cos(\theta - C)} \tag{I.4}$$

$$\int_0^\tau \frac{d\tau}{h^3} = \int_{\theta_0}^{\theta} \frac{d\theta}{[1 + B\cos(\theta - C)]^2} \tag{I.5}$$

where h_0, B, C, and θ_0 are four arbitrary constants of integration. This result can be easily verified by differentiating Eqs. (I.2) through (I.5) with respect to τ, taking into account Eq.

136

(I.1), and by checking that Eqs. (4.6) through (4.9) are identically satisfied. Eqs. (I.2) through (I.5) reduce to Eqs. (4.15) through (4.18) when $Q=A=$constant. Note that if Q is not *explicit* in τ, then Eqs. (I.3), (I.4) still constitute two exact quadratures, while obtaining two more quadratures in such a case may or may not be possible depending on the functional dependence of Q. Note also that again, as in Eq. (4.17), Eq. (I.4) describing the trajectory is *identical* in form with the trajectory equation corresponding to two-body Keplerian motion! Thus, the constants B and C can again be called the *generalized eccentricity* and the *generalized orientation* respectively, since they play qualitatively the same role as the eccentricity and orientation constants e and ω do in Keplerian motion.

Apart from its kinship with Keplerian motion, the importance of the motion arising under the Keplerian class of thrust programs comes partly from the following claim[55]: If the throttling function Q is small, and if the time derivatives of the throttling function $d^n Q/d\tau^n$ $n=1,2,3...$ are much smaller than the throttling function itself, then the corresponding motion under Keplerian thrust, described by Eqs. (I.2) through (I.5), can presumably be expected to be nearly-optimal when performed with a power-limited propulsion system. This claim can be argued upon by examining[55] the costate system of Eqs. (4.54) through (4.56), and the transversality conditions, Eqs. (4.106), (4.109), (4.110), under the assumption that the optimal power-limited thrust is approximately Keplerian. Note that for long duration maneuvers one can easily find members of the Keplerian class for which the above conditions on the throttling function Q are satisfied[55]. In particular, one can introduce four classes of such members each one of which is suitable for treating a special type of finite-time problem that may be encountered during orbital operations. These four classes will be given the names the *Tangential*, the *Linear*, the *Quadratic*, and the *Cubic class*, and correspond to the (Keplerian) thrust programs for which the throttling function Q is respectively a zero, first, second, and third degree polynomial of time τ.

A thrust program will be called *tangential* if and only if the corresponding thrust acceleration vector is tangent to the vehicle's flight path for all time τ for which the thrust program is defined.

Note now that:

(i) The throttling function Q, and the corresponding thrust program, depend on one, two, three, and four arbitrary constants for the Tangential, the Linear, the Quadratic, and the Cubic (sub)classes of (Keplerian) thrust programs respectively.

(ii) When $dQ/d\tau$ is small compared to Q, that is, when Q is slowly varying, then the corresponding thrust is nearly-tangential.

137

(iii) A *Keplerian* thrust program is *tangential* if and only if it is a member of the Tangential (sub)class.

(iv) For the Tangential class of thrust programs Q is a zero degree polynomial, namely a constant.

(v) The class of thrust programs proposed in Eq. (4.10) of Section 4.3 was none other than the Tangential (sub)class of (Keplerian) thrust programs.

(vi) Chapter IV of this report treated in some detail the motion that can be executed under the Tangential class of thrust programs.

It can be verified[55] that near-optimality (in the power-limited sense) and controllability appear as two opposing trends as one goes from the (simplest) Tangential class toward the (most sophisticated) Cubic class of thrust programs. One can satisfy the first-order necessary conditions for optimality extremely well using the Tangential class (see Section 4.6.5), but the vehicle is not completely controllable under the corresponding thrust programs (see for example Theorem 4.1 of Section 4.11, and Appendix F). On the other hand, using the Cubic class one may not be able to satisfy the first-order necessary conditions as well, but the vehicle is much more controllable under the corresponding thrust programs[55]. In fact, it is straightforward to show the following theorem about controllability with regard to the Cubic class (the proof is given in Ref. 55):

Theorem. If h_0, h_f, r_0, r_f, and $\tau_f - \tau_0$ are all *strictly positive*, then, any *given* initial state $(h_0, x_0, r_0, \theta_0)$ at a *given* initial time $\tau = \tau_0$ can be driven to any *given* final state $(h_f, x_f, r_f, \theta_f)$ at a *given* final time $\tau = \tau_f$ by a thrust program belonging to the Cubic class.

The four subclasses introduced above are suitable for treating the following finite-time problems (Note that h_0, e_0, ω_0, e_f and ω_f are always fixed):

(a) Escape problems: For all such problems θ_0, θ_f, and h_f are all left free. The time duration τ_f of the maneuver is fixed. The throttling function Q should depend on (at least) one arbitrary constant. The Tangential class of thrust programs for which the throttling function is an arbitrary constant is uniquely suitable for treating these problems. In this report this was done in Sections 4.9 and 4.10.

(b) Transfer problems: For these problems θ_0 and θ_f are left free, but h_f is fixed. The time duration τ_f of the maneuver may be fixed or free. If τ_f is left free then Q should depend on (at least) one arbitrary constant, meaning that the Tangential class is the suitable one to choose in such cases. This was done in this report in sections 4.8 and 4.10. If τ_f is fixed then Q should depend on (at least) two arbitrary constants and the Linear class may be used.

(c) **Mixed Transfers-Rendezvous:** For these problems h_f is fixed, and only one among θ_0 or θ_f is left free, while the other is fixed. The time duration τ_f of the maneuver may be fixed or left free. If τ_f is left free then Q should depend on (at least) two arbitrary constants, meaning that the Linear class is the suitable one to choose in such cases. If τ_f is fixed then Q should depend on (at least) three arbitrary constants and the Quadratic class may be used.

(d) **Rendezvous Problems:** For these problems θ_0, θ_f, and h_f are all fixed. The time duration τ_f of the maneuver may be fixed or left free (in practice it is usually desirable to have a fixed τ_f). If τ_f is left free then Q should depend on (at least) three arbitrary constants, making the Quadratic class the suitable one to choose in such cases. If τ_f is fixed then Q should depend on (at least) four arbitrary constants and the Cubic class may be used.

This Appendix concludes by supplying a comparison between Keplerian motion and the motion arising under Keplerian thrust, which can be summarized as in Table I.1 that follows. The reader is advised to compare Table I.1 with Table H.1 (page 135) of Appendix H.

Table I.1 Comparison between Keplerian motion and motion under Keplerian thrust

Type of motion:	Keplerian	Present
Thrust:	Zero	Keplerian
Thrust acceleration:	$\varepsilon_r = 0$; $\varepsilon_\theta = 0$	$\varepsilon_r = \dfrac{xQ + 2r\dot{Q}}{h}$; $\varepsilon_\theta = \dfrac{Q}{r}$
Angular momentum:	$h = h_0 = \text{constant}$	$h = h_0 + \displaystyle\int_0^\tau Q\, d\tau$
Trajectory equation:	$r = \dfrac{h^2}{1 + e\cos(\theta - \omega)}$	$r = \dfrac{h^2}{1 + e\cos(\theta - \omega)}$

Note once more that the generalized eccentricity and orientation constants B and C in Eq. (I.4) have in Table I.1 been denoted as e and ω respectively, to make clear the analogy

with the eccentricity and orientation constants corresponding to Keplerian motion. The detailed theory introducing the Keplerian Class of thrust programs is given in Ref. 55. For applications corresponding to the Keplerian Class of thrust programs the reader is referred to Ref. 56 and to the proceedings of the AIAA Astrodynamics Conference of 1995.

References

1. Ardema, M. D., and Rajan, N., "Separation of Time Scales in Aircraft Trajectory Optimization," *AIAA Journal of Guidance and Control*, Vol. 8, No. 2, March-April 1985, pp. 275-278.

2. Shinar, J., "On Applications of Singular Perturbation Techniques in Nonlinear Optimal Control," *Automatica*, Vol. 19, No. 2, 1983, pp. 203-211.

3. Breakwell, J. V., "Optimal Flight-Path Angle Transitions in Minimum-Time Airplane Climbs," *Journal of Aircraft*, Vol. 14, August 1977, pp. 782-786.

4. Calise, A. J., "Optimal Thrust Control with Proportional Navigation Guidance," *AIAA Journal of Guidance and Control*, Vol. 3, No. 4, July-August 1980, pp. 312-318.

5. Kelley, H. J., and Edelbaum, T. N., "Energy Climbs, Energy Turns, and Asymptotic Expansions," *Journal of Aircraft*, Vol. 7, Jan.-Feb. 1970, pp. 93-95.

6. Ardema, M. D., "Solution of the Minimum Time-to-Climb Problem by Matched Asymptotic Expansions," *AIAA Journal*, Vol. 14, No. 7, July 1976, pp. 843-850.

7. Calise, A. J., "Extended Energy Management Methods for Flight Performance Optimization," *AIAA Journal*, Vol. 15, No. 3, March 1977, pp. 314-321.

8. Calise, A. J., "Singular Perturbation Techniques for On-Line Optimal Flight Path Control," *AIAA Journal of Guidance and Control*, Vol. 4, No. 4, July-Aug. 1981, pp. 389-405.

9. Calise, A. J., and Melamed, N., "Optimal Guidance of Aero-Assisted Transfer Vehicles Based on Matched Asymptotic Expansions," AIAA Guidance, Navigation, and Control Conference, New Orleans, Louisiana, August 12-14, 1991, paper No. 91-2680.

10. Melamed, N., and Calise, A. J., "Evaluation of an Optimal Guidance Algorithm for Aero-Assisted Orbit Transfer," AIAA Guidance, Navigation, and Control Conference, Hilton Head, South Carolina, August 10-12, 1992, paper No. 92-4454.

11. Kokotovic, P., Hassan, K. K., and O'Reilly, J., *Singular Perturbation Methods in Control: Analysis and Design*, Academic Press, 1986, pp. 140-142.

12. Corban, J. E., Calise, A. J., and Flandro, G. A., "Rapid Near-Optimal Aerospace Plane Trajectory Generation and Guidance," *AIAA Journal of Guidance, Control, and Dynamics*, Vol. 14, No. 6, Nov.-Dec. 1991, pp. 1181-1190.

13. Calise, A. J., and Moerder, D. D., "Singular Perturbation Techniques for Real Time Aircraft Trajectory Optimization and Control," NASA CR-3597, Aug. 1982.

14. Calise, A. J., and Pettengil, J. B., "A Comparison of Time-Optimal Intercept Trajectories for the F-8 and F-15 - Final Report," NASA CR-186300, Jan. 1990.

15. Barman, J. F., and Erzberger, H., "Fixed-Range Optimum Trajectories for Short-Haul Aircraft," *Journal of Aircraft*, Vol. 13, No. 10, October 1976, pp. 748-754.

16. Corban, J. E., "Real-Time Guidance and Propulsion Control for Single-Stage-to-Orbit Airbreathing Vehicles," Ph.D. Dissertation, Georgia Inst. of Technology, Atlanta, GA, Dec. 1989.

17. Weston, A. R., Kelley, H. J., and Cliff, E. M., "Energy-State Revisited," *Optimal Control Applications & Methods*, Vol. 7, April 1986, pp. 195-200.

18. Calise, A. J., Markopoulos, N., and Corban, J. E., "Nondimensional forms for Singular Perturbation Analyses of Aircraft Energy Climbs," *AIAA Journal of Guidance, Control, and Dynamics*, Vol. 17, No. 3, May-June 1994, pp. 584-590.

19. Falco, M., and Kelly, H. J., "Aircraft Symmetric Flight Optimization," *Control and Dynamic Systems, Advances in Theory and Applications*, Vol. 10, Academic Press, New York, NY, 1973.

20. McHenry, R. L., Brand, T. J., Long, A. D., Cockrell, B. F., and Thibodeau III, B. F., "Space Shuttle Ascent Guidance, Navigation, and Control," *The Journal of the Astronautical Sciences*, Vol. XXVII, No. 1, pp. 1-38, January-March, 1979.

21. Hargraves, C. R., and Paris, S. W., "Direct Trajectory Optimization Using Nonlinear Programming and Collocation," *Journal of Guidance*, Vol. 10, No. 4, July-August 1987, pp. 338-342.

22. Bryson, A. E., Jr., and Ho, Yu-Chi, *Applied Optimal Control*, Hemisphere Publishing Corp., New York, 1975.

23. Jacobson, D. H., Lele, M. M., and Speyer, J. L., "New Necessary Conditions of Optimality for Control Problems with State-Variable Inequality Constraints," *Journal of Mathematical Analysis and Applications*, 35, pp. 255-284, 1971.

24. Kreindler, E., "Additional Necessary Conditions for Optimal Control with State-Variable Inequality Constraints," *Journal of Optimization Theory and Applications*, Vol. 30, No. 2, Oct. 1982, pp. 241-251.

25. Boykin, W. H., Jr., and Bullock, T. E., "State Constraints and Singular Solutions to Penalty Function Optimization Problems," *AIAA Journal*, Vol. 10, No. 2, Feb. 1972, pp. 137-141.

26. Calise, A. J., "Singular Perturbation Techniques for On-Line Optimal Flight Path Control," *AIAA Journal of Guidance and Control*, Vol. 4, No. 4, 1981.

27. Ardema, M. D., "Solution of the Minimum Time-to-Climb Problem by Matched Asymptotic Expansions", *AIAA Journal*, Vol. 14, pp. 843-850, 1976.

28. Calise, A. J., and Corban J. E., "Optimal Control of Two-Time Scale Systems with State-Variable Inequality Constraints" *Journal of Guidance, Control, and Dynamics*, Vol. 15, No. 2, March-April 1992, pp. 468-476.

29. Calise, A. J., "A New Boundary Layer Matching Procedure for Singularly Perturbed Systems," *IEEE Transactions on Automatic Control*, Vol. AC-23, No. 3, June 1978, pp. 434-438.

30. Jacobson, D. H., and Lele, M. M., "A Transformation Technique for Optimal Control Problems with a State Variable Inequality Constraint," *IEEE Transactions on Automatic Control*, Vol. AC-14, No. 5, Oct. 1969, pp. 457-464.

31. Ardema, M. D., "Nonlinear Singularly Perturbed Optimal Control Problems with Singular Arc," *Automatica*, Vol. 16, No. 1, Jan. 1980, pp. 99-104.

32. Markopoulos, N., and Calise, A. J., "Near-Optimal, Asymptotic Tracking in Control Problems Involving State-Variable Inequality Constraints," Presented at the AIAA Guidance, Navigation and Control Conference, Monterey, California, August 9-11, 1993.

33. Spiegel, M. R., *Mathematical Handbook of Formulas and Tables*, Schaum's Outline Series, McGraw-Hill, New York, 1968.

34. Battin, R. H., *An Introduction to the Mathematics and Methods of Astrodynamics*, AIAA, New York, 1987.

35. Lawden, D. F., "Rocket Trajectory Optimization: 1950-1963," *Journal of Guidance, Control, and Dynamics*, Vol. 14, No. 4, 1991, pp. 705-711.

36. Boltz, F. W., "Orbital Motion Under Continuous Tangential Thrust," *Journal of Guidance, Control, and Dynamics*, Vol. 15, No. 6, 1992, pp. 1503-1507.

37. Cajori, F., *Sir Isaac Newton's Mathematical Principles of Natural Philosophy and his System of the World*, Vol. 1, 2, University of California Press, 1934.

38. Whittaker, E. T., *A Treatise on the Analytical Dynamics of Particles and Rigid Bodies*, Cambridge University Press, Cambridge, England, 1937.

39. Tsien, H. S., "Take-off from Satellite Orbit," *Journal of the American Rocket Society*, Vol. 23, No. 4, pp. 233-236.

40. Benney, D. J., "Escape from a Circular Orbit Using Tangential Thrust," *Jet Propulsion*, Vol. 28, No. 3, pp. 167-169.

41. Lawden, D. F., "Optimal Programming of Rocket Thrust Direction," *Astronautica Acta*, Vol. 1, No. 1, 1955, pp. 41-56.

42. Lawden, D. F., "Optimal Escape from a Circular Orbit," *Astronautica Acta*, Vol. 4, No. 3, 1958, pp. 218-233.

43. Long, R. S., "Escape from a Circular Orbit with Finite Velocity at Infinity," *Astronautica Acta*, Vol. 5, No. 3, 1959, pp. 159-162.

44. Edelbaum, T. N., "Optimum Low-Thrust Rendezvous and Station Keeping," *AIAA Journal*, Vol. 2, No. 7, 1964, pp. 1196-1201.

45. Edelbaum, T. N., "Optimum Power-Limited Orbit Transfer in Strong Gravity Fields," *AIAA Journal*, Vol. 3, No. 7, 1965, pp. 921-925.

46. Grodzovskii, G. L., Ivanov, Yu. N., and Tokarev, V. V., *Mechanics of Low-Thrust Spaceflight*, Israel Program for Scientific Translations, Jerusalem, 1969.

47. Marec, J. P. and Vinh, N. X., "Optimal Low-Thrust, Limited Power Transfers Between Arbitrary Elliptical Orbits," *Astronautica Acta*, Vol. 4, 1977, pp. 511-540.

48. Marec, J. P., *Optimal Space Trajectories*, Elsevier, New York, 1979.

49. Golan, O. M., and Breakwell, J. V., "Minimum Fuel Trajectories for a Low-Thrust Power-Limited Mission to the Moon and to Lagrange Points L_4 and L_5," AIAA/AAS Astrodynamics Conference, Stowe, Vermont, August 7-10, 1989.

50. Haissig, C. M., Mease, K. D., and Vinh, N. X., "Minimum-Fuel, Power-Limited Transfers Between Coplanar Elliptical Orbits" *Astronautica Acta*, Vol. 29, No. 1, 1993, pp. 1-15.

51. Haissig, C. M., "Minimum-Fuel Power-Limited Transfers Between Coplanar Elliptic Orbits," Ph.D. Thesis, Princeton University, Mechanical and Aerospace Engineering, October 1992.

52. Markopoulos, N., "Analytically Exact Non-Keplerian Motion for Orbital Transfers," AIAA/AAS Astrodynamics Conference, Scottsdale, Arizona, August 1-3, 1994, paper No. 94-3758.

53. Markopoulos, N., "Analytical Investigations in Aircraft and Spacecraft Trajectory Optimization and Optimal Guidance," Ph.D. Thesis, Georgia Institute of Technology, Aerospace Engineering, August 1994.

54. Chapra, S. C., and Canale, R. P., *Numerical Methods for Engineers*, McGraw-Hill, 1985.

55. Markopoulos, N., "Non-Keplerian Manifestations of the Keplerian Trajectory Equation, and a Theory of Orbital Motion Under Continuous Thrust," Proceedings of the AAS/AIAA Space Flight Mechanics Conference, Albuquerque, New Mexico, February 13-16, 1995, paper No. 95-217.

56. Markopoulos, N., "Explicit, Near-Optimal Guidance for Power-Limited Transfers Between Coplanar Circular Orbits," AIAA Guidance, Navigation, and Control Conference, Baltimore, Maryland, August 7-10, 1995.

Figures
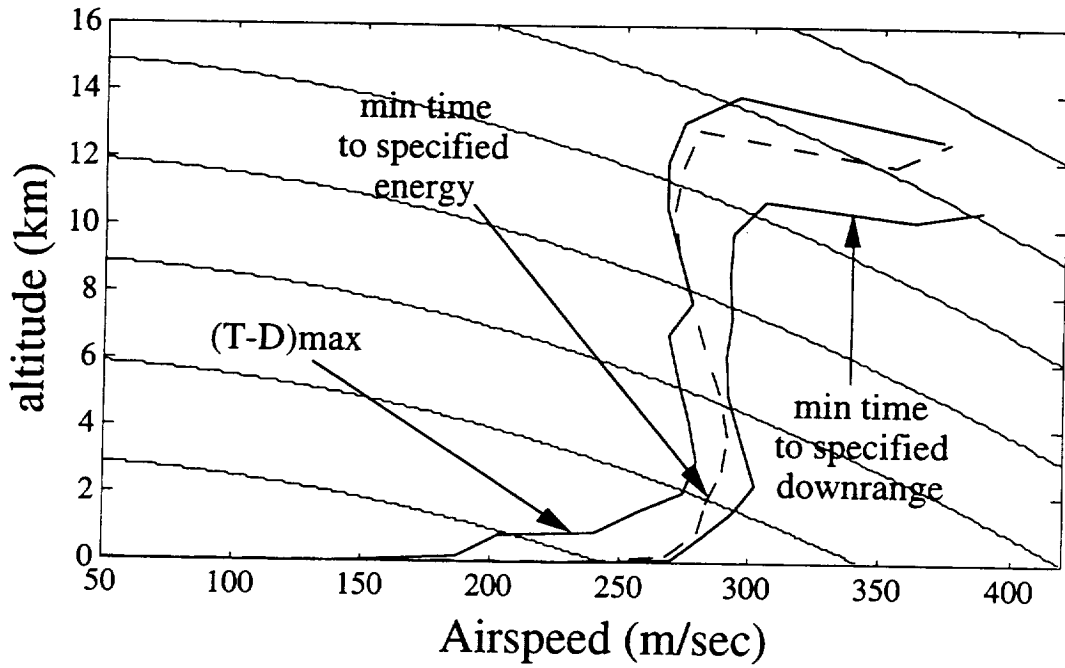
Figure 2.1 Energy climb paths for an F-8 aircraft.
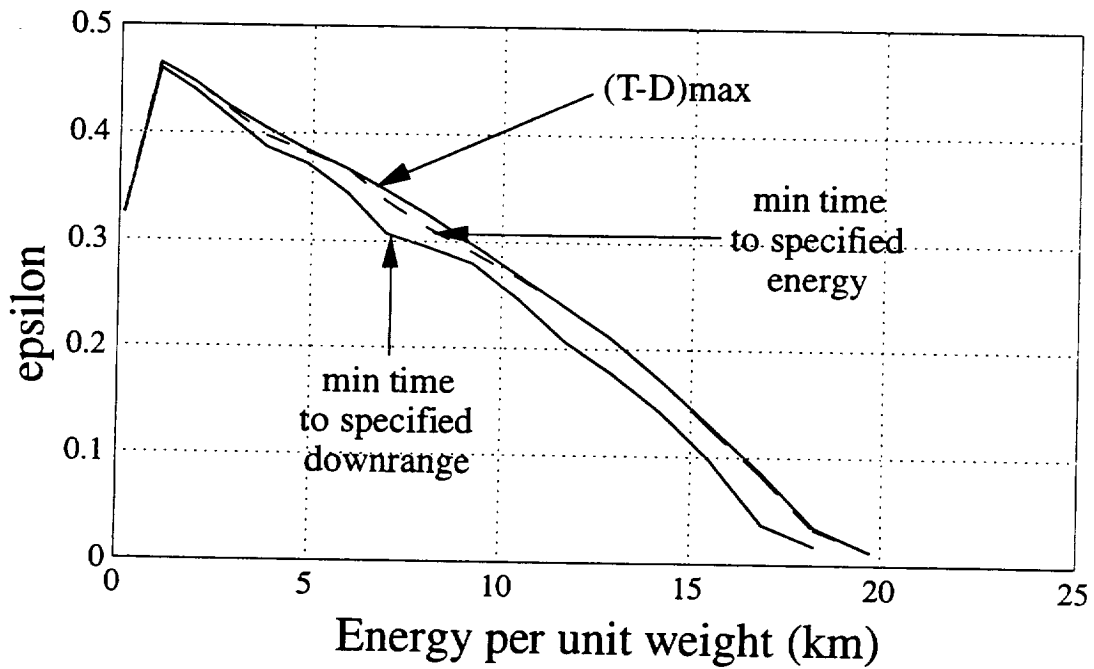
Figure 2.2 Evaluation of ε(E) for an F-8 aircraft.

149
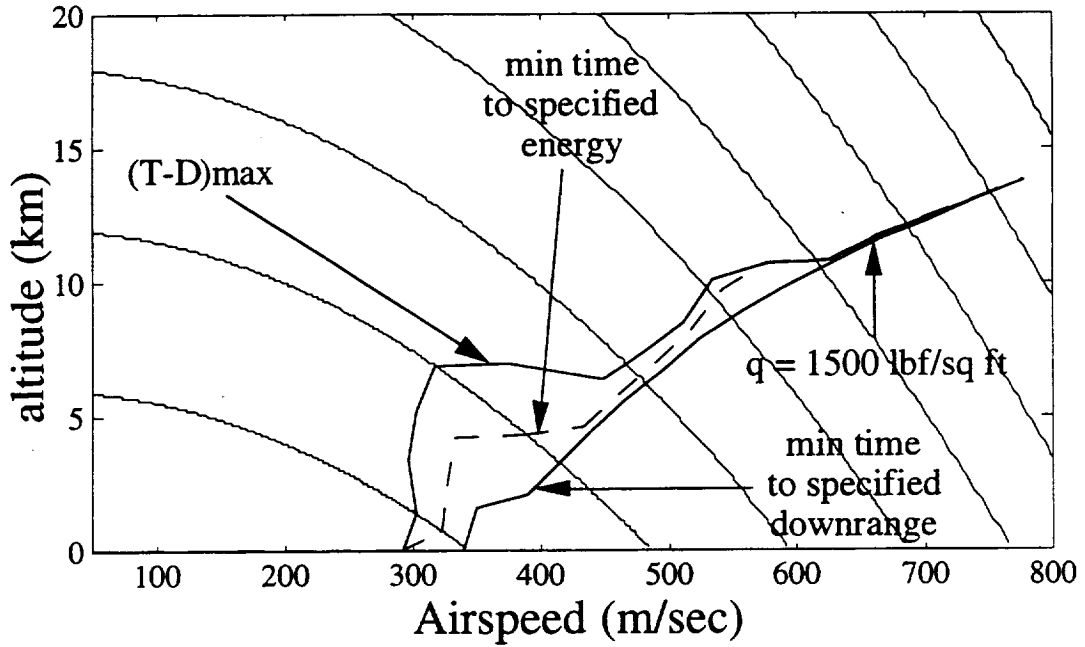
Figure 2.3 Energy climb paths for an F-15 aircraft.
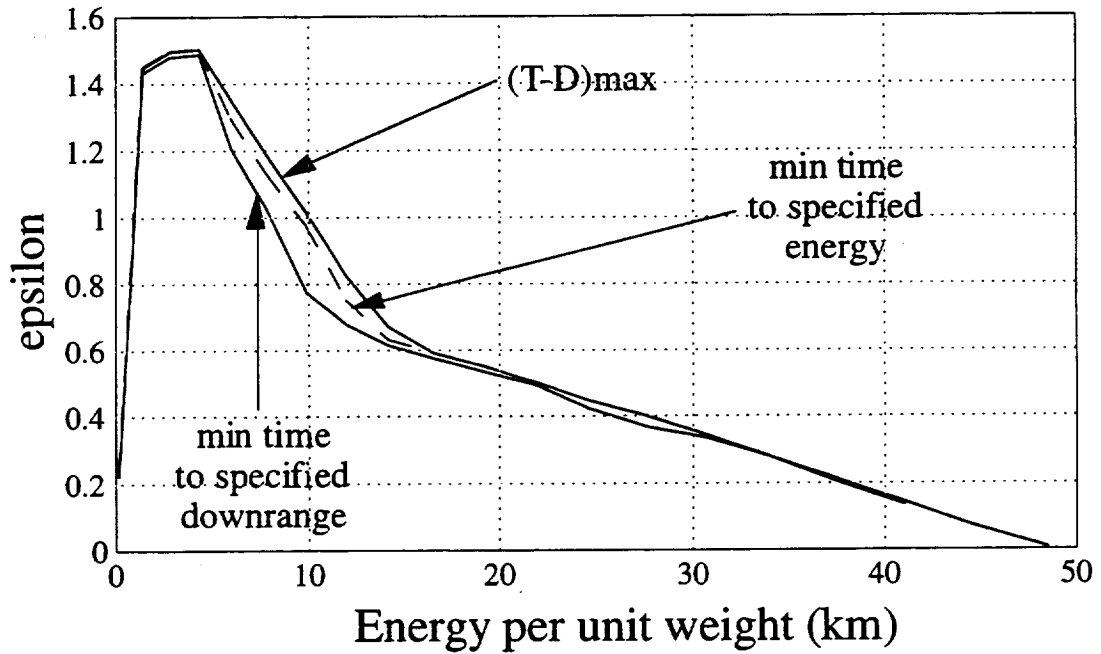
Figure 2.4 Evaluation of ε(E) for an F-15 aircraft.

150
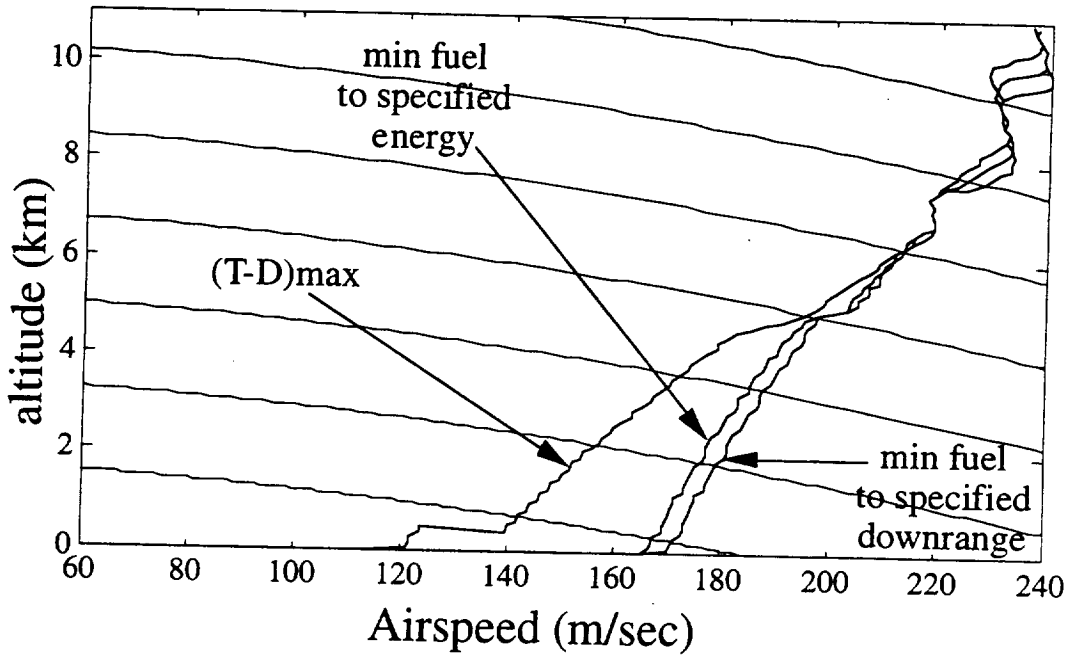
Figure 2.5 Energy climb paths for a short-haul transport aircraft.
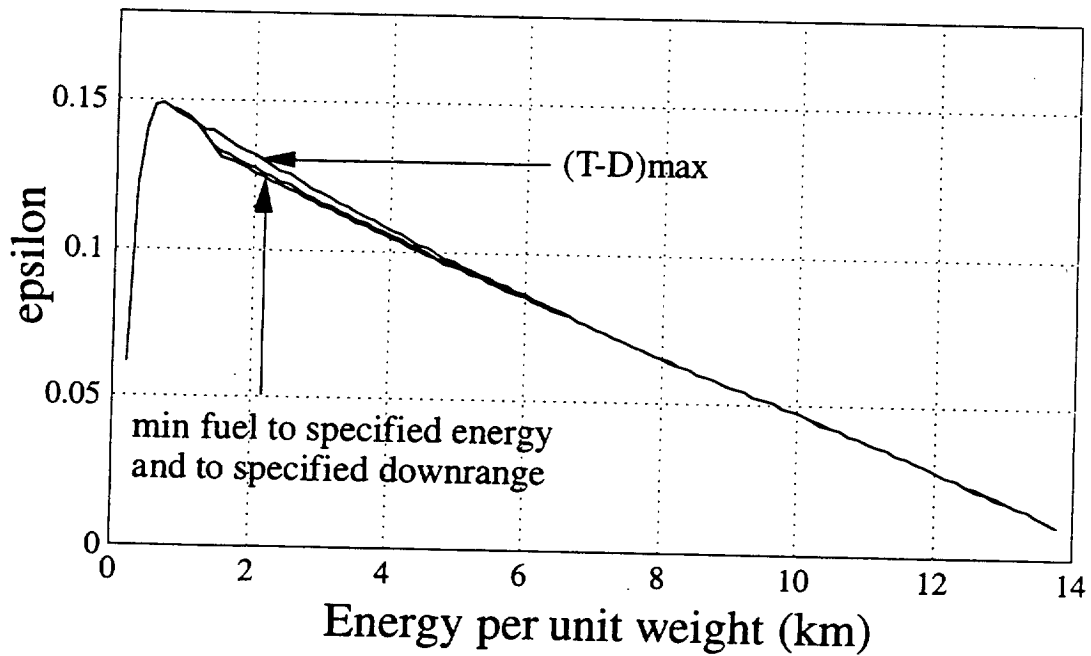
Figure 2.6 Evaluation of ε(E) for a short-haul transport aircraft.

151
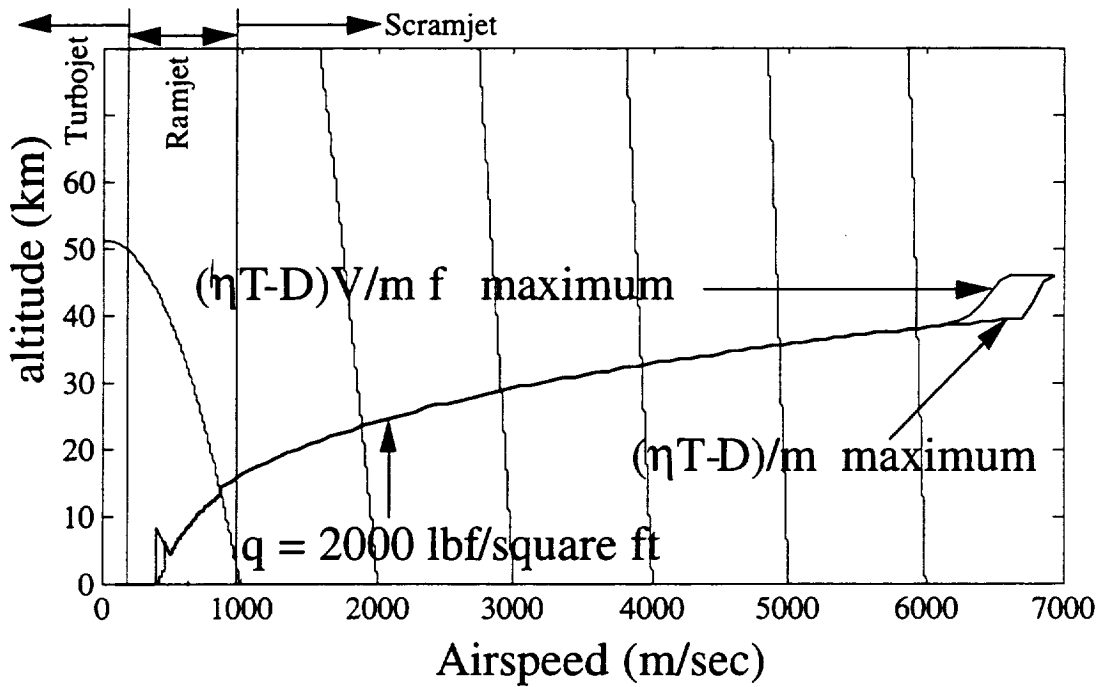
Figure 2.7 Energy climb paths for a generic hypersonic vehicle.
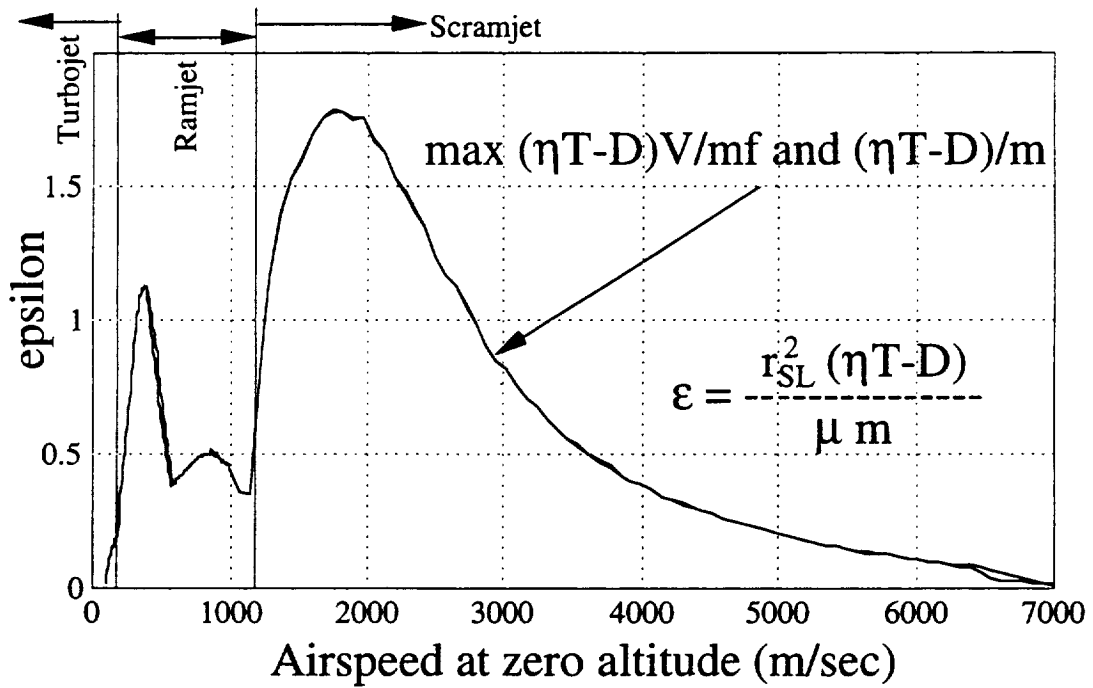
Figure 2.8 Evaluation of ε(E) for a generic hypersonic vehicle.
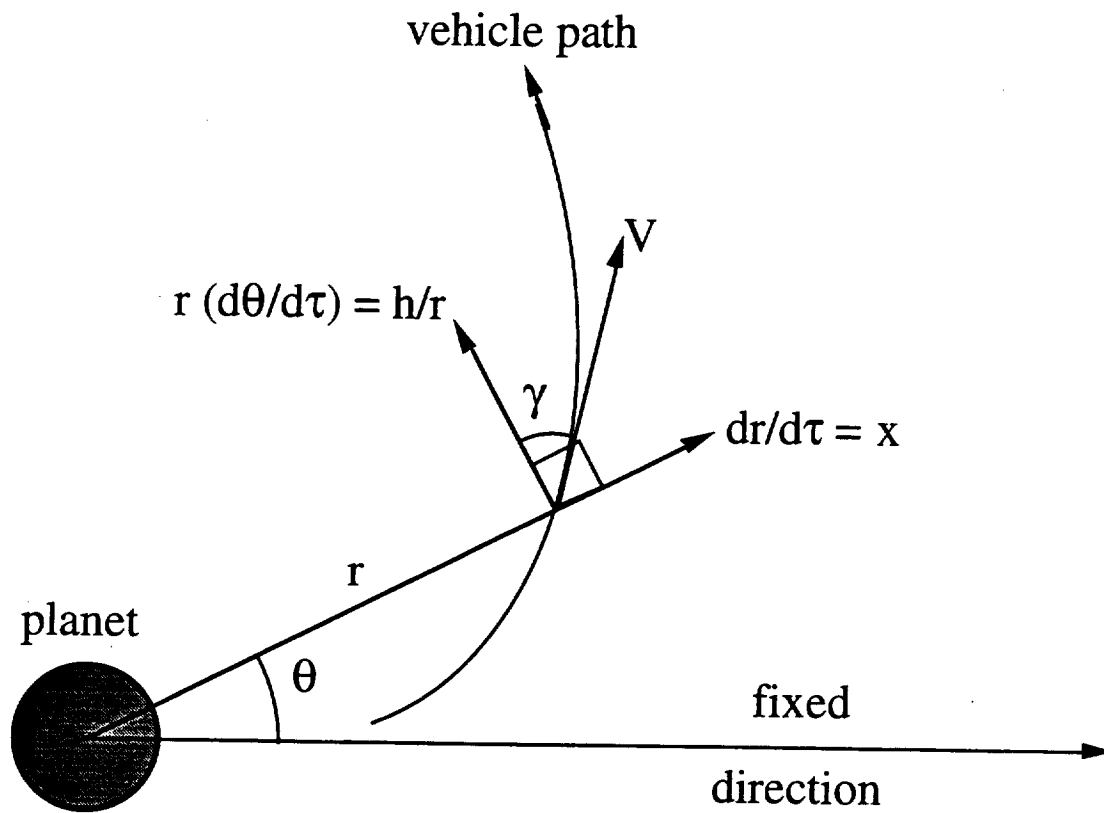
Figure 4.1 Polar coordinates r, θ, and nondimensional state variables
h, x, r, and θ (τ=nondimensional time).
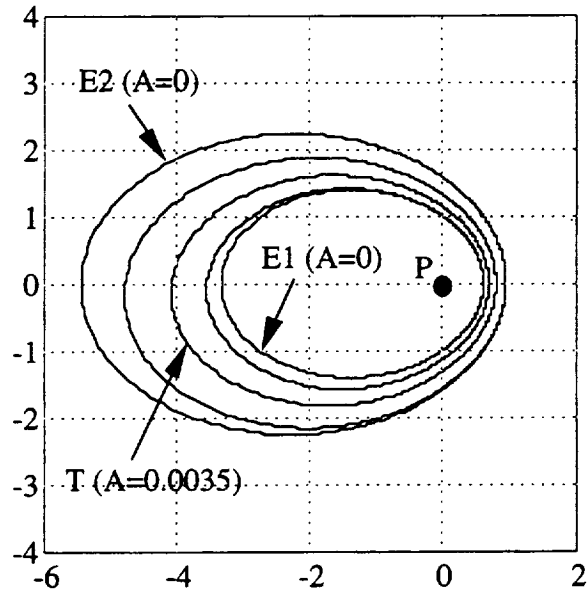
Figure 4.2 Example of transfer between two elliptic orbits.
E1: $h_0=1$, $e_0=0.7$, $\omega_0=0°$, E2: $h_f=1.2568$, $e_f=0.7097$, $\omega_f=0.195°$,
T: A=0.0035, B=0.7000, C=0.3370°, $\theta_0=0°$, $\theta_f=1160°$, $\tau_f=73.361$.
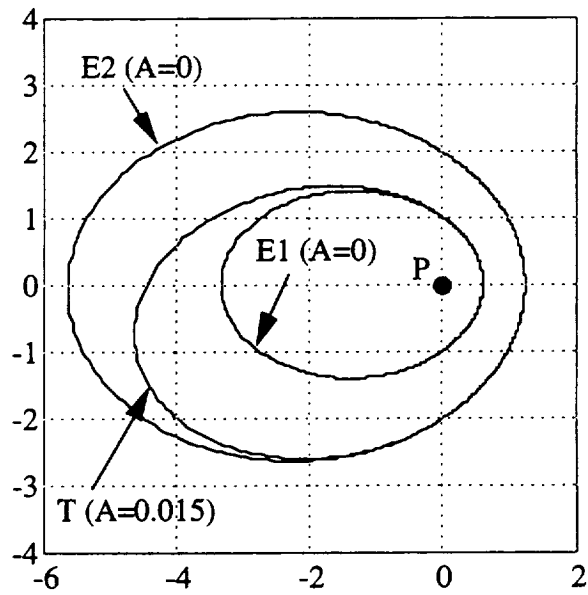
Figure 4.3 Example of transfer between two elliptic orbits.
E1: $h_0=1$, $e_0=0.7$, $\omega_0=0°$, E2: $h_f=1.4114$, $e_f=0.6468$, $\omega_f=0.731°$,
T: A=0.015, B=0.7002, C=1.444°, $\theta_0=0°$, $\theta_f=280°$, $\tau_f=27.426$.
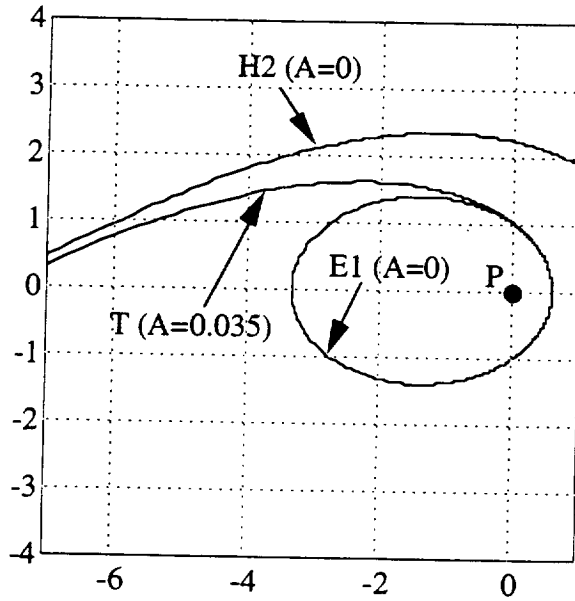
Figure 4.4 Example of elliptic to hyperbolic transfer.
E1: $h_0=1$, $e_0=0.7$, $\omega_0=0°$, H2: $h_f=2.1077$, $e_f=1.0768$, $\omega_f=66.547°$,
T: A=0.035, B=0.7012, C=3.366°, $\theta_0=0°$, $\theta_f=196°$, $\tau_f=31.648$.
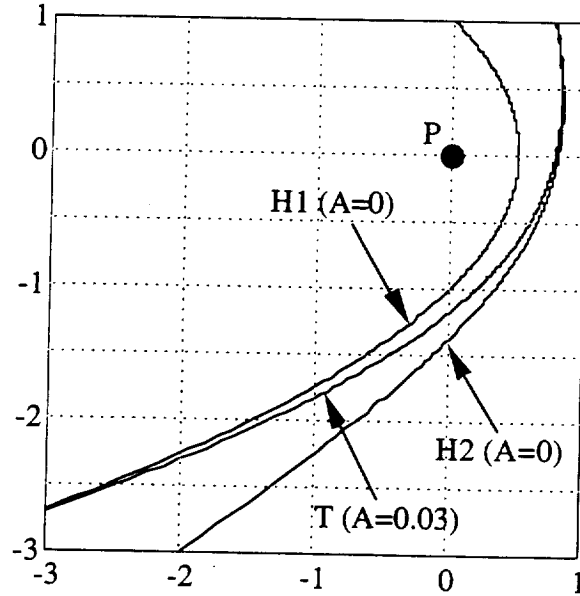
Figure 4.5 Example of hyperbolic to hyperbolic transfer.
H1: $h_0=1$, $e_0=1.01$, $\omega_0=0°$, H2: $h_f=1.3951$, $e_f=1.5071$, $\omega_f=344.030°$,
T: A=0.03, B=1.3164, C=341.640°, $\theta_0=-150°$, $\theta_f=90°$, $\tau_f=13.169$.
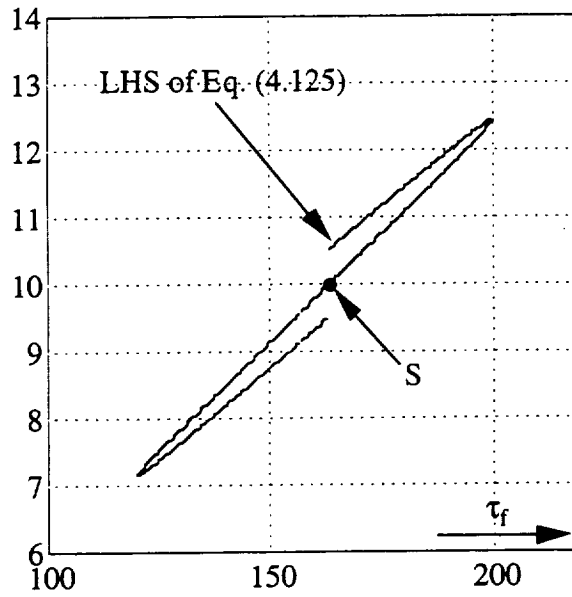
Figure 4.6 Solution search for a circular to circular transfer.
C0: $h_0=1$, $e_0=0$, Cf: $h_f=2$, $e_f=0.05$, $\omega_f=0°$ (Cf is very nearly circular).
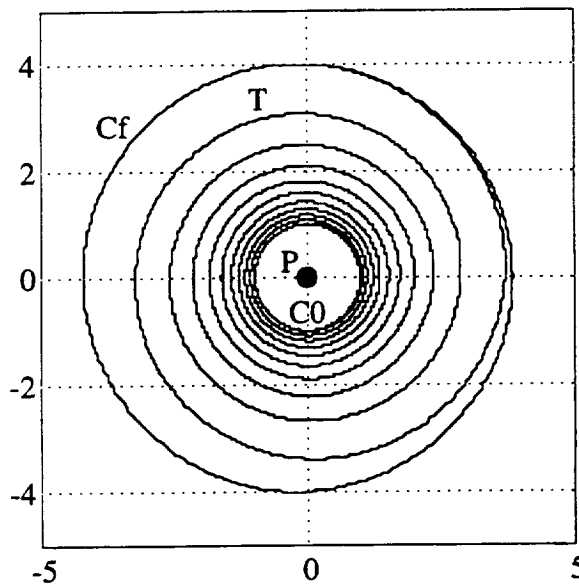
Figure 4.7 Transfer corresponding to point S (with k=10) in Fig. 4.6.T: A=6.1139X10^{-3}, B=1.2228X10^{-2}, C=279.312°, $\theta_0=189.312°$, $\theta_{fp}=104.105°$, $\tau_f=163.563$.

156
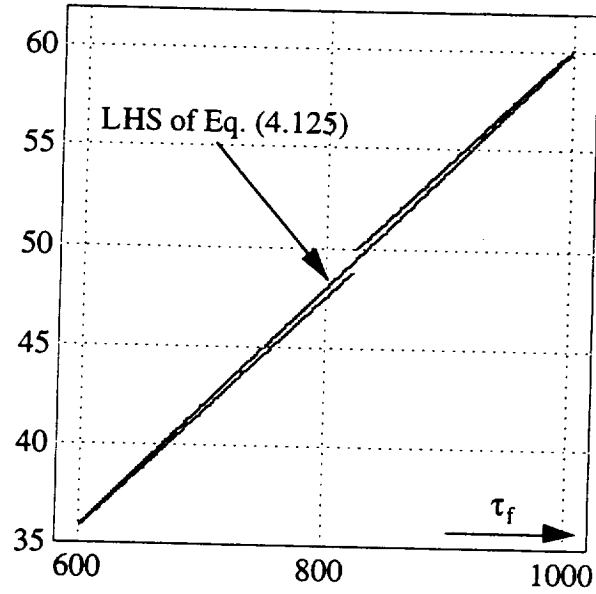
Figure 4.8 Solution search for the same circular to circular transfer as in Fig. 4.6, but with smaller e_f. C0: $h_0=1$, $e_0=0$, Cf: $h_f=2$, $e_f=0.01$, $\omega_f=0°$.
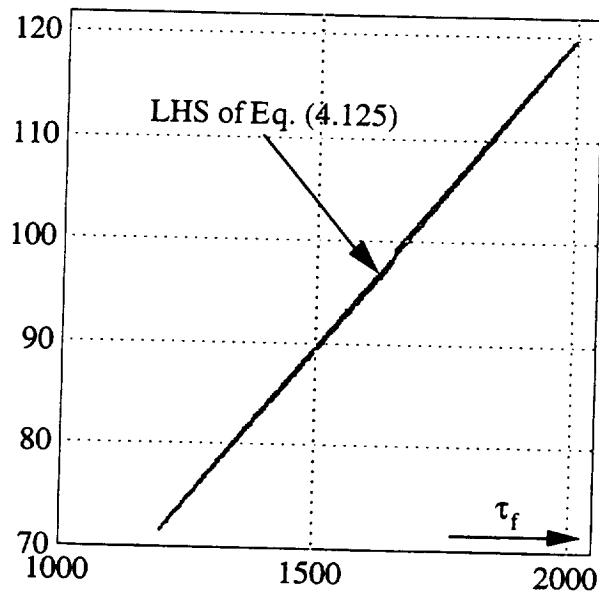
Figure 4.9 Solution search for the same circular to circular transfer as in Fig. 4.6, but with smaller e_f. C0: $h_0=1$, $e_0=0$, Cf: $h_f=2$, $e_f=0.005$, $\omega_f=0°$.
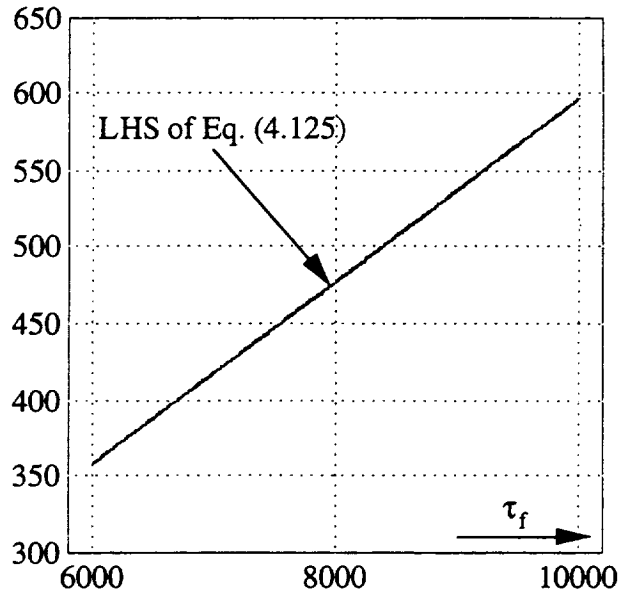
Figure 4.10 Solution search for the same circular to circular transfer as in Fig. 4.6, but with smaller e_f. C0: $h_0=1$, $e_0=0$, Cf: $h_f=2$, $e_f=0.001$, $\omega_f=0°$.
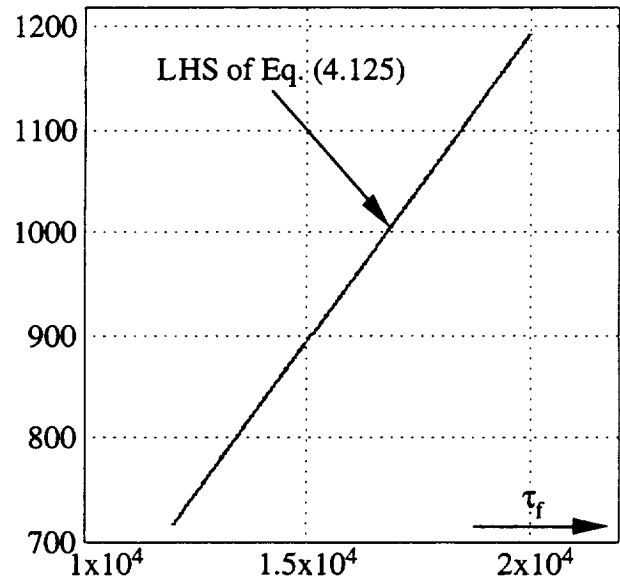
Figure 4.11 Solution search for the same circular to circular transfer as in Fig. 4.6, but with smaller e_f. C0: $h_0=1$, $e_0=0$, Cf: $h_f=2$, $e_f=0.0005$, $\omega_f=0°$.
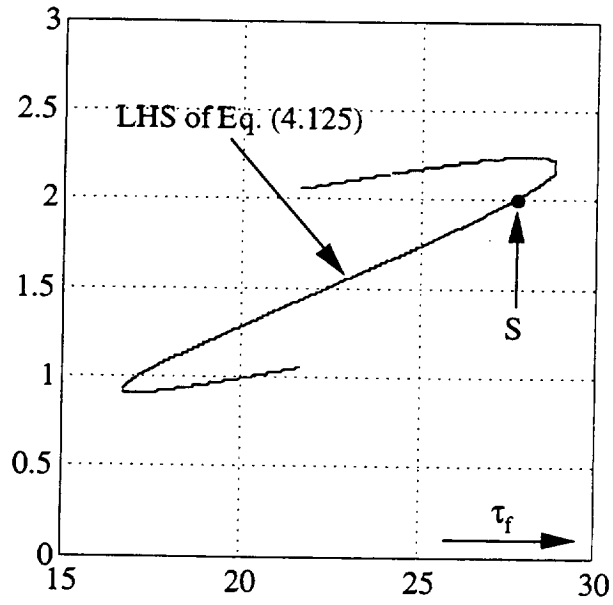
Figure 4.12 Solution search for a circular to elliptic transfer.
C0: $h_0=1$, $e_0=0$, Ef: $h_f=2$, $e_f=0.35$, $\omega_f=0°$.
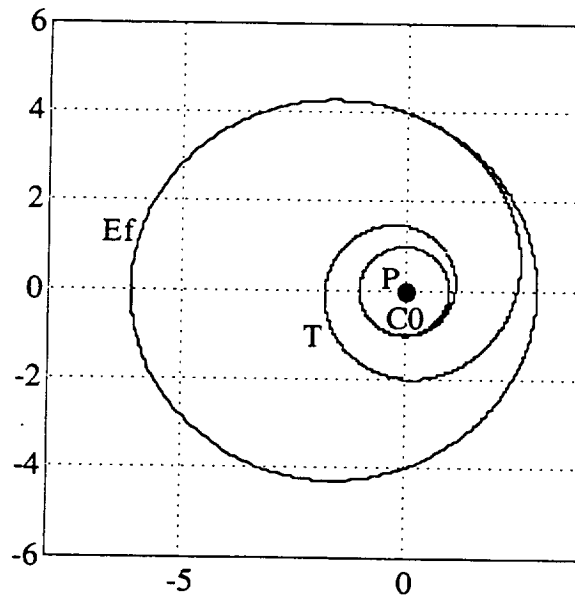
Figure 4.13 Transfer corresponding to point S (with k=2) in Fig.4.12. T: $A=3.6210\times10^{-2}$,
$B=7.2420\times10^{-2}$, $C=309.249°$, $\theta_0=219.249°$, $\theta_{fp}=100.446°$, $\tau_f=27.617$.

159
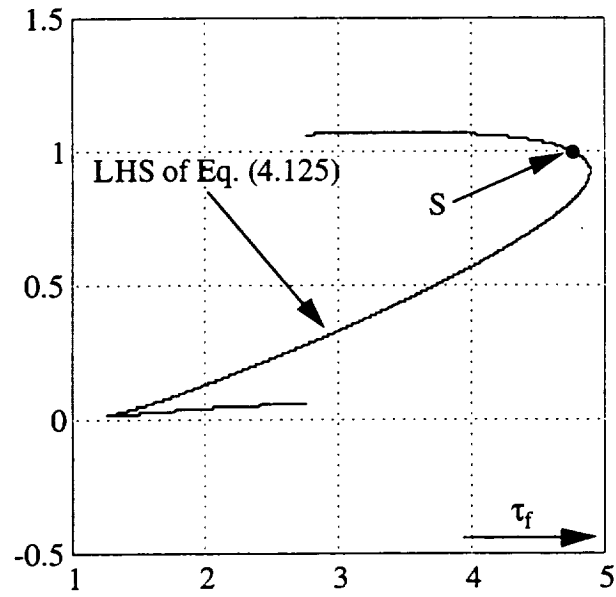
Figure 4.14 Solution search for a circular to elliptic transfer.
C0: $h_0=1$, $e_0=0$, Ef: $h_f=1.5$, $e_f=0.7$, $\omega_f=0°$.
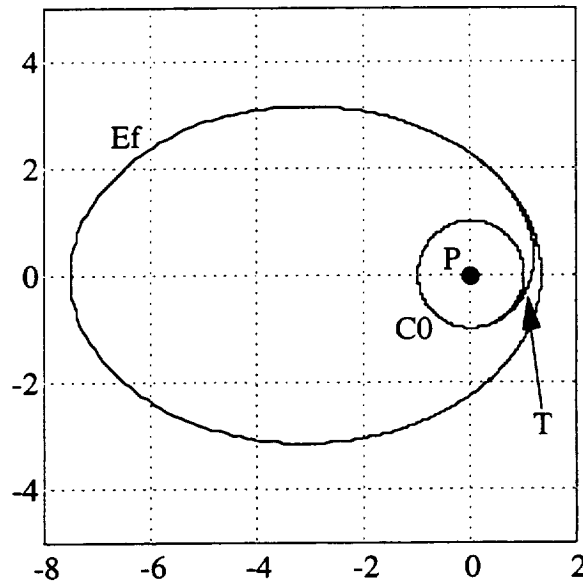
Figure 4.15 Transfer corresponding to point S (with k=1) in Fig. 4.14.
T: A=0.10542, B=0.21084, C=353.501°, $\theta_0=263.501°$, $\theta_{fp}=92.785°$, $\tau_f=4.743$.

160
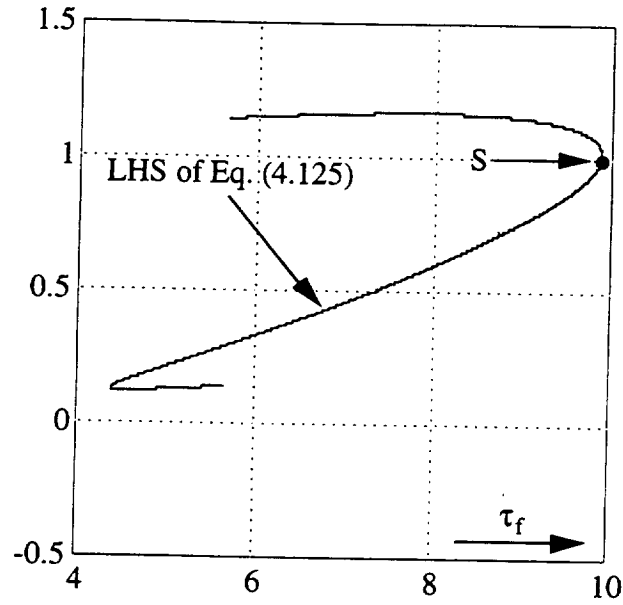
Figure 4.16 Solution search for a circular to hyperbolic transfer.
C0: $h_0=1$, $e_0=0$, Hf: $h_f=2$, $e_f=1.1$, $\omega_f=0°$.
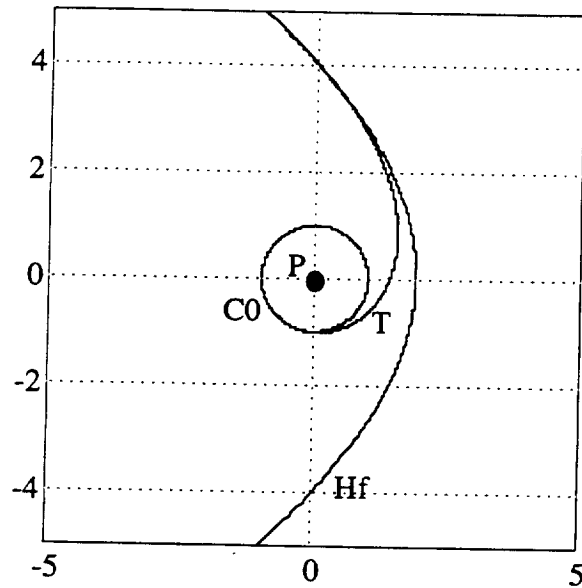
Figure 4.17 Transfer corresponding to point S (with k=1) in Fig. 4.16.
T: A=0.10131, B=0.20261, C=312.109°, $\theta_0=222.109°$, $\theta_{fP}=98.861°$, $\tau_f=9.871$.

161
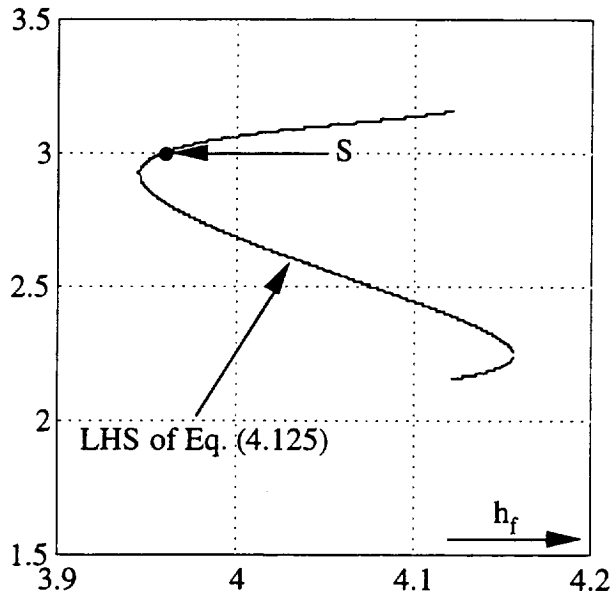
Figure 4.18 Solution search for an escape from a circular orbit at $\tau_f=100$.

C0: $h_0=1$, $e_0=0$, Pf: $h_f=$free, $e_f=1$, $\omega_f=0°$.
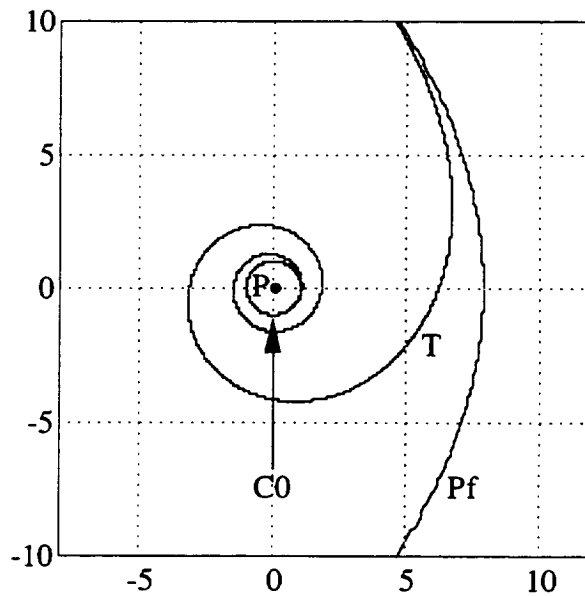
Figure 4.19 Transfer corresponding to point S (with $k=3$, $h_f=3.9601$) in Fig. 4.18.

T: $A=2.9601\text{X}10^{-2}$, $B=5.9202\text{X}10^{-2}$, $C=346.123°$, $\theta_0=256.123°$, $\theta_{fp}=90.863°$, $\tau_f=100$.
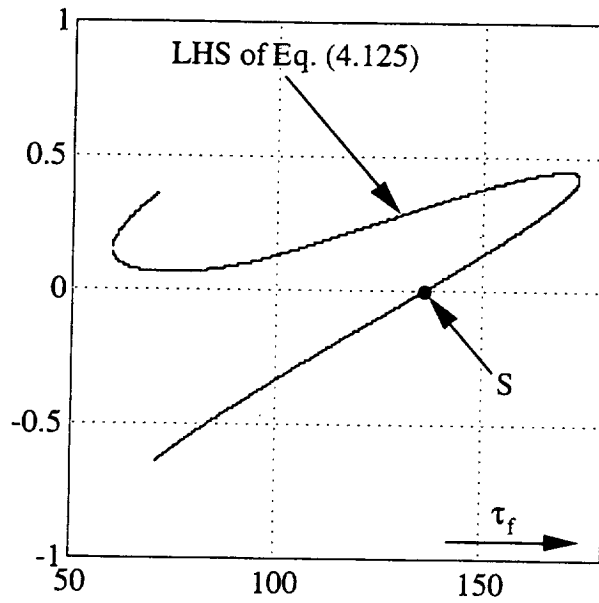
Figure 4.20 Solution search for an elliptic to elliptic transfer.
E0: $h_0=1$, $e_0=0.9$, $\omega_0=0°$, Ef: $h_f=2$, $e_f=0.8$, $\omega_f=0°$.
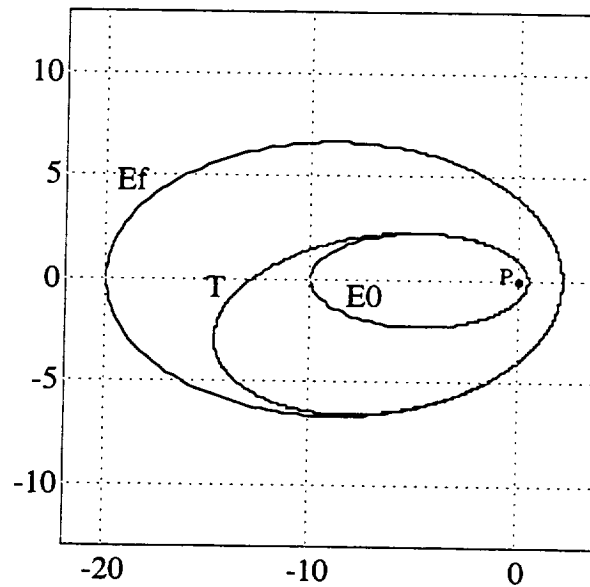
Figure 4.21 Transfer corresponding to point S (with k=0) in Fig. 4.20.
T: $A=7.3577 \times 10^{-3}$, $B=0.87362$, $C=358.544°$, $\theta_0=129.783°$, $\theta_{fP}=253.156°$, $\tau_f=135.913$.
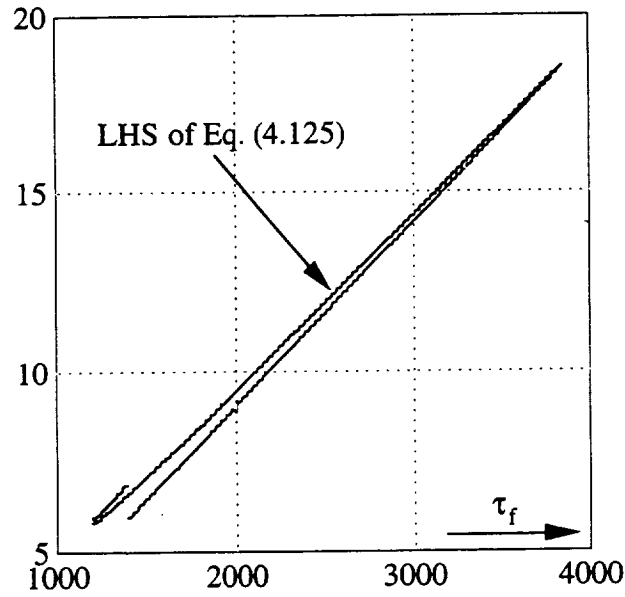
Figure 4.22 Solution search for an elliptic to elliptic transfer involving a small change in eccentricity. E0: $h_0=1$, $e_0=0.9$, $\omega_0=0°$, Ef: $h_f=2$, $e_f=0.895$, $\omega_f=0°$.
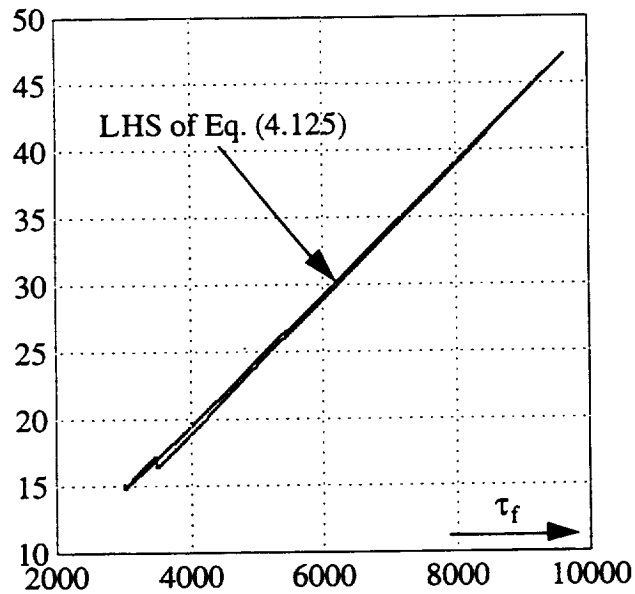
Figure 4.23 Solution search for (practically) the same elliptic to elliptic transfer as in Fig. 4.22. E0: $h_0=1$, $e_0=0.9$, $\omega_0=0°$, Ef: $h_f=2$, $e_f=0.898$, $\omega_f=0°$.
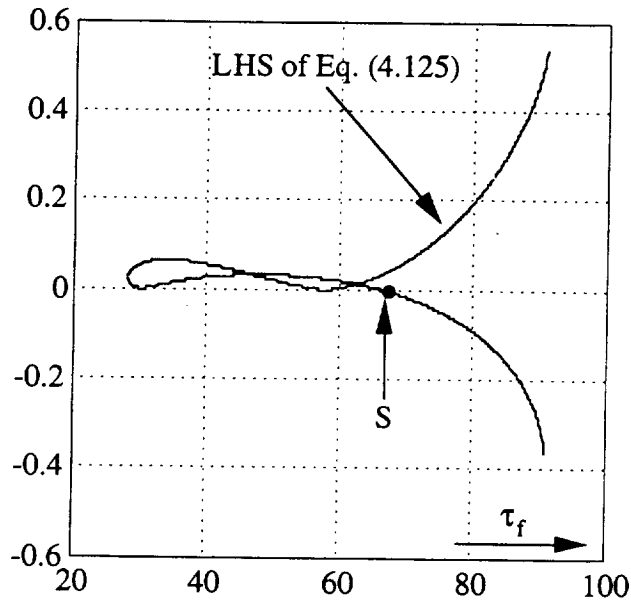
Figure 4.24 Solution search for an elliptic to elliptic transfer with orientation change.
E0: $h_0=1$, $e_0=0.9$, $\omega_0=0°$, Ef: $h_f=2$, $e_f=0.8$, $\omega_f=30°$.
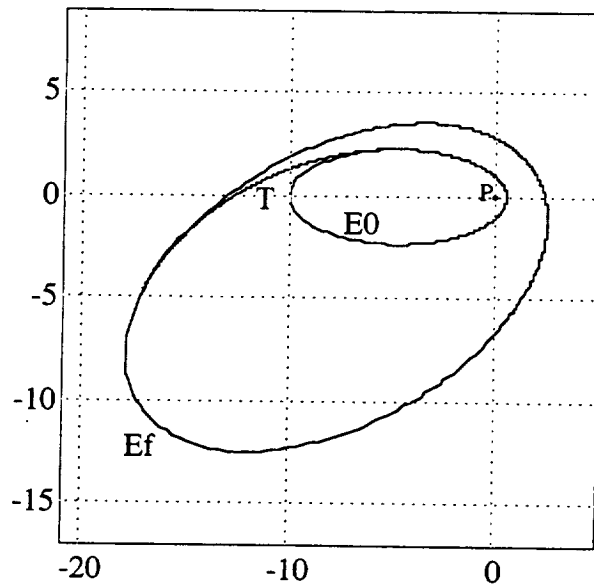
Figure 4.25 Transfer corresponding to point S (with k=0) in Fig. 4.24.
T: $A=1.5121 \times 10^{-2}$, $B=0.83962$, $C=352.146°$, $\theta_0=149.252°$, $\theta_{fP}=195.104°$, $\tau_f=66.134$.
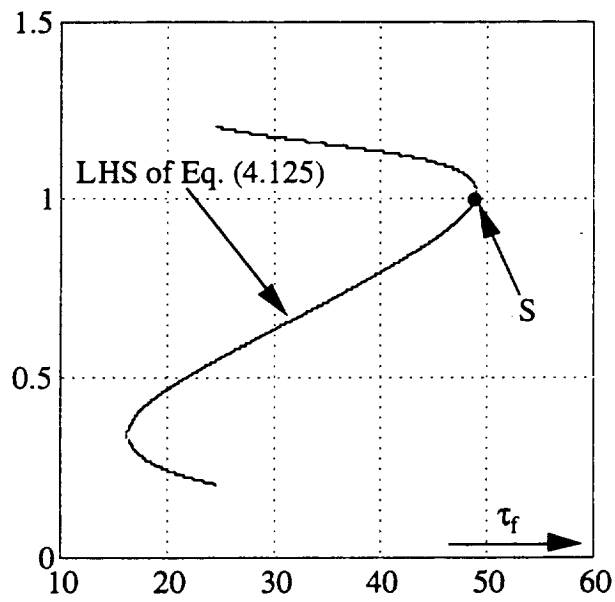
Figure 4.26 Solution search for an elliptic to hyperbolic transfer.
E0: $h_0=1$, $e_0=0.8$, $\omega_0=0°$, Hf: $h_f=2$, $e_f=1.5$, $\omega_f=30°$.
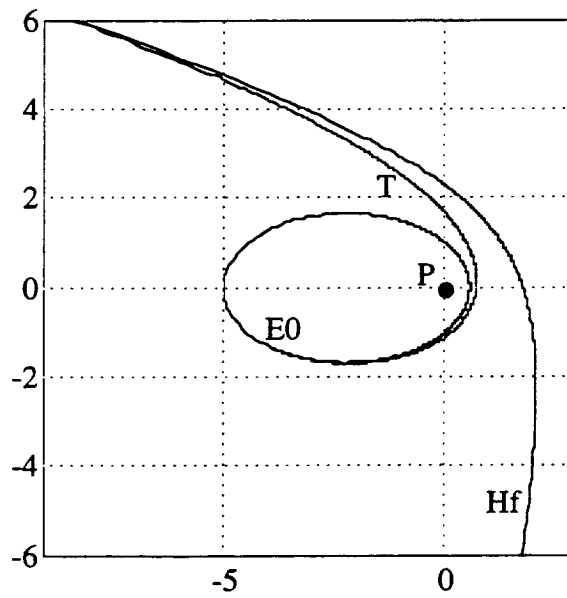
Figure 4.27 Transfer corresponding to point S (with k=1) in Fig. 4.26.
T: $A=2.0519 \times 10^{-2}$, $B=0.86914$, $C=349.330°$, $\theta_0=198.586°$, $\theta_{fp}=153.967°$, $\tau_f=48.736$.
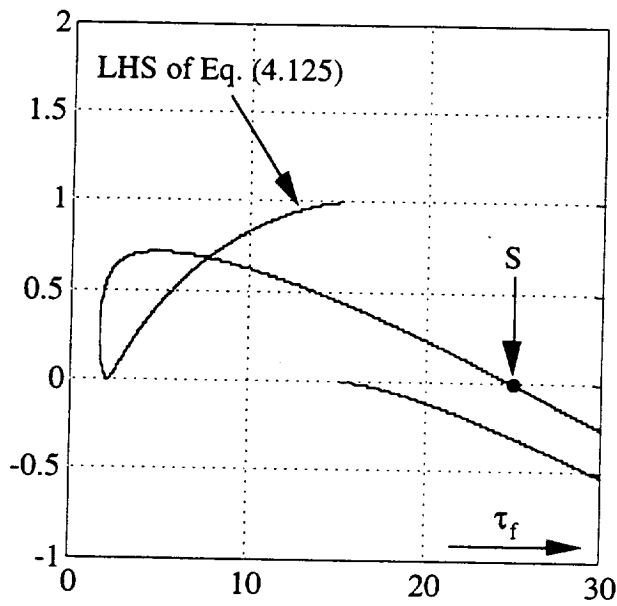
Figure 4.28 Solution search for a hyperbolic to hyperbolic transfer.
H0: $h_0=1$, $e_0=1.1$, $\omega_0=0°$, Hf: $h_f=2.3$, $e_f=3.4$, $\omega_f=320°$.
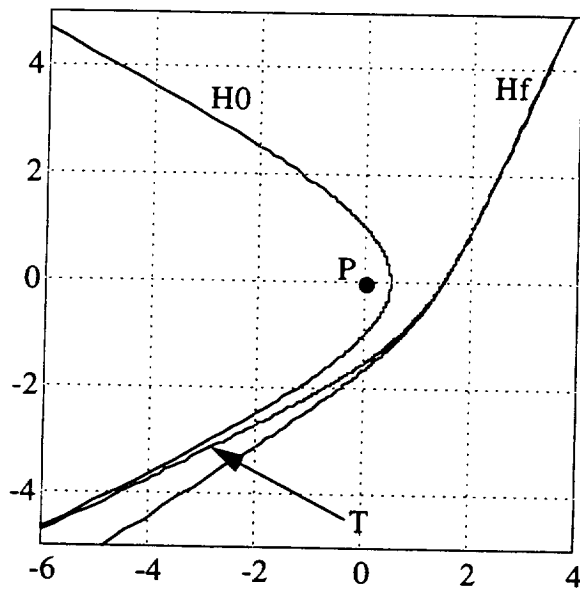
Figure 4.29 Transfer corresponding to point S (with k=0) in Fig. 4.28.
T: $A=5.2151 \times 10^{-2}$, $B=2.8264$, $C=319.870°$, $\theta_0=-149.782°$, $\theta_{fP}=50.642°$, $\tau_f=24.928$.
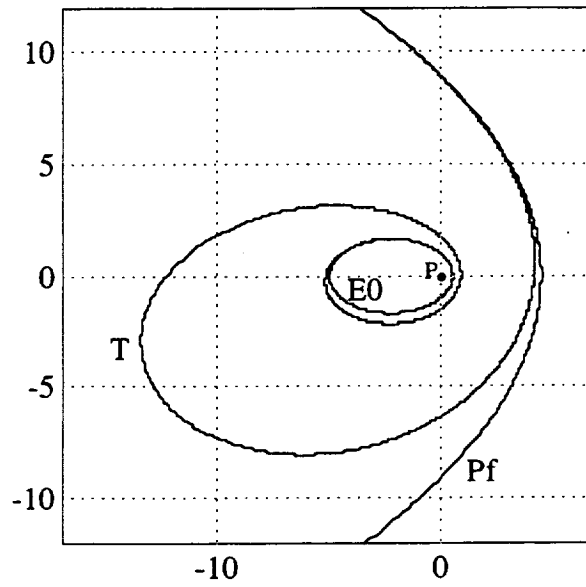
Figure 4.30 Escape from an elliptic orbit at τ_f=200, first solution (ω_f is free).
E0: h_0=1, e_0=0.8, ω_0=0°, Pf: h_f=3, e_f=1, ω_f=0.3562°, T: A=0.01, B=0.76944,
C=355.827°, θ_0=149.787°, θ_{fP}=104.974°, k=2, τ_f=200.
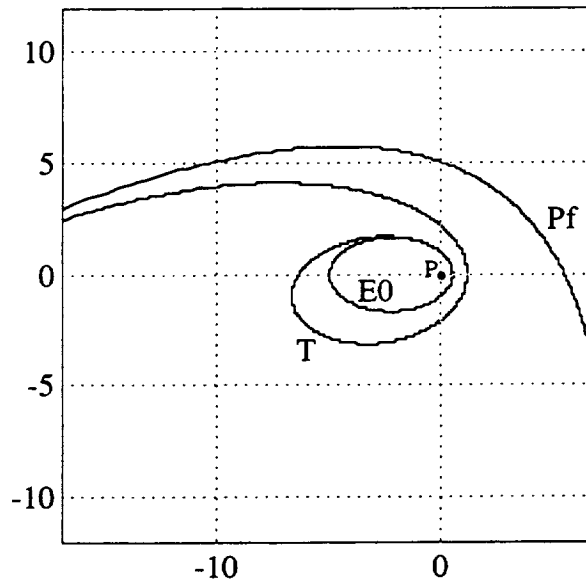
Figure 4.31 Escape from the same elliptic orbit (as in Fig. 4.30) at τ_f=200, second
solution (ω_f is free). E0: h_0=1, e_0=0.8, ω_0=0°, Pf: h_f=3, e_f=1, ω_f=51.459°, T: A=0.01,
B=0.78853, C=0.5593°, θ_0=56.212°, θ_{fP}=192.057°, k=1, τ_f=200.
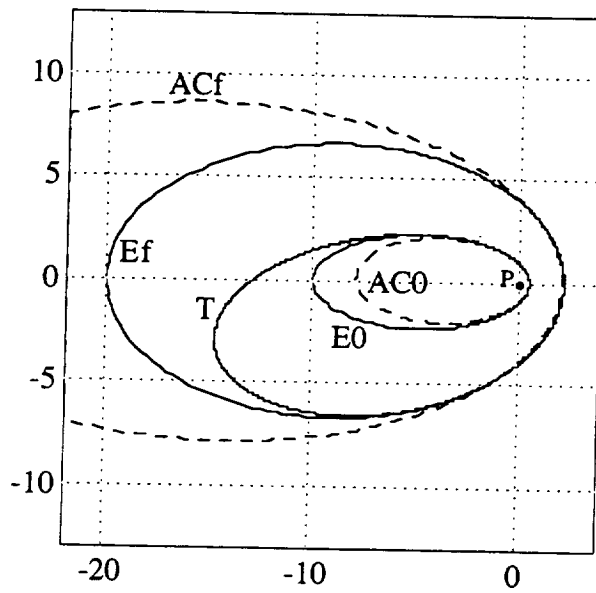
Figure 4.32 The two associated conics (dotted lines) at the initial and final times, for the transfer given in Fig. 4.21. AC0: $h_0=1$, $e_0=0.87362$, $\omega_0=358.544°$, ACf: $h_f=2$, $e_f=0.87362$, $\omega_f=358.544°$.
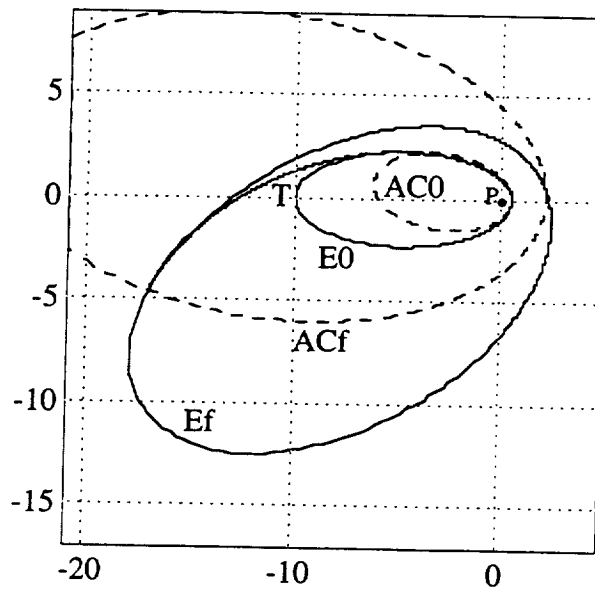
Figure 4.33 The two associated conics (dotted lines) at the initial and final times, for the transfer given in Fig. 4.25. AC0: $h_0=1$, $e_0=0.83962$, $\omega_0=352.146°$, ACf: $h_f=2$, $e_f=0.83962$, $\omega_f=352.146°$.
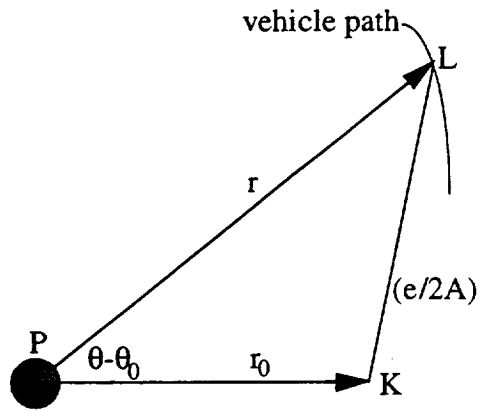
Figure 4.34 The geometry of departure from a circular orbit (Lemma 4.3).
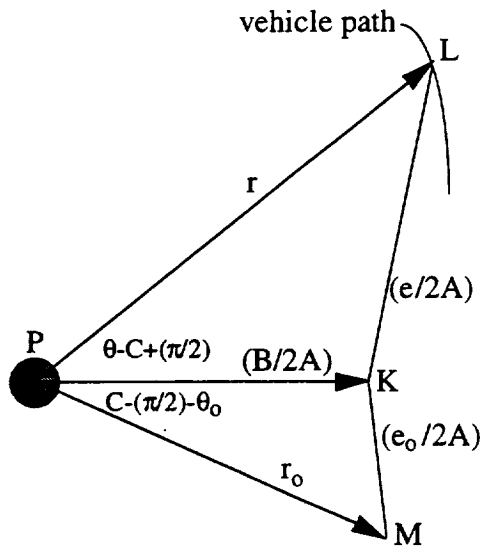
Figure 4.35 The geometry of departure from an arbitrary conic (Lemma 4.4).
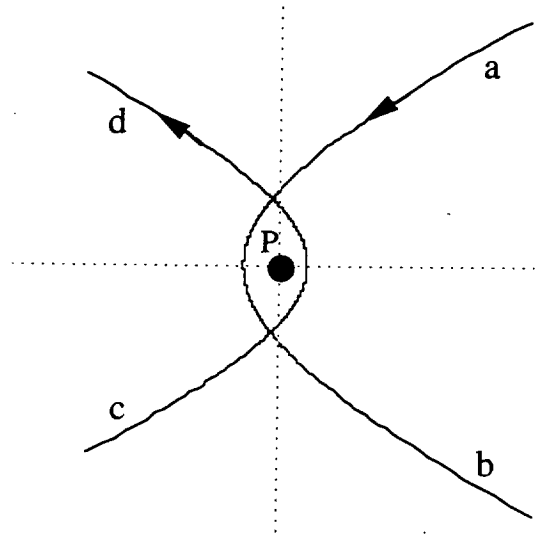
Figure 4.36 Two hyperbolic trajectories having opposite orientation.
A one-segment (transfer) solution cannot exist in such a case.
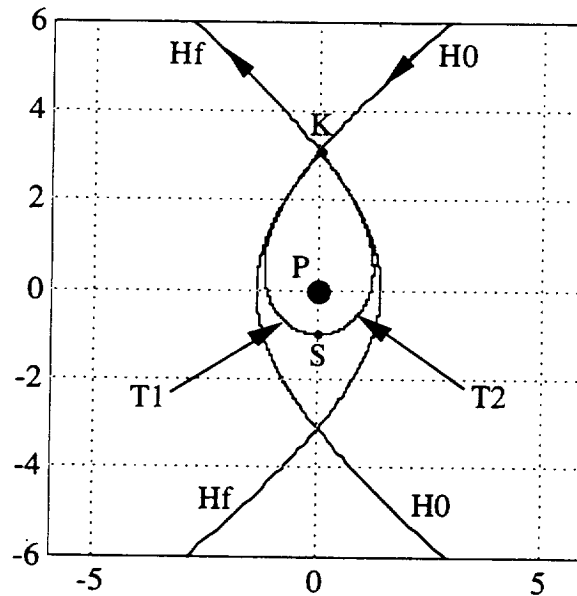
Figure 4.37 A two-segment transfer between two hyperbolic orbits for a case similar to the one given in Fig. 4.36. H0: h_0=1.7604, e_0=1.2297, ω_0=180°, Hf: h_f=1.7604, e_f=1.2297, ω_f=0°, T1: A=-0.15, B=0.3, C=180°, θ_0=90°, θ_f=270°, τ_f=5.0690, T2: Symmetric to T1 about θ=90° with A=0.15 (Note: In Table 4.1, Section 4.13, the costs are the total costs, while ϵ_0 and ϵ_f correspond only to T2).

171
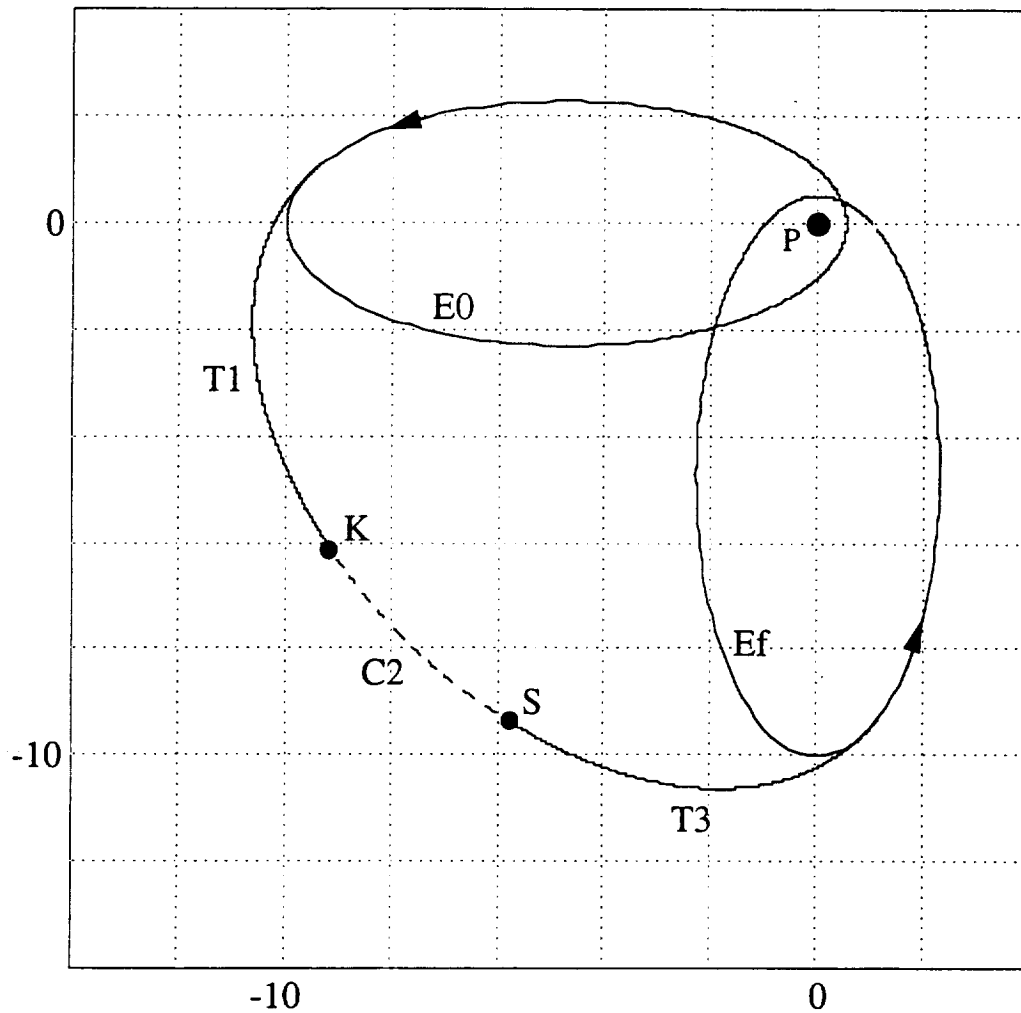
Figure 4.38 An example of a three-segment (thrust(T1)-coast(C2)-thrust(T3)) transfer for changing the orientation of an elliptic orbit by 90 degrees. E0: $h_0=1$, $e_0=0.9$, $\omega_0=0°$, Ef: $h_f=1$, $e_f=0.9$, $\omega_f=90°$, T1: A=6.3771X10^{-2}, B=1.4030, C=302.441°, $\theta_0=172.904°$, $\theta_K=212.441°$, $\tau_{0K}=36.327$, T3: Symmetric to T1 about $\theta=225°$ with A=-6.3771X10^{-2}, C2 (dotted line) is just a circular (Keplerian) segment with A=0 (Note: In Table 4.1, Section 4.13, the costs are the total costs, while ε_0 and ε_f correspond only to T1).
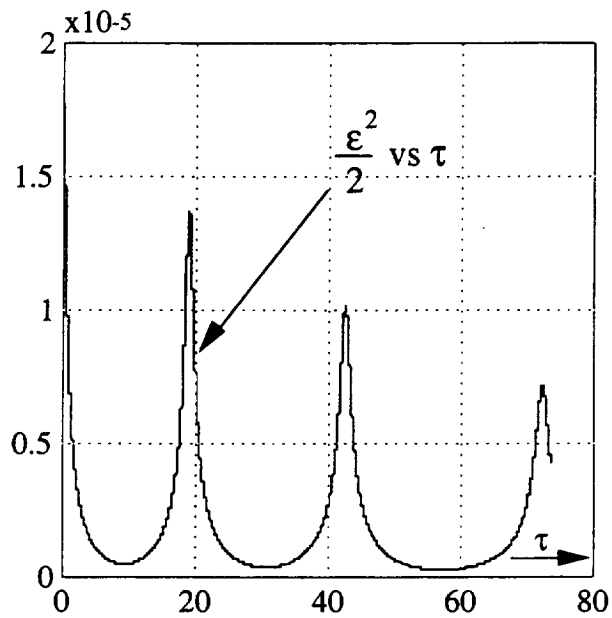
Figure 4.39 Variation of one-half times the square of the (nondimensional) thrust acceleration with (nondimensional) time for the transfer example of Fig. 4.2.
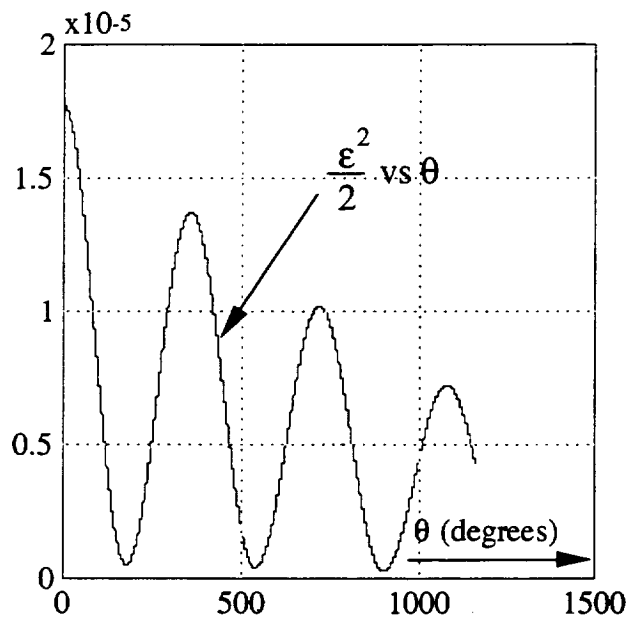
Figure 4.40 Variation of one-half times the square of the (nondimensional) thrust acceleration with the argument of latitude for the transfer example of Fig. 4.2.

173
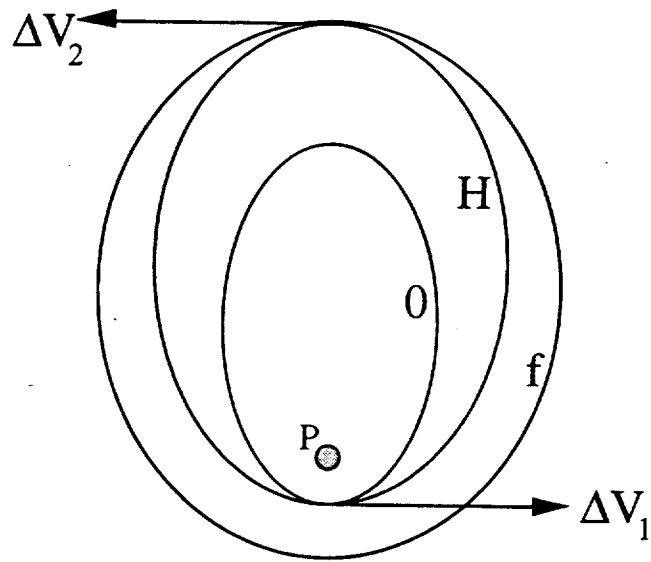
Figure 4.41 The Hohmann transfer (H) between two coplanar elliptical orbits having the same orientation.
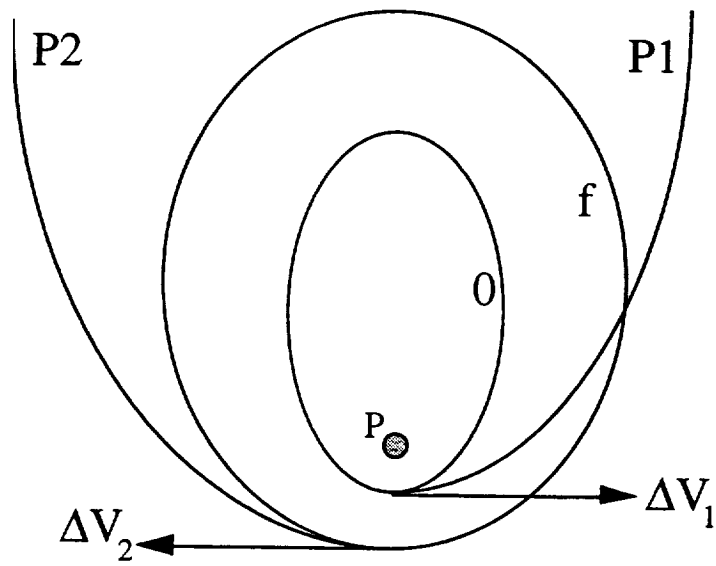
Figure 4.42 The Biparabolic transfer (P1), (P2) between two coplanar elliptical orbits having the same orientation.

174

13. ABSTRACT (Maximum 200 words)

A collection of analytical studies is presented related to unconstrained and constrained aircraft (a/c) energy-state modeling and to spacecraft (s/c) motion under continuous thrust. With regard to a/c unconstrained energy-state modeling, the physical origin of the singular perturbation parameter that accts. for the observed 2-time-scale behavior of a/c during energy climbs is identified and explained. With regard to the constrained energy-state modeling, optimal control problems are studied involving active state-variable inequality constraints. Departing from the pract. deficiences of the control programs for such problems that result from the traditional formulations, a complete reformulation is proposed for these problems which, in contrast to the old formulation, will presumably lead to practically useful controllers that can track an inequality constraint boundary asymptotically, and even in the presence of 2-sided perturbations about it. Finally, with regard to s/c motion under continuous thrust, a thrust program is proposed for which the equations of 2-dimensional motion of a space vehicle in orbit, viewed as a pt. mass, afford an exact analytic solution. The thrust program arises under the assumption of tangential thrust from the costate sys. corresponding to minimum-fuel, power-limited, coplanar transfers between two arbitrary conics. The thrust prog. can be used not only with power-limited propulsion systems, but also with any propulsion sys. capable of generating continuous thrust of controllable magnitude, and, for propulsion types and classes of transfers for which it is sufficiently optimal the results of this report suggest a method of maneuvering during planetocentric or heliocentric orbital operations, requiring a minimum amount of computation, thus uniquely suitable for real-time feedback guidance implementations.

14. SUBJECT TERMS Optimal Guidance, Trajectory Optimization, Perturbation Methods			15. NUMBER OF PAGES 187
			16. PRICE CODE A09
17. SECURITY CLASSIFICATION OF REPORT Unclassified	18. SECURITY CLASSIFICATION OF THIS PAGE Unclassified	19. SECURITY CLASSIFICATION OF ABSTRACT	20. LIMITATION OF ABSTRACT